WHAT MAKES THE LYSIS CLOCK TICK?

A STUDY OF THE BACTERIOPHAGE LAMBDA HOLIN

A Dissertation

by

REBECCA LYNN WHITE

Submitted to the Office of Graduate Studies of
Texas A&M University
in partial fulfillment of the requirements for the degree of

DOCTOR OF PHILOSOPHY

May 2008

Major Subject: Microbiology

WHAT MAKES THE LYSIS CLOCK TICK?

A STUDY OF THE BACTERIOPHAGE LAMBDA HOLIN

A Dissertation

by

REBECCA LYNN WHITE

Submitted to the Office of Graduate Studies of
Texas A&M University
in partial fulfillment of the requirements for the degree of

DOCTOR OF PHILOSOPHY

Approved by:

Chair of Committee,	Ryland F. Young, III
Committee Members,	Deborah A. Siegele
	Susan S. Golden
	Siegfried M. Musser
Head of Department,	Vincent M. Cassone

May 2008

Major Subject: Microbiology

ABSTRACT

What Makes the Lysis Clock Tick?

A Study of the Bacteriophage Lambda Holin. (May 2008)

Rebecca Lynn White, B.S., University of North Texas

Chair of Advisory Committee: Dr. Ryland F. Young, III

The timing of host lysis is the only decision made in the bacteriophage lytic cycle. To optimize timing, double-stranded DNA phages use a 2-component lysis system consisting of a muralytic enzyme, the endolysin, and a small membrane protein, the holin, which controls the timing of lysis. The best characterized holin gene to date is the *S* gene of bacteriophage λ.

One unusual feature of the *S* gene is that it produces two proteins of opposing function: the holin, S105, and the antiholin, S107. Raab et al isolated and characterized a number of *S* mutants, but all of them expressed both the holin and the antiholin; it is possible, then, that the true extent of the holin-holin interactions were masked by interactions with the antiholin. Thus, a large number of S105 mutants were created, and their phenotypes characterized in the absence of the antiholin. The interaction between those mutants and the wild-type were examined in an attempt to better understand what determines the timing of hole formation by S105.

S105 and S107 differ only by two amino acids at the N-terminus; S107 has an additional Met-Lys sequence. Previous studies have shown that S107 may have a

different topology to S105, where the N-terminus of S107 is located in the cytoplasm and is cannot flip through the membrane because of the extra cationic side chain. This study investigates the role of the N-terminal transmembrane domain of the S proteins in terms of hole formation and its role in the antiholin character of S107.

Previous results suggest that S105 forms hole via a large oligomeric structure termed the "death raft". The death raft model states that after S105 is inserted into the membrane, it forms "rafts", which grow in size until a spontaneous channel forms leading to depolarization of the membrane and hole formation. This study investigates the pathway of hole formation at the single-cell level, using a C-terminal fusion of S105 and green fluorescent protein, and attempts to address several of the predictions posed by the death raft model.

DEDICATION

To Phil and Macy: thanks for everything – I couldn't have done it without you.

Love always, Rebecca

ACKNOWLEDGEMENTS

I would like to thank Ry, Susan, Sig, Jim, and particularly Debby for their guidance and support, and Doug for input and ideas. I would also like to thank the members of the Young Lab λ Group –Ing-Nang, John, Joel, Christos, Jill, and Chelsey – for the camaraderie, ideas, feedback, and support. I would like to thank Chelsey in particular for her hard work and tremendous efforts, and Joel for the many brainstorming sessions and random help. Special thanks go to Daisy for her ability to get things done, and the encouragement and dedication she always gives. Dr. Kit Pogliano and Dr. Shinobu Chiba, and the members of Kit's lab at UCSD, were incredibly instrumental in the completion of my localization project and I will always be grateful for their teachings, support, and hospitality; I am very grateful to have worked with such a kindred spirit as Shinobu.

Many thanks go to my friends TP (Taehyun), Carrie, Joel, Jamie Rae, Karla, and especially Libby, for all the jokes, good times, honesty, sensibility, support, heartfelt advice, sympathy, and the occasional swift kick in the rear. Joel, thanks for being my friend and roommate when I needed one the most! I can never thank my family enough, in particular Dad, Mom, Sandra, Mam-maw and Papa, although I should spend the rest of my days trying. Thanks for the hope, prayers, calls and cards, and unconditional support. I am especially grateful to Gill and Jimmy for generously saving the day when I was at my most frustrated point in writing. Phil, I love you and sincerely appreciate your acceptance, patience, and steadfastness. I hope I've made you all proud.

TABLE OF CONTENTS

CHAPTER Page

CHAPTER Page

LIST OF FIGURES

FIGURE Page

FIGURE Page

LIST OF TABLES

CHAPTER I

INTRODUCTION

Lysis by dsDNA bacteriophage

Bacteriophage, or phage, are intracellular bacterial parasites that commandeer bacterial cells for the production of progeny virions. For many phage, release of progeny is achieved by lysis of the host cell. It is not generally appreciated that, in a phage infection, lysis of the host cell is a programmed event. In fact, other than the lysis-lysogeny switch affected by temperate phages, the decision of when to lyse the host, and thus terminate the infection and release the progeny virions, is the only decision of consequence. All other events, including macromolecular synthesis and morphogenesis, have presumably evolved to proceed at an optimal rate, to maximize the accumulation of progeny in the infected cell.

In the evolutionary search for a perfect lysis time, environmental factors are critical, as can be seen from considering the boundary conditions (79). In a "host-rich" environment, curtailing the infective cycle and accepting a reduced production per cell, is advantageous because the released progeny can begin new infections, thus allowing exponential increase in progeny. Conversely, in a "host-deficient" environment, extending the infective cycle to allow more particles to assemble is advantageous, because the released progeny would not likely be able to begin new infections. Thus for billions of years, the lysis systems of bacteriophage have been selected by rigorous,

---

This dissertation follows the style of the Journal of Bacteriology.

opposing evolutionary pressures (79). As a result of these pressures, double-stranded DNA (dsDNA) tailed bacteriophage have evolved a two-component, "holin-endolysin" system to effect host lysis in a programmed manner capable of adjustment to changing physiological conditions in both a real-time and evolutionary sense (80).

The endolysin is a phage-encoded muralytic enzyme that degrades the cell wall of the host. For many phages, including λ, the endolysin is a soluble cytoplasmic protein that requires the holin to access the cell wall. The holin is a small membrane protein that forms lesions in the inner membrane of the host cell, allowing the endolysin access to its substrate, the cell wall. The process of lesion formation will be called "hole formation" in this work, although the nature of the holin-induced lesion is not understood at the molecular or cytological level. The holin accumulates in the inner membrane without harming the host until, at an allele-specific time, the lesion is formed and the endolysin is released to degrade the cell-wall, and subsequently cause the host cell to lyse. Hole formation occurs suddenly, without prior deterioration in membrane integrity or the proton motive force (pmf), and precedes lysis by only the few seconds it takes for the released endolysin to degrade the cell wall (38). Hole formation can be effected prematurely by depleting the pmf, either by stopping the aeration of a culture in which cells are expressing the holin, or by adding an energy poison such as dinitrophenol (DNP) or potassium cyanide (KCN). In any case, the timing of host cell lysis, and thus the release of progeny, is determined by the kinetics of hole formation, a parameter that is uniquely defined by the primary structure of the holin protein.

The bacteriophage λ lysis cassette

For bacteriophage lambda (λ), the lysis genes are found in a cluster immediately downstream of the late ($P_{R'}$) promoter (Figure 1.1). The *S* gene encodes two proteins of opposing function: the 105 residue holin (S105), which has three transmembrane domains (TMDs) and a predicted N-terminus-out, C-terminus-in topology, and the 107 residue antiholin, S107 (34) (Figure 1.2). This "dual start motif", where both the holin and antiholin are expressed from the same coding sequence with only small differences in the resulting proteins, occurs in many dsDNA phage genomes, although λS was the

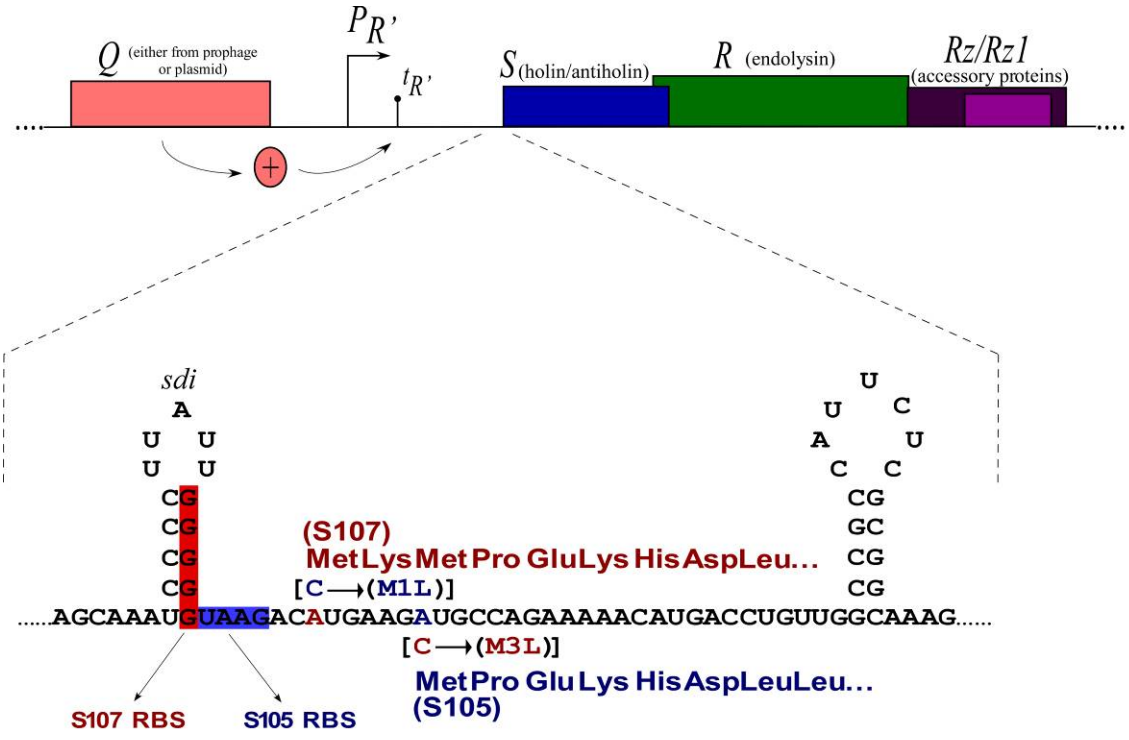

Figure 1.1. The λ lysis cassette and dual start motif.

first example discovered and is the most well-characterized (11), and S105 is the prototype for the Class I holins (Figure 1.2). Excluding the antiholin, previous studies have failed to find any host (R. Young, unpublished data) or λ proteins (30) with which the holin interacts. It has been shown that lysis timing by S is a genetically programmed event; there are missense alleles of the S protein that exhibit lysis times ranging from 11 minutes to more than 2 hours (36-37, 43, R. White, et.al, unpublished data). A null mutation in S extends the vegetative cycle so profoundly that at least ten-fold more progeny accumulate intracellularly compared to the yield in a wild-type infection (80). No other λ gene has a comparable phenotype, indicating that S alone determines when the infection is terminated by killing of the host (60).

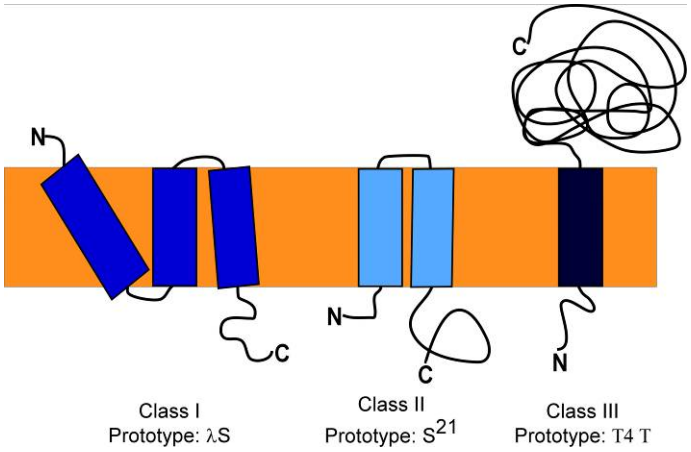

Figure 1.2. The three holin classes. Class I holins have 3 TMDs with N-out, C-in topology, Class II holins have 2 TMDS with N-in, C-in topology, and Class III holins have 1 TMD with N-in, C-out topology. The prototypes for each class are listed.

The *R* gene overlaps the *S* gene by 17 nts in a +1 reading frame. The R endolysin is a 158-residue, 17 kiloDalton (kDa) transglycosolase; it cleaves the MurNac-GlcNac

glycosidic linkage of the cell wall, releasing a non-reducing disaccharide (24, 86-87). The products of the accessory genes *Rz* and *Rz1* have no known function, and to date are only known to be required for lysis in the presence of divalent cations (78). Both Rz and Rz1 are required for lysis in the presence of divalent cations, and genetic evidence suggests that the two proteins interact (78). The *Rz* gene overlaps the *R* gene by 1 nucleotide, and the *Rz1* gene is entirely embedded in the *Rz* gene in a +1 reading frame. The normal lysis time of λ is approximately 50 minutes under standard laboratory conditions (LB medium at 37˚C with aeration), and yields approximately 100 virions per cell.

History of the* S *gene

The first mutations in *S* (*ts_{68}* and *ts_{9B}*) were isolated in 1967 by Harris et al., as a unique class of mutants that did not cause lysis of the host cell, but accumulated endolysin activity to normal levels (39). Interestingly, one of the mutants, *ts_{9B}*, showed a delay in normal lysis timing under permissive conditions and both mutants showed a significant increase in phage production (*ts_{68}* was found to be completely lysis defective) (39, 59). Mapping of these mutants and others isolated later indicated a previously unidentified cistron between the *Q* and *R* genes. (39, 59). The authors proposed that the product of this newly identified cistron must contribute to host cell lysis, and that the activity affected by the product of this gene is required for lysis of λ infected cells (39). This new gene was designated "*S*" (49). Non-sense *S* mutants isolated by Goldberg and Howe (most notably, λ*Ssus7*, later called λ*Sam7*) also exhibit the characteristics first

observed in *ts* mutants, and proved to be useful for isolating large quantities of λ DNA since they accumulate progeny to large excess (31, 59). Given that these mutations were suppressible, it was suggested that the product of the S gene was a protein. Since null mutations in *S* allowed cell growth to continue long after the normal lysis time, the effects of mutations in *S* on DNA synthesis and oxygen uptake were investigated (2, 59). It was determined that DNA synthesis continued to increase following the induction of an S^- lysogen, but decreased after induction of an S^+ lysogen. Expression of the *S* gene also caused cessation of oxygen uptake, which explained why a mutation in the *S* gene would allow the host cells to continue to grow. Since 1) termination of DNA replication and oxygen uptake did not occur immediately after the expression of *S* (2), 2) suppression of the non-sense mutants isolated by Goldberg and Howe required a strong amber suppressor (31), 3) the percentage of wild-type λ in a co-infection with a λ *S* mutant dictated the extent of lysis (59), and 4) *S*-mutant phage were inefficient in complementation tests (59), it was concluded that *S* gene dosage is important for its gene product function possibly because product accumulation was required for its function.

Later studies by Reader and Siminovitch (60) found that *S* gene expression lead to the cessation of host cell respiration, and were the first to show that lysis could be prematurely affected by the addition of an energy poison such as cyanide (CN^-) or 2,4-dinitrophenol (DNP) (60). Additionally, they showed that expression of *S* caused plasmolysis and treatment of these cells caused the cytoplasmic contents of the cells to leak out. Attempts to create spheroplasts from cells expressing *S* resulted in the immediate reduction of cells to debris. The authors concluded that the *S* gene product

physically alters the membrane to allow the endolysin access to the cell wall, and that this alteration, prior to the action of the endolysin, is necessary for lysis (60). This conclusion was validated by studies that indicated that release of periplasmic enzymes such as alkaline phosphatase require both S and R and that while the R product was present in cells expressing R but not S, it could not degrade the cell wall and cause release of periplasmic proteins in the absence of S (6). These studies also showed that the R product could cause lysis from the outside of the cell in the absence of S provided that the outer membrane was destabilized with ethylenediaminetetraacetic acid (EDTA). The authors concluded the inner membrane acted as a physical barrier to prevent R-dependent degradation of the cell wall, and that S eliminates this barrier to allow R access to its substrate. Interestingly, the authors also noted that the small release of periplasmic proteins seen in the induction of S^+R^- lysogen is probably due to the release of bacterial lytic enzymes when S damages the membrane (6), indicating that the inner membrane damage caused by S is at least somewhat non-specific.

Studies of the *S* gene by Rolfe and Campbell (8, 14, 63-64) seem to indicate that S had some interaction with TolB, either directly or indirectly. TolB is a component of a multi-protein complex that transports Group A colicins into cells, killing them (1). In a *tolB*$^-$ background, S was not necessary for lysis and λS^- phage exhibited a 1000-fold higher plating efficiency (e.o.p.) on *tolB*$^-$ strains than on *tolB*$^+$ strains. (8, 63). Further experiments showed that addition of chloramphenicol, like the addition of CN^- or DNP, could prematurely cause lysis of λ infected cells, but did so in both λS^+ and λS^- infections, and in λS^+ infections, the addition of chloramphenicol blocked the ability of

CN^- or DNP to cause premature lysis (14); in the *tolB*$^-$ background, however, chloramphenicol has no effect on lysis. Additionally, the authors note that shifting an induced lysogen to 48°C in the latter portion of the latent period causes premature lysis. Based on these results, the authors believed that t an inhibitor of S is also required for proper lysis function. λ*rex*, which was only known to mediate exclusion of phage T4 rII mutants at the time (48), was proposed to be the inhibitor, since the host mutants that allowed for λ*S*$^-$ phage to plate in the absence of suppression also hindered the exclusion of T4rII phage plating by λ*rex*$^+$ prophage. In their model, λ*rex* functioned to inhibit S-dependent lysis by creating an energy pathway with which the phage could coordinate intracellular processes, environmental conditions, and progeny production (14). Further efforts to characterize the function of λ*rex* in host cell lysis revealed that *rex* was not essential for lysis under normal laboratory conditions, but did affect timing under different growth conditions (64); however, similar effects in lysis timing were observed for other λ mutants. Experiments to further characterize a number of λ*S* and other mutants, as well as the effects of *λrex* and *tolB* on lysis timing, revealed no clear interaction between rex and S or tolB and S, although the authors conclude that the role of rex is to insulate the lysis regulator from factors that would disrupt lysis timing (therefore making it dispensable under normal growth conditions). Later studies of λ*rex* showed that the λ*rex* locus encodes two proteins, RexA and RexB (48), which function as a two component system to effect exclusion of other phage, and this exclusion is dependent on the ratio of the two proteins (53). RexB has also been show to interact with ClpP and to prevent the degradation of the λO protein. Given the multiple

functions of RexB, and the pleiotropic effects of *tol* mutations, it is likely that the *rex* phenotypes exhibited by the *tol* mutants tested had nothing to do with the *S* phenotypes exhibited, and instead were coincidental. Also, given that *tol* mutations have been shown to cause leakage of periplasmic proteins and to decrease the integrity of the cell envelope (7), it is likely that the compromised envelope of *tolB* mutants make them more fragile or more susceptible to the stress produced by the continuous production and accumulation of progeny phage, which would account for the phenotypes reported by Rolfe and Campbell (8, 14, 63-64). Nonetheless, this does not explain the reported ability of λ*S*⁻ phage to plate on other host mutants, such at *cya*, *uncA*, *mutU*, or *uvrD* (63), although these experiments have never been reproduced. It is likely that these mutants exhibit pleoitropic effects that allow λ*S*⁻ phage to plates. Experiments by Garrett et al. (29) using the cloned λ lysis cassette could not reproduce any of the effects of chloramphenicol on *S*⁻ cells, which suggested that the effect of chloramphenicol was caused by the deterioration of the host due to the stress of progeny production, rather than an independent lysis system. Furthermore, this study showed that lysis timing is solely dependent on the *S* gene since expression of the cloned lysis genes occurred in the absence of all other λ genes (i.e., λ*rex*). It did not, however, rule out the possibility that host proteins might affect S function (29).

Although these early studies postulated that S acted on the membrane, S was first formally proposed to be a 15 kDa membrane protein by 2-D PAGE (84), although later studies were unable to confirm the identity of the protein identified by 2-D PAGE, and instead showed that S was in fact an 8.5 kDa membrane protein (4-5, 87). Although this

apparent molecular weight is somewhat smaller than the predicted molecular weight, this irregularity can be accounted for by the highly hydrophobic nature of the protein, which can cause proteins to migrate at a lower apparent molecular weight on SDS-PAGE (5). S function was also shown to robustly inhibit active transport of α-methyl glycoside, proline, glutamine, and fructose in whole cells and membrane vesicles, and that inhibition occurred within minutes of lysis (84). Experiments using the cloned λ lysis cassette showed that PEP-phosphotransferase system dependent transport of glucose was also inhibited by S function (30). Additionally, S permeabilized the membrane to sucrose, glycine, sodium chloride (NaCl), and polyethylene glycol (PEG) 6,000, as well as the nucleotide pool and metabolic intermediates from inside of the cell. Notably, although S activity inhibited respiration, it does not do so by directly inhibiting the respiratory chain; rather, the leakage of components from inside the cell prevents the formation of NADH and thus interrupts electron transport. Assays of membrane protein activity in inverted membrane vesicles showed that activities for several membrane proteins required for respiration and energy production were unaffected by S, again indicating an indirect effect of S on respiration (84). The endolysin, R, is trapped inside the cell, as evidenced by the fact that it was not released by osmotic shock but was released by methods that damage the inner membrane. Thus, authors proposed that S formed a channel through the inner membrane, allowing the passage of the endolysin into the periplasm and leakage of the cytoplasmic contents (i.e., ATP and other molecules), thereby causing cessation of respiration. Importantly, the authors noted that this model allows for the accumulation of large amounts of endolysin in the cytoplasm,

which explained the ability of the phage to rapidly degrade the cell wall at the time of lysis, and that this would minimize the time of the progeny phage in a dead host (84). Based on the experiments using the cloned λ lysis cassette, it was also proposed that S must accumulate to a certain level in order to "trigger" lysis; that is, to effect lesion formation and allow release of the endolysin (30).

Previous experiments showed that S insertion into the membrane is independent of both the *sec* translocon and the proportion of acidic phospholipids in the inner membrane (61). These results, combined with the fact that no host proteins had been shown to interact with S, led to studies of lesion formation by S in different organisms. S was shown to be lethal in both *Saccharomyces cerevisiae* (29) and mammalian cells (3). Surprisingly, expression of *S* was lethal to both types of cells (29, 3). Biochemical analysis of these cells indicate that S is inserted in the membrane of yeast, as well as into the mitochondrial membranes and the endoplasmic reticulum of mammalian cells, confirming that S function requires insertion into the membrane. These results indirectly supported the notion that S does not require a host protein to function, although it is formally possible that a highly-conserved, essential protein might interact with S.

Once S was firmly established as a membrane protein essential for lysis, and that functioned by permeabilizing the membrane to allow the endolysin access to the cell wall, genetic studies were undertaken to explore the molecular mechanisms of S function (56, 57). These studies first focused on non-lethal alleles of *S*, since these were simple to isolate using the cloned λ lysis cassette. 34 alleles in 24 different codons, mostly clustered in the first two-thirds of the *S* coding sequence, were isolated, along with 2

nonsense mutations and 3 mutations in the region immediately upstream of the coding sequence. Analysis of these mutations revealed that the S protein most likely had 3 TMDs, with the N-terminus in the periplasm and the C-terminus in the cytoplasm, and although most of the mutations could be rationalized in terms of the resulting changes in polarity and charge, a number of the mutations could not be explained (56). All of these mutations, including those upstream of the coding sequence, were then recombined into λ in order to characterize them in the context of the phage, and to determine their effects on the wild-type protein when the two are co-expressed (57). Less than half of the alleles (75) isolated exhibited a negative dominant character, either partially or completely inhibiting the function of the wild-type. Fourteen of the alleles were recessive, having little or no effect on wild-type lysis timing. The remaining 7 alleles caused a synergistic phenotype – that is, they accelerated lysis timing more so than when two copies of the wild-type were expressed. Surprisingly, all three of the upstream mutations proved to be dominant (57). When these upstream mutations were first isolated, it was hypothesized that they resulted in decreased translation of S, causing them to be non-lethal (56). However, the dominance exhibited by the upstream mutations when co-expressed with the wild-type could not be explained by translational defects, and upon closer examination of the upstream region, it was proposed that there were actually two proteins produced from the coding sequence (57). The longer one, produced from Met1, was called S107, and the S107 ribosome binding sequence (GGGGG) was precluded in a stemloop structure called the *sdi* (site-directed initiation) stemloop. The shorter product, produced from Met3, was called S105, and the although

S105 ribosome binding site was unusual (UAAG), it could be used when the *sdi* stemloop structure was formed. The two proteins differed only by the Met_1-Lys_2 N-terminal extension on S107. These findings were strengthened by the *Met3Ile* mutation, since it exhibited a nearly complete loss of function, and the *Met1Leu* mutation, which was a more lethal allele (57). Interestingly, the authors explain the synergistic phenotype exhibited by some of the alleles by saying that the mutant protein(s) must interact with $S107_{wt}$ to titrate it out, leaving $S105_{wt}$ free to cause lysis (57). While this may explain the *in trans* effects of the mutant alleles that cause lysis slightly faster than the wild-type alone, it does not address those mutants that cause lysis as fast or faster than two copies of the wild-type; later studies invalidate the $S107_{wt}$ titration model (36).

Early attempts to determine the number of S molecules (S105 + S107) per cell yielded numbers ranging from the low hundreds to around 5,000 (17). The translation rate of S was determined to be approximately 0.85 molecules per minute per *S* mRNA, which is very low compared to other genes, such as β-galactosidase (17). The region upstream of the *sdi* stemloop is required for translation of the S proteins (16-17) since a deletion of that region, known as *Δ119*, causes a 10-fold decrease in the overall translation of S, and results in poor lysis more than 2.5 hours after induction. Since the wild-type reaches those same levels very early after induction, the authors hypothesize that hole formation requires both S accumulation and an appropriate rate of accumulation (17). Taken together, these results indicated that translation of the S gene is tightly controlled in order to limit the amount of S produced and the rate at which it accumulates.

λS_{A52V} (56-57), was used to isolate the first lytic timing mutant of S. When λS_{A52V} was plated, there were a few tiny plaques among the larger, presumably revertant, plaques (43). The phage (called λrj1) from these tiny plaques was isolated and used to make a lysogen. Induction of this prophage caused lysis at 20 minutes, significantly reduced burst size, and when the resulting lysate was plated, tiny to pinpoint plaques were observed. The premature lysis defect in λrj1 was mapped to the *S* gene, and sequencing revealed that the mutation was *A52G* (43). Further tests of this mutant indicated that the A52G mutation did not alter the expression rate of the *S* gene, nor did it affect the accumulation of S in the membrane (although the amount of S_{A52G} at the time of lysis was approximately 5-fold less than that of S_{wt}), and it was shown to be dominant over the wild-type. S_{A52G} could be prematurely triggered to cause lysis well before the S_{wt} could, indicating that the ability to form holes earlier than S_{wt} also conveys the ability to be prematurely triggered earlier (43). These results indicated that timing of lysis is regulated not only by the amount of S produced and the rate at which it accumulates, but also by the inter- and intra-molecular interactions of the S protein in the lesion-forming complex, which would be dictated by the amino acid sequence of the S protein.

The dual-start motif

The "dual-start motif", where one gene in a phage genome encodes both the holin and the antiholin and the two differ only by a few amino acids, one of which is positively charged, has been found in a number of phages (11); however, the best

characterized dual-start motif is that of phage λ. After the discovery of the *sdi* stemloop, subsequent studies characterized the two translational starts and their respective ribosome binding sites (9). In addition to the *sdi* stemloop, a second stemloop was found approximately 30 nucleotides (nt) downstream of the first translational start (Figure 1.1). It was confirmed that both methionine codons were used for initiation (both *in vivo* and *in vitro*) and the proteins produced by the Met1 and Met3 starts gave different phenotypes: S107 was not lytic, and S105 was lytic, and in the absence of S107 (produced by a *Met1Leu* mutation), S105 caused lysis slightly faster than S_{wt}. Further studies showed that both proteins were stable and could be detected in *in vivo* samples, and that both were membrane proteins (10). Additionally, toeprinting assays (16), which measure ribosome binding to mRNAs (40-41), showed that the predicted ribosome binding sites were corrected, despite the unusual sequence of the S105 ribosome binding site, and that the two stemloop structures directed initiation. Destabilizing the *sdi* stemloop by mutation, like the ones isolated by Raab et al. (56), increases the amount of S107 produced and thus affects lysis timing negatively (9). Destabilizing the downstream stemloop also increased the amount of S107 (17).

S107 was shown to act *in trans*, and that its antiholin character was dependent on the positive charge of the N-terminal extension (10). Energy poisons caused S107 to become lytic, indicating that the collapse of the membrane potential allowed it to cause hole formation. The authors postulated that S107 molecules would retard hole formation by interacting with S105 molecules until an oligomer sufficiently rich in S105 formed and caused the first pore. This pore formation would collapse the membrane potential,

thus both alleviating the block imposed by S107 and allowing S107 molecules to participate in hole formation (10). Increasing the positive charge of the N-terminal extension by either adding additional positively charged residues or by mutating the negatively charged residues to neutral ones created non-lytic alleles that could not be triggered to cause hole formation by the addition of energy poisons (76). Mutating the N-terminus so that the net charge was either neutral or negative resulted in S107 alleles that behaved as holins. These results indicated that the positive charges on the N-terminus of S107 prevented it from acting as a holin, and that the N-terminus of S107 plays an important role in the inhibition of S105. It was later shown that both S proteins require the N-terminus to be localized to the periplasm for hole formation (33-34), and that perhaps S107 has an altered topology due to the positive charge of the N-terminus (11, 34).

Since S107 causes inhibition *in trans*, it seemed that inhibition was caused by direct interactions between the holin and antiholin. Copper phenanthroline ($Cu(Ph_3)$) crosslinking was used to show that S107 preferentially heterodimerizes with S105, and that this heterodimerization is required for inhibition. Mutants of S107 that show decreased inhibition also show decreased crosslinking (35). Since S107 preferentially heterodimerizes with S105, the ratio of S105 to S107 would be important for regulating lysis time. Altering this ratio has already been shown to have effects on lysis timing, with too much S107 causing a delay in lysis and eliminating S107 altogether accelerates lysis slightly (9). Investigations of the ratio of S105 to S107 showed that, at the time of lysis, the ratio is approximately 2-2.5:1 (16-17). The studies also showed the ratio

apparently remained constant, which indicated that although the stemloop structures present in the *S* mRNA control the expression of *S*, there is no temporal regulation of the ratio of S105:S107 under standard laboratory conditions (17).

Although the regulation of *S* and the λ dual-start motif have been studied extensively (10-11, 16-17, 33-35, 76), little is known about the details of the S107 antiholin's role in λ lysis, and further studies are needed to elucidate the features of S107 that convey antiholin character and how it affects hole formation *in vivo*.

Studies of S105, the λ holin

More recent studies have focused on S105, the holin, since it is the effector of lysis. Given that no other phage proteins are involved in the timing of lysis (30), and that the inter- and intra-molecular interactions of S may play some role in the regulation of lysis timing (43), it seemed likely that S105 must oligomerize to affect lesion formation. Oligomerization studies using the cross-linker dithiobis(succinimidylpropionate) (DSP) showed that indeed S105 does oligomerize to at least octamers (the largest species detectable on SDS-PAGE) (36, 87) and that certain non-lytic mutants of S105, such as $S105_{A52V}$, are blocked after dimer formation. This indicated that oligomerization was necessary for hole formation, although since the mutant $S105_{R59C}$ showed an identical crosslinking pattern to that of $S105_{wt}$, oligomerization was not sufficient for hole formation (36). Experiments using the cysteine-specific crosslinker copper phenanthroline ($Cu(Ph_3)$) showed, using the native cysteine at position 51, that S105 homodimer formation is very strong. Using a

collection of single-cysteine mutants in TMD2, it was also shown that S105 homodimer formation is very strong on the opposite side of TMD2, since crosslinking occurred very efficiently between I53C and M50C, I53C, and I54C (36), indicating that interactions occur on both sides of the S105 molecule. This same set of single cysteine mutants demonstrated conclusively that regulation of lysis timing is programmed into the primary structure of the holin molecule; lysis times for the collection ranged from 20' ($S105_{C51S/S76C}$) to non-lytic (several alleles, including $S105_{C51S/A52C}$) (36). $Cu(Ph_3)$ crosslinking was also used to show that co-dominant alleles, such as $S105_{A52V}$, and synergistic alleles, such as $S105_{A48V}$, altered lysis timing of the wild-type by directly interacting with it. This nullified the previous hypothesis of $S107_{wt}$ titration since there was no S107 present in cells and because the direct interaction was shown biochemically (36). Additional testing of this collection using the cysteine-specific, membrane-impermeable reagent 4-acetamido-4'-((iodoacetyl)amino)stilbene-2,2'-disulfonic acid (IASD), revealed that S105 indeed has three TMDs with an N-terminus out, C-terminus in topology (37). Studies of the cytoplasmic S105 tail region indicated that although it was dispensable (62), the distribution of charges in that region can affect lysis timing, signifying that the C-terminal domain has a regulatory role in lysis timing, although for the most part, lysis timing is controlled by the three TMDs (12).

Early models of hole formation suggested that accumulation of S caused a leak of protons or other ions that depleted the pmf until the triggering point was reached; this, however, is not the case. A tethered cell assay, where cells are tethered to a glass slide via the flagella, was used to demonstrate that S105 causes sudden cell death, followed by

a few seconds of delay, after which the degradation of the peptidoglycan by R causes catastrophic lysis of the host cell (38). Since flagellar rotation is directly correlated to the pmf, the speed at which the cells rotate on the slide is correlated to their pmf (26-27). Tethered cells carrying the plasmid-encoded lysis cassette were induced and monitored. The rotational speed of the cells remained constant until they suddenly stopped a few seconds before lysis. The point at which they stopped corresponded to holin triggering, the delay between triggering and lysis was shown to be dependent on lysozyme activity (38). Additional experiments using DNP showed that holin triggering occurs when the pmf has been depleted 30% or more (38). These experiments were significant because they showed that the holin accumulates harmlessly until the time of triggering, leaving the host healthy for the entire span of the vegetative cycle. Furthermore, since they showed that triggering occurs rapidly when the membrane is fully depolarized, they explain the so-called "sentinel function" of the holin. A number of phages cause temporary depolarization of the membrane when they inject their DNA (32, 46); this depolarization would trigger the holin, causing lysis and thus releasing the progeny phage already accumulated and resulting in an abortive infection of the secondary infecting phage.

While much has been learned about the regulation of S and its function, almost nothing is known about the structure or size of the hole formed. Previous studies indicate that it is large enough to allow the membrane to be permeable to PEG-6,000 (84). The λ endolysin, R, has dimensions of 40 x 32 x 32 Å (24), and would require a hole size greater than 3 nm in diameter to be released into the periplasm. A fusion of R and β-

galactosidase (RΦlacZ), which forms a tetramer with a MW of approximately 500 kDa, was released efficiently from cells expressing *S105* or $S105_{A52G}$ (81). This indicated that although $S105_{A52G}$ produces much less protein than *S105*, the holes made by both proteins were at least large enough to release RΦlacZ, and that the holes must be at least 15 nm in diameter (81). Prematurely triggered S105 was unable to release RΦlacZ, which suggested that lesions formed by prematurely triggering the holin are smaller than those formed by normal holin triggering (81). Since the S protein is so small, and the holes formed by it appear to be very large, it was proposed that S must form two-dimensional arrays or "rafts" in the membrane, oligomerize, and then somehow effect hole formation (81).

Biochemical characterization of the S105 protein

Since studying the S105 protein biochemically required purified S105 protein, and S105 is a small and hydrophobic protein that is difficult to detect and lethal to cells, it was determined that affinity chromatography was the method of choice for purifying the S protein (72). Given the lethal nature of S at low concentrations (only 1,000 to 2,000 molecules per cell (17)), experiments were first conducted to see if over-expression of S was even possible. The *S* gene was cloned into a T7 over-expression vector and cells carrying the plasmid were infected with λCE6 (lambda carrying the T7 RNA polymerase gene) (71). Results showed a 100-fold increase in S protein compared to expression of S from the native λ context, and the yield from this over-expression was approximately 1 μg of S105 protein per ml of induced culture (71). Since the λ *R*, *Rz*

and *Rz1* gene are expressed in a λCE6 infection and this lead to lysis of the cells, it was determined that the BL21(DE3) cell line should be used instead, since the T7 RNA polymerase is under the control of the *lacUV5* promoter, and induction of that promoter with IPTG would not also induce the other lysis genes (77). Initial experiments showed that the basal level of *S* expression in these cells was toxic, but that fresh transformants could be grown in liquid culture and induced. Induction of *S* expression caused an almost immediate, dramatic and rapid drop in cell viability; and the S protein produced was found in the inner membrane fraction and the amount of S was much greater than the expression levels of *S* from λ (71). The ability of S to "hyperaccumulate" suggested that although there is a minimal rate of accumulation required for S function, significantly exceeding that rate does not cause the aggregation or oligomerization processes, or any conformational changes required to affect hole formation to proceed any faster. This lead to the conclusion that those steps required a minimum amount of time to occur (approximately 10 minutes) and that the minimum amount of time required was independent of the expression system (71). Attempts to insert a histidine-tag ($G_2H_6G_2$; His-tag; designated as "τ") into the S105 gene so that immobilized metal affinity chromatography (IMAC) could be used as the purification method yielded surprising results. Only the mutants with his-tag insertions at positions 94 and 88 showed lysis profiles that were similar to the wild-type, although several more were somewhat functional, and showed very late, slow lysis (73). Since the mutant $S105_{\tau 94}$ showed the lysis profile most similar to wild-type, it was chosen for further study. Following IMAC purification, purified S105 was used in a calcein-release assay; S105

was added to calcein-loaded liposomes and the release of calcein was monitored by the increase in fluorescence. This experiment showed that S105 did indeed cause release of calcein, and did so in a concentration dependent manner. The non-lytic mutant, $S105_{A52V}$, was also purified and assayed in this manner, and did not cause release of calcein (72), indicating that calcein-release by S105 is correlated to the *in vivo* ability to form holes.

One issue of the calcein release assay was that most of the S105 ended up in insoluble aggregates (72). In an effort to improve the assay, Deaton et al. showed that GroEL could solubilize large complexes of S105 and deliver them efficiently to calcein-loaded liposomes, and that the S105 delivered to the liposomes caused release of calcein in a concentration dependent manner (21). Further characterization of purified S105 showed that in non-ionic or mild zwitterionic detergent, S105 forms rings (67). The thickness of the rings is close to that of the bilayer (67), although the inner diameter of the rings is significantly smaller than that of the predicted hole formed by S105 (81). Based on protease accessibility studies, it was found that the tertiary structure of S105 in rings is similar to that of S105 in inverted membrane vesicles. While it is not clear that the rings are a physiologically relevant form of S105, it is clear that the ability to form rings is correlated to the *in vivo* ability to form holes (purified $S105_{A52V}$ does not form rings) (67), and thus may reveal important intermolecular interactions that are analogous to those formed in the bilayer.

Summary and goals

Although S105 is the most-studied holin to date, little is known about the nature of the lesion or its structure, or about the role of the antiholin in lesion formation. What is known about the holin can be summarized in a few sentences. The λS gene produces two proteins of opposing function from the same coding sequence, the holin, S105, and the antiholin, S107. Both are small membrane proteins, and the antiholin inhibits the holin by directly interacting with it. The two are produced at a 2-2.5:1 ratio (S105:S107). The holin is the only protein that controls the timing of lysis, although the normal amount of antiholin produced under standard laboratory conditions causes a slight delay, and lysis timing is programmed into the primary structure of the holin protein. Holin triggering is somehow tied to membrane polarization, in that it causes collapse of the pmf and artificially collapsing the pmf will cause holin triggering. The holin oligomerizes in the inner membrane, and this oligomerization is necessary but not sufficient for hole formation. The hole formed by S105 is larger than any other characterized transmembrane channel formed by alpha-helical proteins, and 1,000-2,000 molecules of holin are required for hole formation, although it is not known if there are many holes or one large one.

In light of these facts, the goals of this project are four-fold: to use mutational analysis to better understand the timing mechanism of holin triggering, to determine the feature of S107 that cause it to inhibit S105, to visualize the lesion formed by S105 in the inner membrane of *E. coli* cells and to elucidate the effects of the anti-holin on lesion

formation. The results from the experiments conducted in pursuit of these goals will be used to formulate a model of hole formation by λS.

CHAPTER II

MUTATIONAL ANALYSIS STUDIES

Introduction

The holin-endolysin system is used by all dsDNA phages to accomplish lysis of the host cell (86). In the case of bacteriophage λ, the endolysin is a soluble muralytic enzyme that is trapped in the cytoplasm and relies on the holin to allow it access to its substrate, the cell wall. Holins are small membrane proteins that form lesions in the inner membrane of the host cell, releasing the endolysin so that the peptidoglycan can be degraded and the progeny released (86). The holin is responsible for not only the release of the endolysin, but for timing the release such that a sufficient number of progeny have been assembled and potential other host cells remain in the environment for subsequent infections (86). The holin protein of λ, S105, is encoded by the λ*S* gene (Figure 2.1), and is the best-characterized holin to date. It is the prototype of the Class I holins and has been the subject of extensive genetic and biochemical characterization (86). Although S105 is very small, only 105 residues in length, it forms holes that are at least 15 nm in diameter; these holes are the largest known transmembrane channels formed by alpha helical proteins (81). This indicates that S105 must oligomerize, since it would take many molecules of S105 to form a lesion this large. S105 has, in fact, been shown to oligomerize (36, 87), and this oligomerization is required for hole formation (36). Additionally, crosslinking has been shown that S105 can form dimers via the

interactions of two faces of TMD2 (36), although a comprehensive study of TMD interactions has not yet been completed.

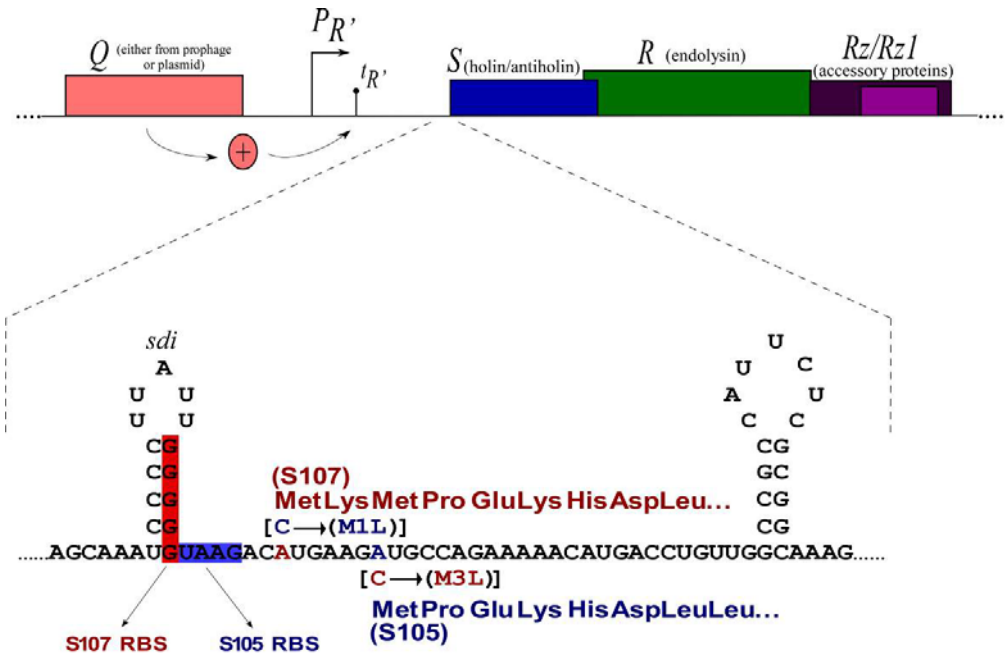

Figure 2.1. The λ lysis cassette and dual start motif.

The first genetic study of *S* found a number of non-functional mutants in all three TMDs of the protein, and that expressing these non-functional alleles *in trans* to the wild-type gave unpredictable results (57). This study also indicated that there was more than one protein produced from the S gene, further studies showed that the second protein functioned as an inhibitor of the holin (10, 35). The translation of these two proteins is controlled by a "dual-start" motif, where the longer product, S107 (the antiholin) is translated from Met1, and the shorter product, S105 (the holin), is translated

from Met3 (11) (Figure 2.1). One complication of the Raab et al. (57) study was that both the holin, S105, and the antiholin, S107, were expressed from both the wild-type phage and the mutant phage, making it difficult to determine which of the possible interactions was affecting lysis timing. Later studies of *S105* using site-directed mutagenesis to introduce single-cysteine mutations also showed that making mutations anywhere in the protein caused lysis times to vary (36-37), indicating that perhaps all three TMDs must interact in order to accomplish hole formation. Since none of the previous studies were comprehensive, however, the variations in lysis time caused by missense mutations could not be predicted. This study attempts to clarify and expand upon the results of Raab et al. (57) by introducing those mutations and others into pS105 via site-directed mutagenesis and characterizing their effects on lysis timing.

Materials and methods

Materials, strains, bacteriophage, plasmids, and growth media

All reagents were of the highest purity commercially available. The *E. coli* strain XL1Blue, the lysis-defective thermoinducible prophages *λΔSR,* and the lysis-proficient thermoinducible prophages λ*S105* (expressing *S105*) have been described previously (35, 57, 70, 73). The strains, phage, and plasmids used in this work are described in Table 2.1.

Table 2.1. Strains, phage and plasmids.

Strain, phage or plasmid	Genotype/features	Source or reference
Strains		
MC4100 *ΔtonA*	E. coli K-12 F$^-$ *araD139 Δ(argF-lac)U169 rpsL15relA1flbB3501 deo pstF25 rbsR ΔtonA*	Lab stock
MG1655 *ΔtonA lacI^q*	F$^-$ *ilvG rfb50 rph1 ΔtonA lacI^q*	Lab stock
MDS12 *ΔtonA*	MG1655 with 12 deletions, totaling 376,180 nt including cryptic prophages; *ΔtonA*	(45)
XL1Blue	E. coli K-12 *recA endA1 gyrA96 thi1 hsdR17 supE44 relA1 lac* [F' *proAB lacZΔM15::tn10*]	Stratagene
Phages		
λΔSR	*Δ(stf-tfa)::cat cI$_{857}$* Δ(*SR*)	(72)
λ*S105*	*Δ(stf-tfa)::cat cI$_{857}$ S$_{M1L}$*	(73)
Plasmids		
pQ	λQ cloned into pZS*24, *kan^R*	(38)
pS105	λ lysis gene region with *S$_{M1L}$* cloned into pBR322, *amp^R*	(36)
pS105$_{C51S}$	Same as pS105, but with *C51S* mutation	(37)
pKB1	Same as pS105, but with *Sam7* mutation	(36)

Media, growth conditions, IPTG induction and thermal induction of the λ lysis genes from a prophage and/or plasmid have been described previously (17, 37-38, 72). Bacterial cultures were grown in standard LB medium supplemented with ampicillin (100 μg/ml), kanamycin (40 μg/ml) and chloramphenicol (10 μg/ml) for the maintenance of plasmids and prophage, respectively. Lysis curves were repeated a

minimum of three times, and the lysis times listed in for each mutant in Table 2.2 are accurate within ± 1 minute.

Standard DNA manipulations, PCR, site-directed mutagenesis, and DNA sequencing

Isolation of plasmid DNA, DNA amplification by PCR, DNA transformation, and DNA sequencing were performed as previously described (37). Primers were obtained from Integrated DNA Technologies, Coralville, IA, and were used without further purification. Restriction and DNA-modifying enzymes were purchased from New England Biolabs; all reactions using these enzymes were performed according to the manufacturer's instructions. Site-directed mutagenesis was performed using the QuikChange kit from Stratagene as described previously (37). pS105 was used as the template for all primers, except the cysteine mutation primers (excluding A52C For/Rev). $pS105_{C51S}$ was used as the template for all of the cysteine mutation primers. Primers used for site-directed mutagenesis are listed in Appendix A. The DNA sequence of all constructs was verified by automated fluorescence sequencing performed at the Laboratory for Plant Genome Technology at the Texas Agricultural Experiment Station.

Generation of recombinant bacteriophage

Recombinant phage were constructed as follows: Plasmids were transformed into MDS12 *ΔtonA* (*λΔSR*) and individual transformants were grown up and induced as

previously described (37). Chloroform (final concentration, 1%) was added to the cultures 2 hours after induction, or when lysis was complete. Lysates were cleared by centrifugation (3,000 rpm in a clinical centrifuge) and used to reinfect early-log (A_{550} = 0.2) cultures of MDS12 *ΔtonA* at a multiplicity of infection (m.o.i.) of 5. Two hours after infection, chloroform was added and the lysate cleared. This enrichment step was repeated twice more, and the final lysate was used to lysogenize MC4100 *ΔtonA*. Lysogens were selected for by plating on LB plates containing chloramphenicol and were screened using Single Prophage PCR (SPP) (55) to determine which candidates contained a single prophage. These candidates were then cross-streaked against λ86 (λ^{imm434} c^- $R_{am54am60}$) to verify the presence of a functional endolysin; positive candidates were used for lysis curves and to create phage stocks.

TCA precipitation

1 ml or 5 ml culture aliquots were added to 111 µl or 555 µl, respectively, of cold, 6.1 N trichloroacetic acid, then placed on ice for 30 minutes. The precipitate was collected by centrifugation (15,000 rpm in a tabletop microcentrifuge or 3,000 rpm in a clinical centrifuge, respectively) and washed once with acetone, resuspending the pellet completely. Pellets were air-dried and resuspended in SDS-PAGE loading buffer. Proteins were separated on 16.5% SDS-PAGE with a 4% stacking gel. Western blotting and immunodetection with anti-S antibodies were performed as previously described (38).

Results

Comparison of induction systems

There are currently three ways to express the λ lysis genes from the native λ late promoter ($P_{R'}$): transactivation of pS105 or derivative via the pQ induction system, where the *Q* gene is under the control of the P_L*lac/ara* promoter on a low copy plasmid (38); transactivation of pS105 or derivative via production of Q from thermal induction of the λΔSR prophage (72); and thermal induction of a prophage if the *S* gene of interest has been recombined onto the phage genome (56). For lytic alleles of *S*, these three induction systems are roughly equivalent, although the rate of S accumulation differs causing different lysis times (Figure 2.2). For non-lytic alleles of *S*, however, these methods of induction are not equivalent, since membrane protein toxicity effects can mimic slow and inefficient lysis, thus making the rate of S accumulation very important when testing alleles with unknown lysis times. Accumulation of large amounts of the accessory proteins Rz and Rz1 is also toxic, which further complicates the analysis of non-lytic alleles. The membrane protein toxicity effects are seen most in the pQ induction system (data not shown), making it the least favorable of the three for testing new alleles of *S*. The labor- and time-intensive process of recombining alleles onto the phage genome creates a significant block to productively testing large numbers of alleles in a reasonable amount of time, so although it is the best method for testing alleles in terms of S accumulation rate, it is the least favorable in terms of feasibility of strain construction. Therefore, for the purposes of this study, the λ*ΔSR* transactivation system

was chosen, since it combines the ease of using plasmid-borne S alleles with near-prophage levels of S accumulation.

Figure 2.2. Western blot comparison of S105 protein expression systems. Lanes 1 and 18, molecular weight marker, lanes 2-7, λ*S105* samples taken at 0', 15', 30' 40', 45', and 50', respectively; lanes 8-11, λ*ΔSR* pS105 samples taken at 0' 15', 30', and 35', respectively; lanes 12-17, pQ pS105 samples taken at 0', 15', 30', 35', 40', 45' and 50', respectively; lane 14, molecular weight marker. Lysis occurs at ~50' for λS105, 35' for λ*ΔSR* pS105, and 45' for pQ pS105.

Lysis timing in S105 mutants

101 S105 mutants were created and their lysis times tested (Table 2.2). Among the alleles were those first isolated by Raab et al. (56) and those created by Zheng et al. (89) using site-directed mutagenesis (alleles were chosen by a randomizing computer algorithm). Two sets of alleles were created by mutating positions 51 and 52 to all possible amino acids. Additional mutants were chosen at random.

For the position 51 and 52 series, analysis of lysis times (listed in Table 2.2; Figure 2.3) yielded no patterns for the effects of substitutions on lysis timing. Although the obvious characteristics of amino acids – size, volume, hydrophobicity – were plotted against lysis time, no patterns were of lysis time were revealed. A similar mutation series of positions 49 and 50 are currently being created and characterized.

Dominance/recessiveness of S105 alleles

Raab et al. (57) tested the dominance/recessiveness of the alleles they isolated by making lysogens with double prophages; one prophage carried the wild-type *S* gene, and the other the mutant allele. Since the large number of mutants in this study made using double prophages unfeasible, we used λ*S105* with $pS105_{mut}$ *in trans* for the dominance/recessiveness studies. Like Raab et al., we also found four classes of mutants: dominant, co-dominant, recessive, and synergistic (phenotypes are listed in Table 2.2 for the alleles tested); the dominant class can be split into the lytic dominant alleles and the non-lytic dominant alleles. One example of each is shown in Figure 2.4. One caveat of these experiments, especially for mutants that reveal a dominant phenotype, is since the mutants are expressed from the plasmid and the wild-type is expressed from the prophage, the mutants will have a slight advantage in accumulation, assuming that the mutation present does not affect the translation rate of the mutant protein.

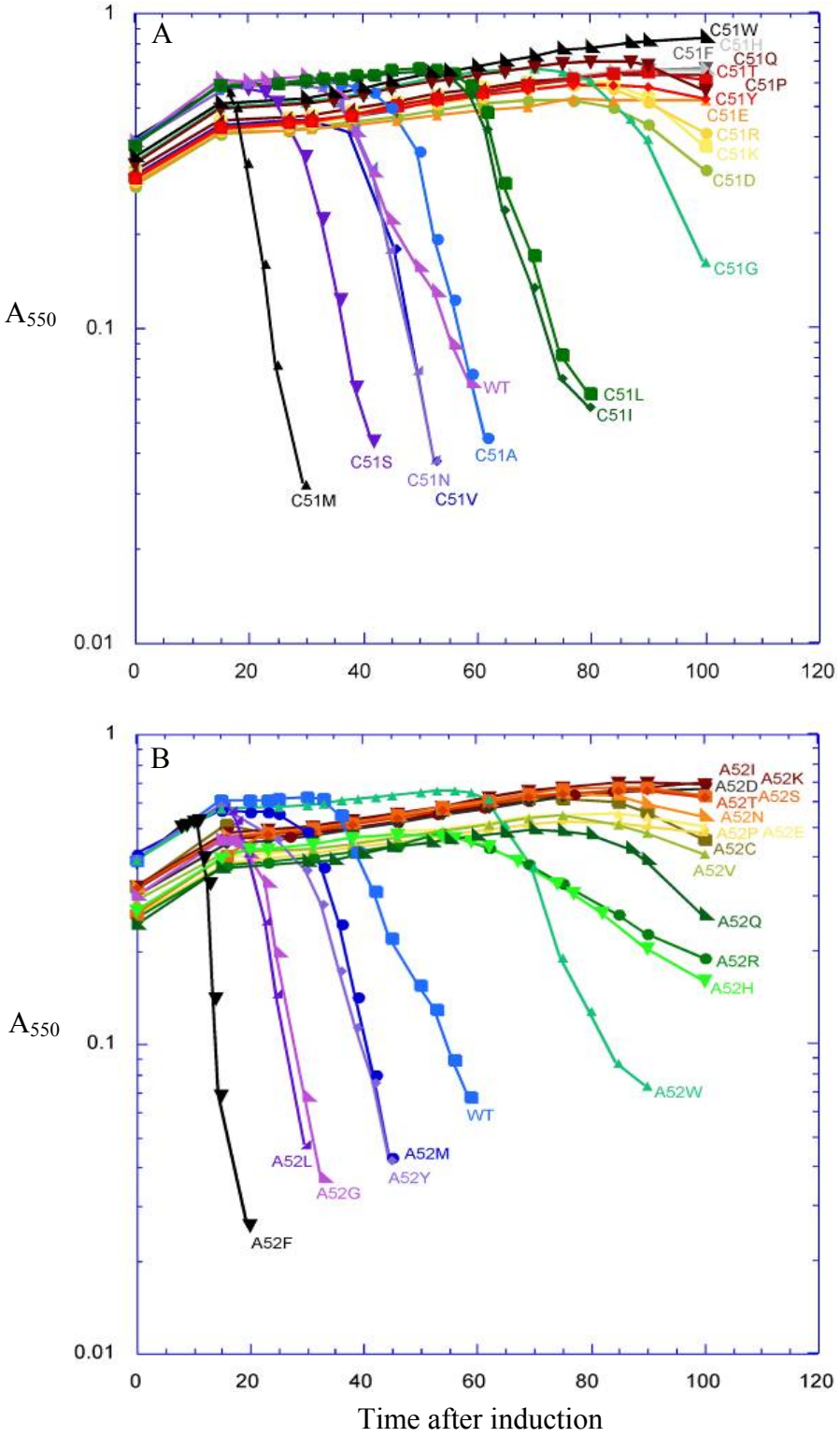

Figure 2.3. Lysis curves of position 51 and 52 mutant series. Mutations are labeled on the graph. A, Position 51 series. B, Position 52 series. No pattern of lysis time vs. substitution was observed.

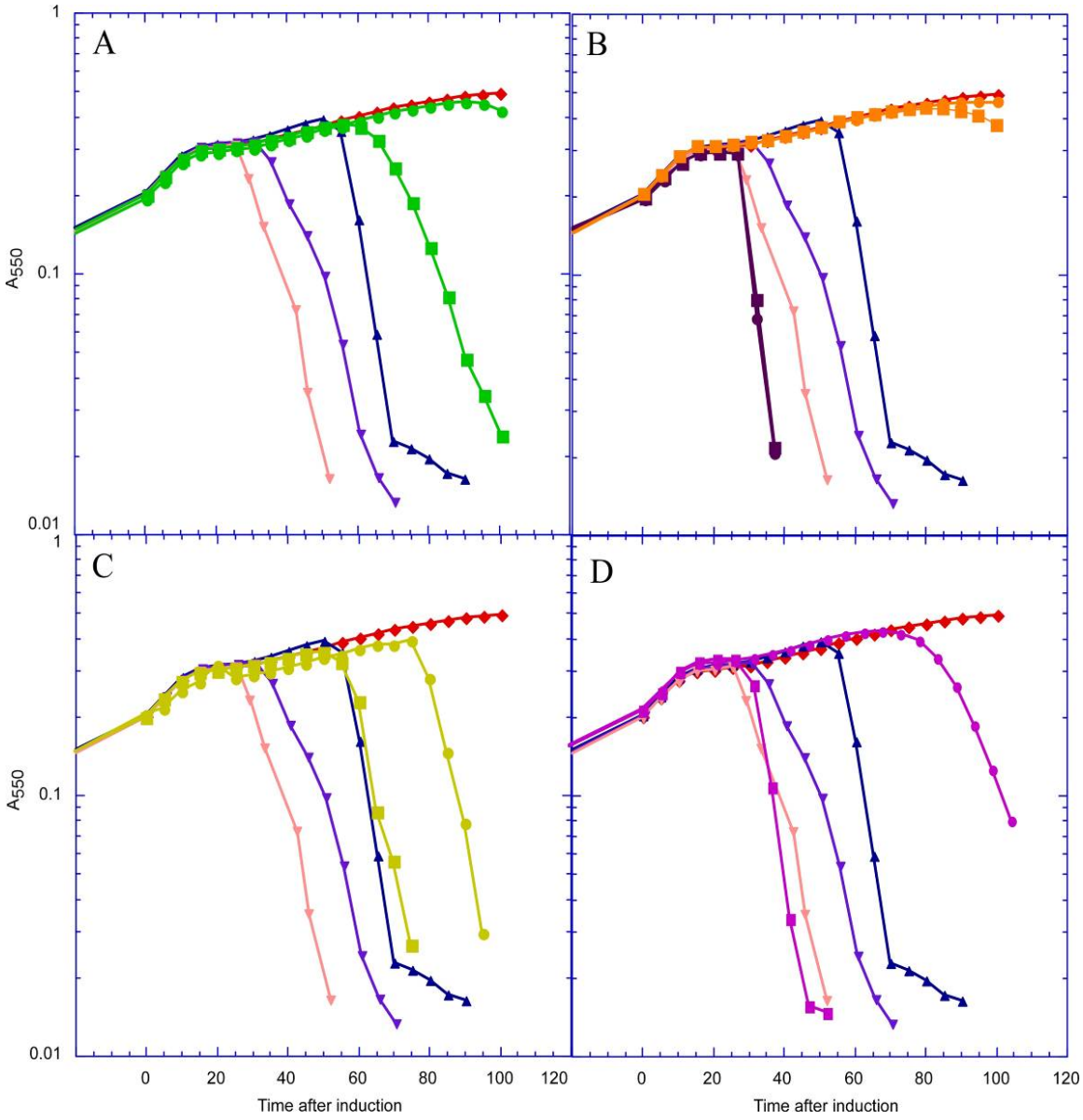

Figure 2.4. Examples of co-dominant, dominant, recessive and synergistic mutants in S105. In each panel, the controls are (♦) λ*ΔSR* + pKB1, (▲) λ*S105* + pKB1, (▼) λ*ΔSR* + pS105, and (▼) λ*S105* + pS105; and the mutants are (●) λ*ΔSR* + $pS105_{mut}$, (■) λ*S105* + $pS105_{mut}$. Panel A, co-dominant mutant I87Y, panel B, dominant lytic mutant G66E in purple, dominant non-lytic mutant I53Y in orange, panel C, recessive mutant R59H, panel D, synergistic mutant M50G.

Table 2.2. Lysis times of mutants and phenotypes *in trans* to $S105_{wt}$.

Codon	Mutant	Lysis time (λ*ΔSR*)	Lysis time (λ*S105*)	Phenotype *in trans* to wt	Raab et. al. phenotype (57)
3	M1L	30’	25’	--	--
12	A12T	30’	35’	cD	--
16	A16N	30’	30’	D(l)	--
18	E18K	non-lytic	non-lytic	D(n)	(S)
21	I21T	25’	25’	D(l)	--
22	G22R	non-lytic	non-lytic	D(n)	cD
22	G22W	non-lytic	60’	cD	cD
22	G22E	20’	25’	cD	S
23	A23T	80’	55’	cD	R
23	A23V	non-lytic	non-lytic	D(n)	R
25	L25G	non-lytic	70’	cD	--
25	L25V	non-lytic	non-lytic	D(n)	R
28	A28T	25’	25’	D(l)	--
29	M29I	72’	45’	(S)	R
30	A30S	38’	55’	cD	R
30	A30V	non-lytic	non-lytic	D(n)	S
31	Y31I	30’	30’	D(l)	--
33	R33C	non-lytic	non-lytic	D(n)	cD
33	R33H	non-lytic	non-lytic	D(n)	D(n)
33	R33L	non-lytic	non-lytic	D(n)	cD
34	G34S	non-lytic	non-lytic	D(n)	cD
35	R35K	non-lytic	55’	cD	--
38	G38S	non-lytic	non-lytic	D(n)	cD
39	G39D	20’	16’	S	S
39	G39V	23’	22’	D(l)	--
47	D47Y	non-lytic	35’	(S)	S
48	A48T	non-lytic	25’	S	(S)
48	A48V	non-lytic	40’	(S)	S
50	M50A	non-lytic	22’	S	--
50	M50G	70’	25’	S	--
50	M50I	90’	50’	R	R
51	C51A	36’	22’	S	--
51	C51D	77’ (slow)	35’	S	--
51	C51E	non-lytic	45’	(S)	--
51	C51F	non-lytic	45’	(S)	--
51	C51G	70’	47’	S	--
51	C51H	non-lytic	24’	S	--
51	C51I	53’	27’	S	--

Table 2.2. Continued

Codon	Mutant	Lysis time (λ*ΔSR*)	Lysis time (λ*S105*)	Phenotype *in trans* to wt	Raab et. al. phenotype (57)
51	C51L	53’	25’	S	--
51	C51M	16’	16’	D(l)	--
51	C51N	30’	25’	S	--
51	C51P	non-lytic	37’	(S)	--
51	C51Q	non-lytic	25’	S	--
51	C51R	non-lytic	50’	R	R
51	C51S	25’	25’	D(l)	--
51	C51T	non-lytic	45’	(S)	--
51	C51V	33’	24’	S	--
51	C51W	non-lytic	50’	R	--
51	C51Y	non-lytic	40’	(S)	S
52	A52C	80’ (slow)	55’ (slow)	cD	--
52	A52D	non-lytic	non-lytic	D(n)	--
52	A52E	non-lytic	50’	R	--
52	A52F	11’	11’	D(l)	--
52	A52G	17’	17’	D(l)	--
52	A52H	53’ (slow)	50’	R	--
52	A52I	non-lytic	55’	cD	--
52	A52K	non-lytic	52’	R	--
52	A52L	15’	17’	D(l)	--
52	A52M	23’	25’	cD	--
52	A52N	non-lytic	non-lytic	D(n)	--
52	A52P	non-lytic	45’	(S)	--
52	A52Q	75’ (slow)	38’	(S)	--
52	A52R	53’ (slow)	55’	cD	--
52	A52S	non-lytic	75’ (slow)	cD	--
52	A52T	non-lytic	non-lytic	D(n)	--
52	A52V	non-lytic	non-lytic	D(n)	R
52	A52W	60’	30’	S	--
52	A52Y	15’	15’	D(l)	--
53	I53Y	non-lytic	non-lytic	D(n)	--
55	A55T	70’	30’	S	S
56	W56S	non-lytic	non-lytic	D(n)	--
56	W56Y	21’	19’	D(l)	--
56	W56am (Sam7)	non-lytic	50’	R	R
59	R59C	non-lytic	50’	R	cD
59	R59H	75’	50’	R	cD

Table 2.2. Continued

Codon	Mutant	Lysis time (λ*ΔSR*)	Lysis time (λ*S105*)	Phenotype *in trans* to wt	Raab et. al. phenotype (57)
59	R59L	60’	35’	cD	--
60	D60N	non-lytic	57’	cD	cD
62	L62F	75’	35’	cD	(S)
66	G66E	25’	25’	D(l)	--
71	L71F	55’	50’	R	(S)
72	A72C*	50’	15’	S	--
73	Y73C*	80’	15’	S	--
73	Y73F	non-lytic	non-lytic	D(n)	--
73	Y73T	10’	15’	cD	--
75	T75C*	24’	18’	S	--
76	S76C*	20’	20’	D(l)	--
77	V77T	35’	35’	D(l)	--
78	F78G	20’	20’	D(l)	--
79	I79C*	90’	15’	S	--
80	G80C*	75’	35’	(S)	--
80	G80S	non-lytic	non-lytic	D(n)	cD
83	G83D	72’	50’	R	R
83	G83I	non-lytic	non-lytic	D(n)	--
87	I87Y	non-lytic	65’	cD	--
88	G88K	non-lytic	non-lytic	D(n)	--
89	S89C*	20’	19’	D(l)	--
99	A99C*	22’	15’	S	--
101	V101T	35’	35’	D(l)	--
102	E102K	37’	38’	D(l)	R
104	G104C*	35’	22’	S	--
108C	108C*	22’	18’	S	--

*These mutants also have the mutation *C51S*. Key: items in blue need to be tested for dominance/recessiveness, items highlighted in fuchia have not been tested yet; D(l) = lytic dominant, D(n) = non-lytic dominant, cD = codominant, R = recessive, S = synergistic (as fast or faster than λS105 + pS105, or, in the case of G108C, faster than G108C alone); (S) = slightly synergistic (causes lysis faster than a recessive allele, but not as fast as a synergistic).

Discussion

Although many mutants of S105 were tested, analysis of the effects of any given substitution on lysis time revealed no significant patterns. It is not surprising that for the more-or-less random collection of mutants originally isolated by Raab et al. (56) or Zheng et al. (89) there was no pattern observed. However, it is striking that for the position 51 and 52 series of mutants, where those positions were mutated to the other 19 amino acids, that no pattern was observed. Regardless, since the collection of mutations contains mutants on all faces of all three TMDs (Figure 2.5), and all of the mutations affect lysis timing, analysis of these mutants is valuable. The results indicated that the three helices of S105 must interact, probably via helix-packing, to accomplish lesion formation. Additionally, since mutations at the same position have dramatic and unpredictable effects on lysis timing, the TMDs may interact with multiple partner helices via either intra-molecular or inter-molecular interactions, to accomplish lesion formation. It is already known that TMD2 interacts inter-molecularly with other TMD2s at different faces, based on $Cu(Ph_3)$ crosslinking (36). It is possible, then, that interfering with one interaction, for example, between TMD2 of one molecule and TMD2 of another, might not interfere with another interaction, perhaps between TMD2 and TMD3 of the same molecule; the reverse may also be true. Changing a single amino acid may therefore interfere with interactions between one or more partner helices, and whether the substitution influences one or multiple interactions may influence the severity of the phenotype. Also, the severity of the phenotype may depend on the importance of the interaction(s) interrupted. Since S is known to oligomerize (37, 87),

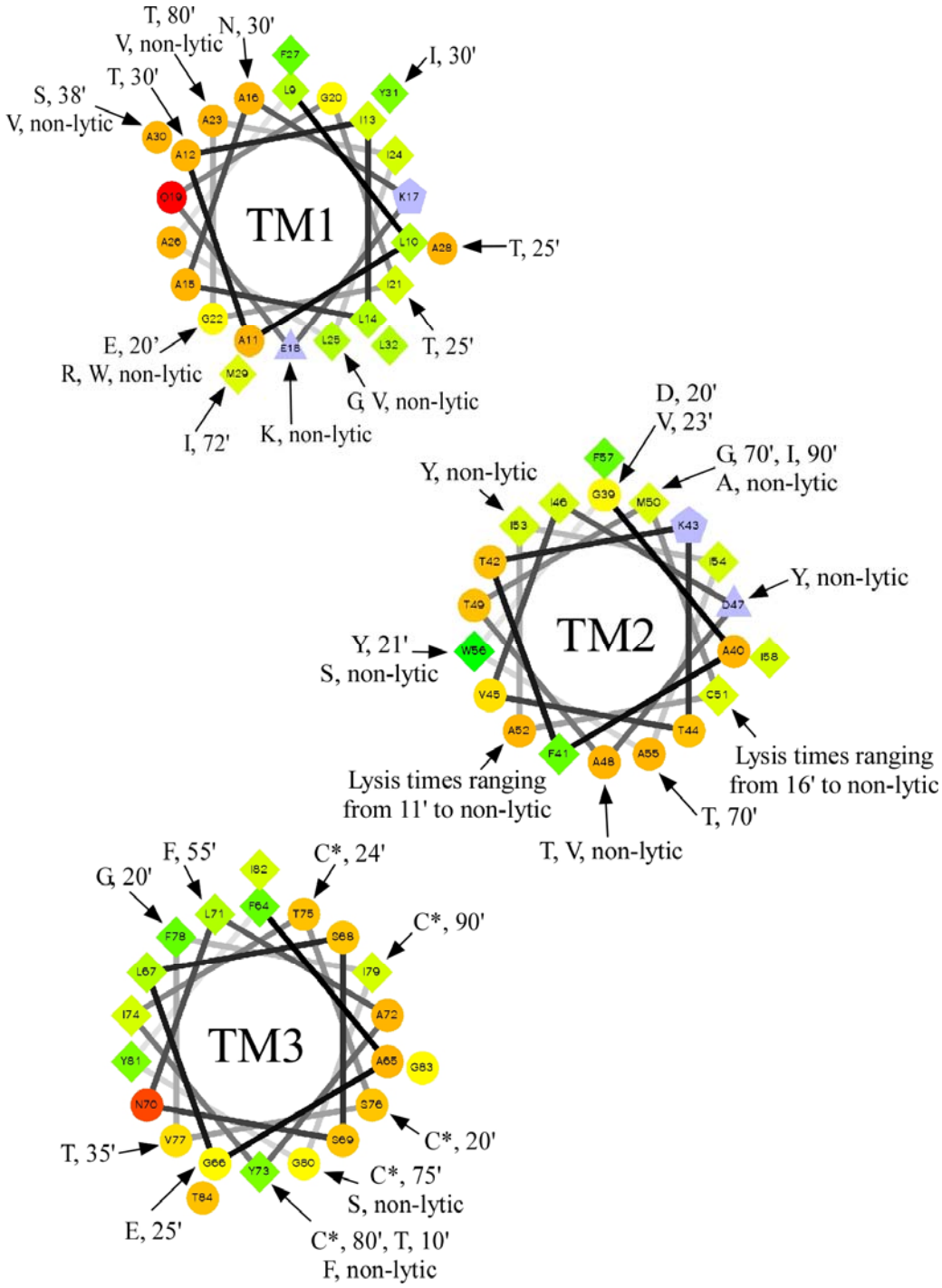

Figure 2.5. Helical wheel diagrams of the three TMDs of S105. Mutations are indicated with their corresponding lysis times. For simplicity, only a few of the position 51 and 52 mutants are indicated.

substitutions that affect the various stages of oligomerization, either impeding them or enhancing them, may have drastic affects. For example, Western blot analysis of the non-lytic $S105_{G83I}$ mutant shows that it forms SDS-resistant dimers and that very little monomer can be detected (89). This indicates that the *Gly83Ile* substitution highly enhances the interactions that lead to dimer formation, and presumably impedes the formation of higher oligomers, since this allele is non-lytic. However, since this allele is dominant to the wild-type, and Western blot analysis shows that wild-type S105 does not form SDS-resistant heterodimers with $S105_{G83I}$ (data not shown), it is probable that the enhancement of dimer interactions is not required for the non-lytic phenotype exhibited by the $S105_{G83I}$.

In the dominance/recessiveness test, the mutants fall into four classes: dominant, co-dominant, recessive, and synergistic; the dominant class can be split into the lytic dominant mutations and the non-lytic dominant mutations. For the co-dominant and synergistic classes, as well as for the non-lytic dominant mutants, it is clear that the wild-type and the mutant proteins interact, since an intermediate lysis time is observed in the presence of the wild-type for the co-dominant and synergistic classes, and no lysis time is observed for the non-lytic dominant alleles even in the presence of the wild-type. It appears that for the lytic dominant and recessive alleles, however, that the wild-type and the mutant form two separate pools of S105 molecules, and these pools do not influence each other (assuming, in the case of the recessive mutants, that the protein accumulates normally). This may mean that these mutants (or the wild-type) have a higher self-affinity, and a lower affinity for the other S105 protein being expressed. One

observation worth of note is that most of the lytic dominant alleles are "fast" lysers – that is to say, that they cause lysis much earlier than the wild-type. It is also interesting to note that although the antiholin was absent in this study, most of the mutants had the same phenotype (11 alleles) or a slightly more negative phenotype (15 alleles) *in trans* $S105_{wt}$ when compared to the Raab et. al. (57). Given that the mutant S105 has a slight expression advantage over the wild-type in this expression system, it is not surprising that mutants identified as co-dominant by Raab et. al. (57) exhibit a more negative effect on the wild-type, or that mutants identified as recessive or synergistic by Raab et. al (57) exhibit a more synergistic effect on wild-type. Mutants that were identified as co-dominant in both studies also exhibit a stronger effect on the wild-type, again probably due to the expression advantage of the mutants. A few mutants were identified as recessive in both studies; a simple explanation for this would be that the protein does not accumulate normally; however, at least one of these proteins, $S105_{G83D}$, accumulates normally (data not shown), supporting the idea that $S105_{G83D}$ and $S105_{wt}$ do not interact. Further studies, using $Cu(Ph_3)$ crosslinking to determine the extent of heterodimer formation between wild-type and either lytic dominant or recessive alleles, are currently underway (20).

Previous studies suggested that all three TMDs interact to affect hole formation; the data presented here support that assertion and suggest that both intermolecular and intramolecular interactions are important for hole formation, and that those interactions influence each other. To test this hypothesis, we are currently attempting to isolate intragenic suppressor mutations; if a mutation only affects one interaction, mutations

that restore that interaction should be easy to isolate. If a mutation disrupts multiple interactions, multiple intragenic suppressors at different locations in the gene should be isolated. However, given that a large number of changes in the same codon can restore lysis (approximately half of both the position 51 and 52 mutants are lytic), mutants will have to be carefully chosen to minimize the possible number of lytic alleles that will arise from reversion of the mutated codon; an example set of possible reversions is shown in Table 2.3. Preliminary results from Dankenbring et. al. (20) show that the apparent reversion rate of an allele corresponds to the number of possible single base mutations that would result in a lytic allele (i.e., the larger the number of possible lytic alleles, the higher the apparent reversion rate). Studies of previously isolated intragenic suppressors (74) are currently underway (20), as are studies of the position 49 and 50 mutant series as well as cysteine scanning studies to probe interactions between all three TMDs.

Table 2.3. Possible (pseudo)revertants of non-lytic C51 and A52 mutants by single base changes.

Codon	Mutant	Lysis time (λ*ΔSR*)	Codon	Mutant	Lysis time (λ*ΔSR*)
TTT	C51F	non-lytic	CCA	A52P	non-lytic
CTT	C51L	53’	TCA	A52S*	non-lytic
ATT	C51I	53’	ACA	A52T	non-lytic
GTT	C51V	35’	GCA	wt	30’
TCT	C51S	25’	CTA	A52L	11’
TAT	C51Y	non-lytic	CAA	A52Q	75’ (slow)
TGT	wt	30’	CGA	A52R	53’ (slow)
TTC	C51F	non-lytic	CCT	A52P	non-lytic
TTA	C51L	53’	CCC	A52P	non-lytic
TTG	C51L	53’	CCG	A52P	non-lytic
TAT	C51Y	non-lytic	ATC	A52I	non-lytic
CAT	C51H	non-lytic	TTC	A52F	11’
AAT	C51N	30’	CTC	A52L	15’
GAT	C51D	77’ (slow)	GTC	A52V	non-lytic
TTT	C51F	non-lytic	ACC	A52T	non-lytic
TCT	C51S	25’	AAC	A52N	non-lytic
TGT	wt	30’	AGC	A52S*	non-lytic
TAC	C51Y	non-lytic	ATT	A52I	non-lytic
TAA	stop	non-lytic	ATA	A52I	non-lytic
TAG	stop	non-lytic	ATG	A52M	23’
CCC	C51P	non-lytic	ACA	A52T	non-lytic
TCC	C51S	25’	TCA	A52S*	non-lytic
ACC	C51T	non-lytic	CCA	A52P	non-lytic
GCC	C51A	36’	GCA	wt	30’
CTC	C51L	53’	ATA	A52I	non-lytic
CAC	C51H	non-lytic	AAA	A52K	non-lytic
CGC	C51R	non-lytic	AGA	A52R	53’ (slow)
CCT	C51P	non-lytic	ACT	A52T	non-lytic
CCA	C51P	non-lytic	ACC	A52T	non-lytic
CCG	C51P	non-lytic	ACG	A52T	non-lytic
CAT	C51H	non-lytic	AAC	A52N	non-lytic
TAT	C51Y	non-lytic	TAC	A52Y	15’
AAT	C51N	30’	CAC	A52H	53’ (slow)
GAT	C51D	77’ (slow)	GAC	A52D	non-lytic
CTT	C51L	53’	ATC	A52I	non-lytic
CCT	C51P	non-lytic	ACC	A52T	non-lytic

Table 2.3. Continued

Codon	Mutant	Lysis time (λ⊿*SR*)	Codon	Mutant	Lysis time (λ⊿*SR*)
CGT	C51R	non-lytic	AGC	A52S*	non-lytic
CAC	C51H	non-lytic	AAT	A52N	non-lytic
CAA	C51Q	non-lytic	AAA	A52K	non-lytic
CAG	C51Q	non-lytic	AAG	A52K	non-lytic
CAA	C51Q	non-lytic	AAA	A52K	non-lytic
TAA	stop	non-lytic	TAA	stop	non-lytic
AAA	C51K	77’ (slow)	CAA	A52Q	75’ (slow)
GAA	C51E	non-lytic	GAA	A52E	non-lytic
CTA	C51L	53’	ATA	A52I	non-lytic
CCA	C51P	non-lytic	ACA	A52T	non-lytic
CGA	C51R	non-lytic	AGA	A52R	53’ (slow)
CAC	C51H	non-lytic	AAT	A52N	non-lytic
CAT	C51H	non-lytic	AAC	A52N	non-lytic
CAG	C51Q	non-lytic	AAG	A52K	non-lytic
CGC	C51R	non-lytic	AGC	A52S*	non-lytic
TGC	wt	30’	TGC	A52C	80’ (slow)
AGC	C51S	25’	CGC	A52R	53’ (slow)
GGC	C51G	70’	GGC	A52G	17’
CTC	C51L	53’	ATC	A52I	non-lytic
CCC	C51P	non-lytic	ACC	A52T	non-lytic
CAC	C51H	non-lytic	AAC	A52N	non-lytic
CGT	C51R	non-lytic	AGT	A52S*	non-lytic
CGA	C51R	non-lytic	AGA	A52R	53’ (slow)
CGG	C51R	non-lytic	AGG	A52R	53’ (slow)
ACA	C51T	non-lytic	GTC	A52V	non-lytic
TCA	C51S	25’	TTC	A52F	11’
CCA	C51P	non-lytic	CTC	A52L	15’
GCA	C51A	36’	ATC	A52I	non-lytic
ATA	C51I	53’	GCC	wt	30’
AAA	C51K	77’ (slow)	GAC	A52D	non-lytic
AGA	C51R	non-lytic	GGC	A52G	17’
ACT	C51T	non-lytic	GTT	A52V	non-lytic
ACC	C51T	non-lytic	GTA	A52V	non-lytic
ACG	C51T	non-lytic	GTC	A52V	non-lytic

Table 2.3. Continued

Codon	Mutant	Lysis time (λ*ΔSR*)	Codon	Mutant	Lysis time (λ*ΔSR*)
GAA	C51E	non-lytic	GAT	A52D	non-lytic
TAA	stop	non-lytic	TAT	A52Y	15’
CAA	C51Q	non-lytic	CAT	A52H	53’ (slow)
AAA	C51K	77’ (slow)	AAT	A52N	non-lytic
GTA	C51V	33’	GTT	A52V	non-lytic
GCA	C51A	36’	GCT	wt	30’
GGA	C51G	70’	GGT	A52G	17’
GAT	C51D	77’ (slow)	GAC	A52D	non-lytic
GAC	C51D	77’ (slow)	GAA	A52E	non-lytic
GAG	C51E	non-lytic	GAG	A52E	non-lytic
TGG	C51W	non-lytic	GAA	A52E	non-lytic
CGG	C51R	non-lytic	TAA	stop	non-lytic
AGG	C51R	non-lytic	CAA	A52Q	75’ (slow)
GGG	C51G	70’	AAA	A52K	non-lytic
TTG	C51L	53’	GTA	A52V	non-lytic
TCG	C51S	25’	GCA	wt	30’
TAG	stop	non-lytic	GGA	A52G	17’
TGT	wt	30’	GAT	A52D	non-lytic
TGC	wt	30’	GAC	A52D	non-lytic
TGA	stop	non-lytic	GAG	A52E	non-lytic

*The allele *Ala52Ser* lysis at 156’ when recombined into λ. This highlights a caveat of using the λΔSR system for determining lysis times; because of toxicity caused Rz and Rz1 expressed from the plasmid, it is not possible to correctly determine lysis times after t = 100’ in this expression system, meaning that some alleles that cause lysis very late will be called non-lytic.

CHAPTER III

ANTIHOLIN STUDIES

Introduction

To achieve saltatory lysis of their hosts, double-stranded DNA bacteriophage rely upon a system with two essential components, a holin and an endolysin. Holins are small membrane proteins which form lesions in the cytoplasmic membranes of their hosts and thereby control access of the endolysin to its substrate, peptidoglycan. The holin protein accumulates in the cytoplasmic membrane throughout late gene expression, without measurable effect on the host. Then, at a time determined by its primary structure, the holin suddenly triggers to permeabilize the membrane, allowing a phage-encoded muralytic enzyme (endolysin) to degrade the cell wall. Lysis of the host occurs within seconds of holin triggering (38).

The best characterized holin gene is the *S* gene of phage λ, which directs the synthesis of two proteins, S105 and S107 (figure 3.1A). S105 results from translational initiation at Met3 of the 107 codon open reading frame of *S* and has been shown to have the membrane disrupting activity expected of a holin. The S105 protein has been shown to have three TMDs with its N-terminus in the periplasm and its C-terminus in the cytosol (figure 3.1B). Remarkably, the full length product of *S*, S107, has an opposing function despite differing from S105 by just the amino-terminal extension, Met-Lys. S107 is a specific inhibitor of S105, acting to delay the triggering time by dimerizing with the holin (10, 35).

The Lys2 residue of S107 is critical for its antiholin activity. Placing a neutral or acidic residue at this position not only abolishes the antiholin function of S107, but converts it into a holin (9-10, 34). Based on this observation, it was proposed that the extra positive charge at the N-terminus of S107 (compared to S105) prevents the movement of the S107 N-terminus through the energized cytoplasmic membrane of the host, thereby preventing the membrane insertion of the sequence that is equivalent to the TMD1 of S105. Thus, nascent S107 has only two TMDs (Figure 3.1B). This model explains why treating cells expressing *S107* with poisons that depolarize the membrane causes the antiholin to trigger like a holin. Upon addition of the energy poison, the membrane potential collapses, allowing the N-terminus of S107 to "flip" through the membrane. The resulting topological isomer of S107 has not only lost its antiholin activity, but behaves as a holin. Further support for this model comes from experiments where a *sec*-dependent signal sequence was fused to the N-terminus of S107 (34). In this case, the fusion only exhibited holin activity since the N-terminus of S107 was exported directly to the periplasm.

It has been proposed that holins form two-dimensional aggregates or rafts in the cytoplasmic membrane before triggering (81). In this "death raft" model, a small channel or defect in the array of tightly packed transmembrane helices arises at some point during the growth of the raft; this causes a local depolarization which promotes conformational changes that lead to the transformation of the raft into a hole. In the case of λS, this hole is large enough to allow the passage of a cytoplasmic endolysin. Presumably, the formation of the initial defect in the raft depends on the strength of the

interactions between the transmembrane helices of the holin protein. Thus, single missense changes in the primary sequence of a holin can lead to dramatically different lysis times by altering the strength of the individual helix-helix interactions in the raft. The ability of λS to form dimers and higher oligomers in the membrane has been demonstrated, as has the ability of S105 and S107 to efficiently form mixed dimers. If these heterodimers do not contribute to raft formation, this would explain the antiholin activity of S107.

Previous studies of the S gene showed that the ratio of S105:S107 is approximately 2-2.5:1 (16-17). Since S105:S107 heterodimers presumably do not contribute to raft formation, and thus retard hole formation, modulation of this ratio would affect lysis timing. It is not known whether the ratio determined by Chang et al. (17) is modified under different growth conditions, although given the secondary structure of the *S* mRNA around the start sites of the coding region, it seems likely that the ratio may be modified in certain conditions (i.e, starvation) to give λ the ability to fine-tune lysis timing on a real-time basis in a given host cell.

Here, we report studies directed at assessing the importance of the N-terminal TMD of S107 in its role as an antiholin and correlating antiholin activity with the ability of an antiholin protein to heterodimerize with a holin. Preliminary results for studies to determine the S105:S107 ratio are also reported. The results are discussed in terms of a general model for the formation of the holin lesion and the modes by which this critical triggering event might be regulated.

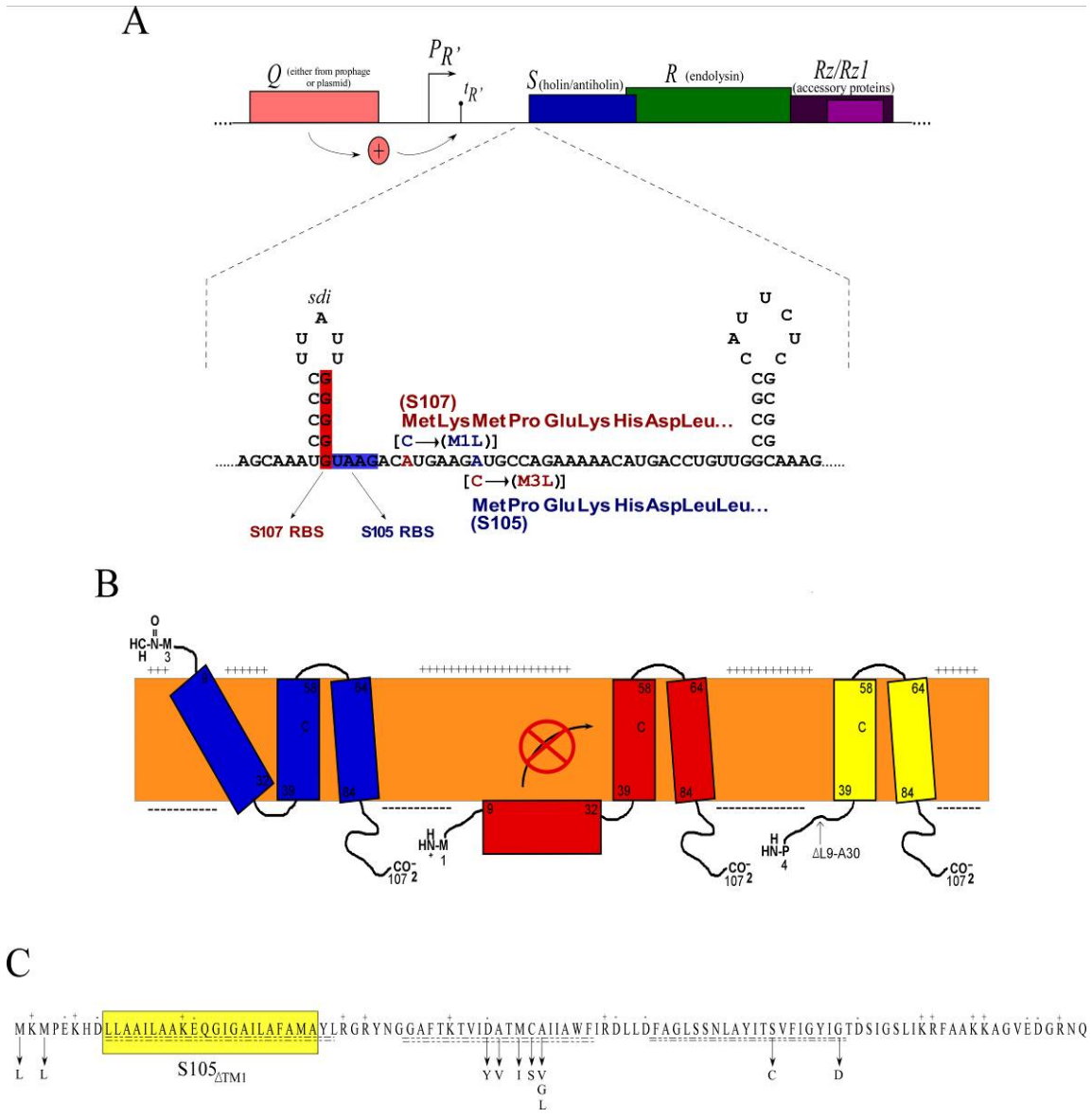

Figure 3.1. Diagram of the λ lysis cassette, the dual-start motif of the λ*S* gene, topologies of S105, S107 and $S105_{\Delta TMD1}$, and sequence of the S protein. A, Diagram of the λ lysis cassette and of the dual-start motif of the λ*S* gene. Text in red or highlighted in red correspond to S107, and text in blue or highlighted in blue correspond to S105. B, Diagram of the topology of S105 (blue) and the predicted topologies of S107 (red) and $S105_{\Delta TMD1}$ (yellow). TMD1 of S107 is prevented from transversing the membrane by the pmf. C, Sequence of the S protein. The yellow box indicates the deletion made to create $S105_{\Delta TMD1}$; missense alleles used in this study are indicated by arrows below the corresponding residue.

Materials and methods

Materials, strains, bacteriophage, plasmids, and growth media

N-Ethylmaleimide (NEM) and 1-10 phenanthroline were purchased from Sigma-Aldrich (St. Louis, MO). All other reagents were of the highest purity commercially available. The *E. coli* strains XL1Blue and BL21(DE3), the lysis-defective thermoinducible prophages *λΔSR* and *λSam7*, and the lysis-proficient thermoinducible prophages λ*S105* (expressing *S105*), and λ*S107** (expressing only S107) have been described previously (35, 57, 70, 73). $\lambda S105_{\Delta TMD1}$ is identical to λ*S105* with the exception that this phage has nucleotides 27-90 of the *S* gene deleted (corresponding to residues L9 to A30) to create the $S105_{\Delta TMD1}$ allele (Figure 3.1C). The strains and plasmids used in this work are described in Table 3.1.

Table 3.1. Strains, phage and plasmids.

Strain, phage or plasmid	Genotype/features	Source or reference
Strains		
MC4100 *ΔtonA*	E. coli K-12 F^- *araD139 Δ(argF-lac)U169 rpsL15relA1flbB3501 deo pstF25 rbsR ΔtonA*	Lab stock
MG1655 *ΔtonA* $lacI^q$	F^- *ilvG rfb50 rph1 ΔtonA* $lacI^q$	Lab stock
MDS12 *ΔtonA*	MG1655 with 12 deletions, totaling 376,180 nt including cryptic prophages; *ΔtonA*	(45)
XL1Blue	E. coli K-12 *recA endA1 gyrA96 thi1 hsdR17 supE44 relA1 lac* [F' *proAB lacZΔM15::tn10*]	Stratagene

Table 3.1. Continued

Strain, phage or plasmid	Genotype/features	Source or reference
Phage	Description	Source
λΔSR	*Δ(stf-tfa)::cat* cI_{857} Δ(*SR*)	(72)
λS105	*Δ(stf-tfa)::cat* cI_{857} S_{M1L}	(73)
λS107*	*Δ(stf-tfa)::cat* cI_{857} S_{M3L}	This study
$\lambda S105_{\tau 94}$	*Δ(stf-tfa)::cat* cI_{857} S_{M1L} *with the His-tag at position 94*	(73)
$\lambda S105_{\Delta TMD1}$	*Δ(stf-tfa)::cat* cI_{857} $S_{M1L\ \Delta L9\text{-}A30}$	This study
$\lambda S105_{\Delta TMD1\ mut}$	*Δ(stf-tfa)::cat* cI_{857} $S_{M1L\ \Delta L9\text{-}A30\ mut}$; see Table 3.3 for list of mutants	This study
Plasmid	Description	Source
pQ	The λ *Q* gene cloned into pZS*24, kan^R	(38)
pS105	λ lysis gene region with $S_{Met1Leu}$ cloned into pBR322, amp^R	(36)
pSwt	Same as pS105, but $Met1^+$	(35)
pKB1	Same as pSwt, but with *Sam7* mutation	(36)
pS107*	Same as pS105, but with $Met1^+$, *Met3Leu*	(35)
$pS105_{\Delta TMD1}$	Same as pS105, but with *ΔTMD1* mutation	This study
$pS105_{\Delta TMD1\ C51S}$	Same as $pS105_{\Delta TMD1}$, but with *Cys51Ser* mutation	This study
pS105 $Rz_{Q100am}Rz1_{W38am}$	Same as pS105, but with Rz_{Q100am} and Rz_{W38am}	Lab stock
pλ81	Same as lysis cassette from λ81 cloned into pS105	This study
pλ81-2	Same as pλ81, but with Rz_{Q100am} and Rz_{W38am}	This study
pS105*-3	Same as pS105, but with $R_{am54am60}$, Rz_{Q100am} and Rz_{W38am} and a unique KpnI site in R	This study
pS107*-3	Same as pS107*, but with $R_{am54am60}$, Rz_{Q100am} and Rz_{W38am} and a unique KpnI site in R	This study

Table 3.1. Continued

Strain, phage or plasmid	Genotype/features	Source or reference
$pS105_{\Delta TMD1}$*-3	Same as $pS105_{\Delta TMD1}$, but with $R_{am54am60}$, Rz_{Q100am} and Rz_{W38am} and a unique KpnI site in R	This study
$pS105_{A52V}$*-3	Same as pS105, but with *Ala52Val* mutation in *S105*, $R_{am54am60}$, Rz_{Q100am} and Rz_{W38am} and a unique KpnI site in *R*	This study
$pS105_{W56am}$*-3	Same as pS105, but with *Trp56am* (*Sam7*) mutation in *S105*, $R_{am54am60}$, Rz_{Q100am} and Rz_{W38am} and a unique KpnI site in *R*	This study
pSS-S107	Same as pSwt, but with signal sequence and ϕ10 ribosome binding site	This study
$pSS\text{-}S107_{A52V}$	Same as pSS-S107, but with *Ala52Val* mutation	This study
$pSS\text{-}S107_{A52V\tau94}$	Same as $pSS\text{-}S107_{A52V}$, but with 6X histidine-tag insertion after codon 94	This study
pTP2	Same as pS105, but with the lysis genes of phage 21 in place of the λ lysis genes	(52)
pET11a	pBR322 origin, T7 promoter, amp^R	Novagen
$pET\text{-}S105_{\tau94}$	pETlla with *S105*	(72)
$pET\text{-}S107^*_{\tau94}$	Same as $pET\text{-}S105_{\tau94}$, but $Met1^+$, *Met3Leu*	This study
$pET\text{-}S105_{\Delta TMD1\tau94}$	Same as $pET\text{-}S105_{\tau94}$, but with *ΔTMD1* mutation	This study
$pET\text{-}SS\text{-}S107_{A52V\tau94}$	pET11a with $SS\text{-}S107_{A52V\tau94}$	This study

Media, growth conditions, and thermal induction of the λ lysis genes from a prophage and/or plasmid have been described previously (17, 37-38, 72). The ability of *S* alleles to be triggered by membrane depolarization was assessed by adding dinitrophenol (DNP) or potassium cyanide (KCN) to a final concentration of 5 mM or 10 mM, respectively. Bacterial cultures were grown in standard LB medium supplemented

with ampicillin (100 μg/ml), kanamycin (40 μg/ml) and chloramphenicol (10 μg/ml) for the maintenance of plasmids and prophage, respectively.

Standard DNA manipulations, PCR, site-directed mutagenesis, and DNA sequencing

Isolation of plasmid DNA, DNA amplification by PCR, DNA transformation, and DNA sequencing were performed as previously described (37). Primers were obtained from Integrated DNA Technologies, Coralville, IA, and were used without further purification. Restriction and DNA-modifying enzymes were purchased from New England Biolabs; all reactions using these enzymes were performed according to the manufacturer's instructions. Site-directed mutagenesis was performed using the QuikChange kit from Stratagene as described previously (37). Primers used for site-directed mutagenesis are listed in Appendix A. $pS105_{\Delta TMD1}$ was used as the template for all the missense mutation primers, with the exceptions that $pS105_{\Delta TMD1\ C51S}$ was used as the template for primers S76C For and Rev and pSwt (35). The DNA sequence of all constructs was verified by automated fluorescence sequencing performed at the Laboratory for Plant Genome Technology at the Texas Agricultural Experiment Station.

Plasmid construction and generation of recombinant bacteriophage

The plasmid $pS105_{\Delta TMD1}$ was constructed by amplifying pS105, excluding nucleotides 27 to 90 of the *S105* gene, using primers Y31 For and D8 Rev. Following digestion with DpnI, the linear PCR product was purified using the PCR Purification Kit

(Qiagen), then treated with T4 Polynucleotide kinase and ligated with T4 DNA ligase. Following transformation into XL1 Blue, individual transformants were screened by colony PCR. The plasmids from candidates that tested positive were sequenced.

The plasmid pλ81 was constructed by first cloning the lysis cassette of λ81 (genotype cI_{857} *Ram54am60*; these amber mutations were previously unsequenced; sequencing showed that the *Ram54* mutation is *Gln26am* and the *Ram60* mutation is *Trp73am*) from the EcoRI site at λ nt 44972 to the ClaI site at λ nt 46448, into pS105 by splicing by overlapping extension (SOE) PCR (42), using SEcoRI For, 2-AatII For, 2-AatII Rev, and Lys Cas Rev; the primers used for the initial amplification mutated the AatII site at λ nt 44592, via silent mutation (C to T at λ nt 44594; the AatII site at λ nt 45563 is destroyed by the Q26am mutation). The 611 bp EcoRV-ClaI fragment from pS105$Rz_{Q100am}Rz1_{W38am}$ containing a portion of the *R* gene and the entire *Rz/Rz1* genes was then cloned into pλ81, creating pλ81-2. The plasmid pS105*-3 was created from pS105 and p λ81-2 by SOE PCR, using primers SEcoRI For, Ram54 KpnI Rev, Ram54 KpnI For, and pS105 ClaI Rev. pS107*-3, $pS105_{A52V}$*-3, $pS105_{\Delta TMD1}$*-3, and $pS105_{W56am}$*-3 were created from pS105*-3 by Quikchange, using the primers S107* For and Rev, A52V For and Rev, Y31 For and D8 Rev, and Sam7 For and Rev, respectively.

The plasmid pSS-S017 was constructed in a two-step Quikchange reaction by amplifying pSwt first using primers SS-S107 For and SS-S107 Rev, then SS-S107 For-2 and SS-S107 Rev. These primers replaced the *sdi* stemloop with the *ϕ10* ribosome binding site and inserted the coding sequence for the 18 residue synthetic signal

sequence (MKWVTFISLLFLFSSAYA). After digestion with DpnI, the linear PCR product was purified using the PCR Purification Kit (Qiagen), then treated with T4 Polynucleotide kinase and ligated with T4 DNA ligase. Following transformation into XL1 Blue, individual transformants were screened by colony PCR. Plasmids from candidates that tested positive were sequenced.

Recombinant phage were constructed as follows: Plasmids carrying non-lytic alleles of S105 (such as $S105_{\Delta TMD1}$) were transformed into MDS12 *ΔtonA* (λΔSR) and individual transformants were grown up and induced as previously described. Chloroform (final concentration, 1%) was added to the cultures 2 hours after induction, or when lysis was complete. Lysates were cleared by centrifugation (3,000 rpm in a clinical centrifuge) and used to reinfect early-log cultures of MDS12 *ΔtonA* at m.o.i. of 5. Two hours after infection, chloroform was added and the lysate cleared. This enrichment step was repeated twice more, and the final lysate was used to lysogenize MC4100 *ΔtonA*. Lysogens were selected for by plating on LB plates containing chloramphenicol and were screened using Single Prophage PCR (55) to determine which candidates contained a single prophage. These candidates were then cross-streaked against λ86 ($\lambda^{imm434}\ c^{-}\ R_{am54am60}$) to verify the presence of a functional endolysin; positive candidates were used for lysis curves and to create phage stocks. Plasmids carrying lytic alleles of S105 (such as $S105_{A52G}$) were transformed into MDS12 *ΔtonA* (λΔSR) and individual transformants were grown up and induced as previously described. Chloroform (final concentration, 1%) was added to the cultures when lysis was complete. Lysates were cleared by centrifugation (3,000 rpm in a clinical centrifuge),

and serial dilutions of lysates were plated on MDS12 *ΔtonA*. Plaques were purified by streaking them on MDS12 *ΔtonA*, and pickates made from purified plaques were used to lysogenize MC4100 *ΔtonA*. Lysogens were selected for by plating on LB plates containing chloramphenicol and were screened using Single Prophage PCR (55) to determine which candidates contained a single prophage. These candidates were then cross-streaked against λ86 (λ^{imm434} c^- $R_{am54am60}$) to verify the presence of a functional endolysin; positive candidates were used for lysis curves and to create phage stocks.

TCA precipitation

1 ml or 5 ml culture aliquots were added to 111 µl or 555 µl, respectively, of cold, 6.1 N trichloroacetic acid, then placed on ice for 30 minutes. The precipitate was collected by centrifugation (15,000 rpm in a microcentrifuge or 3,000 rpm in a clinical centrifuge, respectively) and washed once with acetone, resuspending the pellet completely. Pellets were air-dried and resuspended in SDS-PAGE loading buffer. Proteins were separated on 16.5% SDS-PAGE with a 4% stacking gel. Western blotting and immunodetection with anti-S antibodies were performed as previously described (37).

Purification of *E. coli* deformylase

The plasmid pET-22B-def-CHT, encoding oligohistidine-tagged deformylase, was a gift from Hua Pei (58). The His-tagged deformylase was overexpressed in BL21(DE3) *slyD::Tn10* harboring pET-22B-def-CHT as described (58). The enzyme

was purified by immobilized metal affinity chromatography (IMAC) to a final concentration of 5 mg/ml. The activity of the purified enzyme was determined using the tri-peptide formyl-Met-Ala-Ser (Sigma) as the substrate. The appearance of N-terminal amines was monitored using 2,4,6-trinitrobenzenesulfonic acid (25).

Oxidative disulfide bridge formation in membranes

A culture expressing the desired *S* allele(s) was induced as previously described (35). After lysis was complete or 100 minutes after induction in cases where lysis does not occur, 10 ml aliquots of the induced cultures were disrupted by passage through a French pressure cell (Spectronic Instruments, Rochester, NY.) at 16,000 lb/in^2 (1 lb/in^2 = 6.89 kPa). The samples were then oxidized by the addition of $CuSO_4$ and 1-10 phenanthroline to final concentrations of 20 mM and 60 mM, respectively. After incubation for 60 minutes at room temperature, the reactions were stopped by the addition of NEM (in ethanol) to a final concentration of 0.1 M. Following a 3,000 x *g* clearing spin, the membrane fraction was collected by centrifugation at 100,000 x *g* for 60 min at 18°C. The membrane pellet was resuspended in 50 µl of membrane extraction buffer (1% Empigen BB, 10% glycerol, 0.5 M NaCl, 20 mM Tris-HCl, pH 8.0, 0.1 M NEM) containing 35 mM $MgCl_2$ to stabilize the outer membranes. This mixture was incubated for 12 to 14 h at 37°C and detergent-insoluble material was removed by centrifugation at 100,000 x *g* for 45 min at 18°C. The detergent-soluble fraction was diluted 1:1 with 2X protein sample loading buffer prior to SDS-PAGE analysis. Proteins

were separated on 16.5% SDS-PAGE with a 4% stacking gel. Western blotting and immunodetection with anti-S antibodies were performed as described previously (37).

Phage accumulation after the induction of λ lysogens

Cells lysogenized with *λSam7, λS107**, *λS105,* $\lambda S105_{A52V}$ or $\lambda S105_{\Delta TMD1}$ were grown and thermally induced as previously described (35). At various times after induction, 1 ml aliquots were removed and treated with 1% chloroform to release progeny phage which were then titered by plating on lawns of MDS12 pTP2. This plasmid contains the lysis genes $S^{21}68$, R^{21}, *and* $Rz^{21}/Rz1^{21}$ from phage 21 (52) under control of the λ $P_{R'}$ promoter. Since the holin of phage 21 does not interact with S105, S107, $S105_{A52V}$or $S105_{\Delta TMD1}$ (data not shown), the presence of this plasmid allows even lysis defective lambda phages to form plaques on the indicator lawn. Plaques from triplicate platings were counted after 12-16 hours of incubation at 37˚C, and the averages from 2 experiments were used.

Viability assays

Cultures of MG155 *ΔtonA* $lacI^q$ *ΔlacY* expressing pQ and either pS105*-3, pS107*-3, $pS105_{A52V}$*-3, $pS105_{\Delta TMD1}$*-3 or $pS105_{W56am}$*-3 were induced as previously described (38). At t = 60 and 120, a 2 ml sample of each culture was removed; 1 ml of the sample was serially diluted on ice, and plated in triplicate on LB plates containing kanamycin and ampicillin; the remaining 1ml of sample was TCA precipitated for

Western blotting. Colonies from three separate experiments were counted after 12-16 hours incubation at 37˚C.

Results

The N-terminus of Sl05, but not Sl07, retains its fMet residue

Our current model to explain the functional difference between the antiholin, Sl07, and the holin, Sl05, stipulates that the N-terminus of the former, but not the latter, is blocked from transiting the membrane by the positive-outside potential across the energized cytoplasmic membrane. Thus, while the N-terminus of S107 should be subject to deformylation by the cytoplasmic deformylase enzyme, the N-terminus of S105 might escape this modification. To test this idea, the purified S105 and S107 proteins were subjected to automated N-terminal sequencing. The Sl07 species was found to be fully sequenceable, and the sequence corresponded exactly to that predicted from the dual start motif (Table 3.2). In contrast, Sl05 could not be sequenced, suggesting that the α-amino group of the Metl residue was covalently blocked. To test whether the blockage was due to an N-terminal formyl group, the S105 protein was treated with purified *E. coli* deformylase. When the resulting protein was subjected to N-terminal sequencing, a sequence consistent with translational initiation at Met3 was obtained (Table 3.2), demonstrating that Sl05 indeed carries the N-terminal fMet residue. Not only does this finding directly support our model for a topological

difference between S105 and S107, but it also indicates that the N-terminus of Sl05 exits the cytoplasm very rapidly since it escapes cytoplasmic deformylation.

Table 3.2. N-terminal sequencing of purified S proteins.

Sample	Repetitive yield	Sequence
S105	0%	---
S107* (*M1*$^{+}$, *M3L*)	82%	MKLPEK
$S105_{\Delta TMD1}$	91%	PEKHD
Def treated S105	>95%	XXHDLLA XXXHDLL

TMD1 of S is essential for holin activity

Since the topological difference distinguishing S105 and S107 involves the N-terminal TMD1, it was of interest to see if TMD1 plays a purely regulatory role or whether it is required for the holin function of S105. To answer this question, we deleted codons 9-30 from the *S105* gene in pS105 generating plasmid $pS105_{\Delta TMD1}$ which has the lysis cassette, $S105_{\Delta TMD1}$ *RRzRz1* under control of the λ $P_{R'}$ promoter. This lysis cassette was then recombined into the thermally inducible λ*ΔSR* prophage, resulting in $\lambda S105_{\Delta TMD1}$. While the induction *λS105* and *λS107* caused lysis, induction of $\lambda S105_{\Delta TMD1}$ seemed to have little effect on cell growth for over five hours (Figure 3.2A). During this period, phage continued to accumulate to a level equivalent to the induction of a λ*Sam7* prophage (Figure 3.2B). The inability of $S105_{\Delta TMD1}$ to effect lysis was not due to the instability of the $S105_{\Delta TMD1}$ protein since it accumulated to higher levels than either

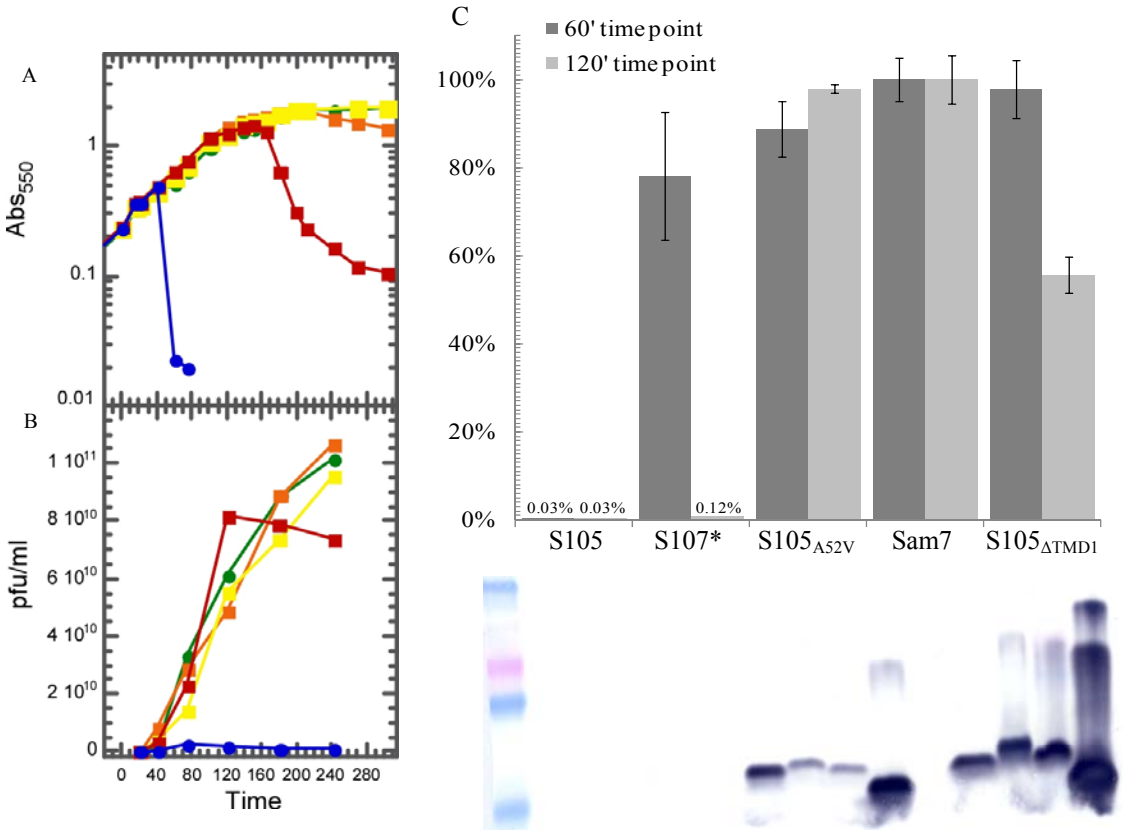

Figure 3.2. Lysis profiles and phage accumulation for λ*S105*, λ*S107**, λ*Sam7*, λ*S105*$_{A52V}$ and λ*S105*$_{\Delta TMD1}$ and viability of cells expressing *S105*,λ*S107**,λ*Sam7*, *S105*$_{A52V}$ and *S105*$_{\Delta TMD1.}$ A, lysis profiles of (●) λ*S105*, (■) λ*S107* (M1*$^{+}$*, M3L)*, (●) λ*Sam7*, (■) λ*S105*$_{A52V}$, and (■) λ*S105*$_{\Delta TMD1}$. λ*S105*$_{\Delta TMD1}$ behaves identically to λ*Sam7*. B, phage accumulation profiles for (●) λ*S105*, (■) λ*S107**, (●) λ*Sam7*, (■) λ*S105*$_{A52V}$, and (■) λ*S105*$_{\Delta TMD1}$. Again, λ*S105*$_{\Delta TMD1}$ behaves identically to λ*Sam7*. C, Viability of cultures expressing pS105, pS107*, pS105$_{A52V}$, pS105$_{W56am}$ (Sam7) or pS105$_{\Delta TMD1}$ 1 hour and 2 hours after induction. D, Western blot of cells expressing pS105, pS107*, pS105$_{A52V}$, pS105$_{\Delta TMD1}$ or pS105$_{W56am}$ (Sam7); lane 1, molecular weight marker, lanes 2-6, samples taken at time 0, lanes 11, samples taken 1 hour after induction, lanes12-16, samples taken 2 hours after induction. Not the severe excess of S105$_{\Delta TMD1}$ in the both the 1 hour and 2 hour sample compared to the others.

S105 or S107 (Figure 3.3). Moreover, N- terminal sequencing of the S105$_{\Delta TMD1}$ protein revealed that its N-terminus was unblocked, indicating that it was retained in the cytoplasm (Table 3.2). Thus, deletion of TMD1 did not appear to affect the topology of

the remainder of the protein. Hole formation by the $S105_{\Delta TMD1}$ protein could not be elicited by treatments that depolarize the cytoplasmic membrane (Fig. 3.4). This stands in stark contrast to S105 and S107, both of which can be artificially triggered to form holes by membrane depolarization (Fig. 3.4). Finally, when lysis cassettes carrying the various *S* alleles were induced using a plasmid-borne *Q* gene, only *S105* was lethal at 60' after induction, consistent with its holin function (Fig. 3.2C), and only S107* was lethal at 120' after induction; the other alleles had little effect. The reduced amount of survival seen at 120' for $pS105_{\Delta TMD1}$ is due to the high amounts of $S105_{\Delta TMD1}$ protein produced, since excessive production of a membrane protein is toxic to cells (Figure 3.2D).

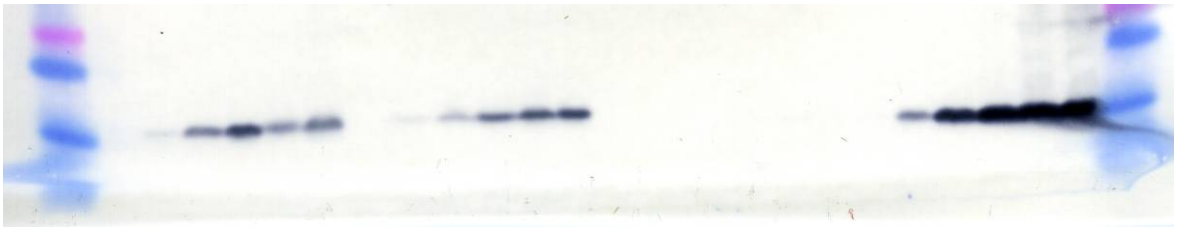

Figure 3.3. Accumulation of S105, S107*, Sam7, and $S105_{\Delta TMD1}$ following prophage induction. Samples were taken at 0', 15', 30', 45', 60', and 90' after induction. Lanes 1 and 26, molecular weight marker, lanes 2-7, S105 samples, lanes 8-13, S107* samples, lanes 14-19, Sam7 samples, lanes 20-25, $S105_{\Delta TMD1}$ samples. In lanes 6 and 7, the decreased amount of S105 is due to variable sample recovery during TCA precipitation because the culture was already lysed at these time points.

When $\lambda S105_{\Delta TMD1}$ was plated on lawns of wild-type *E.coli*, the reversion rate was much lower (~1.5×10^{-8}) than that of $\lambda Sam7$, which reverted at a rate of 2×10^{-5}. It was shown however, that these few pseudorevertants were the result of the acquisition of

lysis genes from cryptic prophages by recombination (44) rather than from the mutational conversion of $S105_{\Delta TMD1}$ to a functional holin (data not shown). When λ$S105_{\Delta TMD1}$ was plated on MDS12, a strain deleted for all known cryptic prophage found in *E. coli* K-12 laboratory strains, no revertants could be isolated, even when the phage was chemically mutagenized prior to plating (data not shown). The behavior of the $S105_{\Delta TMD1}$ allele in both the plasmid and phage context indicates that the N-terminal TMD of λS is essential for its holin function.

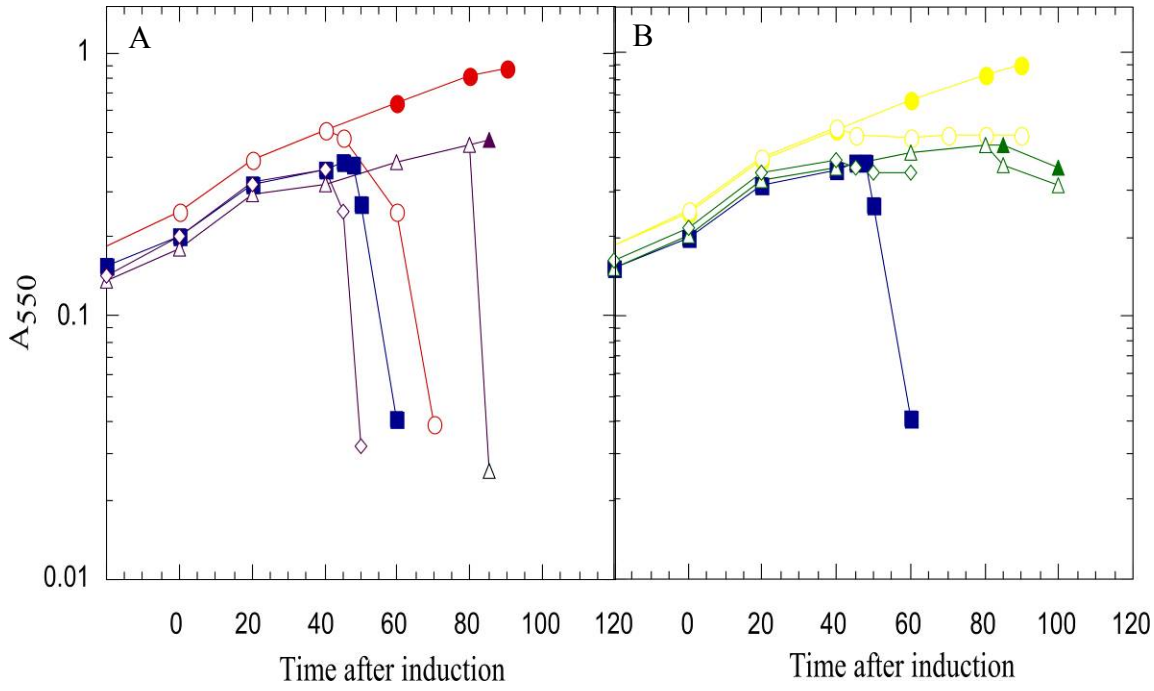

Figure 3.4. DNP treatment of S107* and $S105_{\Delta TMD1}$ with and without S105. A, (■) λ*S105*; (●) λ*S107*; (○) λ*S107* with DNP added at 40 minutes; (▲) λ*S105* + pS107; (◊) λ*S105* + pS107 with DNP added at 40 minutes; (Δ) λ*S105* + pS107 with DNP added at 80 minutes. B, (■) λ*S105*; (●) λ$S105_{\Delta TMD1}$; (○) λ$S105_{\Delta TMD1}$ with DNP added at 40 minutes; (▲) λ*S105* + $pS105_{\Delta TMD1}$; (◊) λ*S105* + $pS105_{\Delta TMD1}$ with DNP added at 40 minutes; (Δ) λ*S105* + $pS105_{\Delta TMD1}$ with DNP added at 80 minutes.

The antiholin character of S107 is due to the absence of TMD 1 from the bilayer

We next examined whether the antiholin activity of nascent S107 was due to the absence of its potential TMD1 from the membrane or to the presence of the N-terminus in the cytoplasm. When either the antiholin gene, *S107*, or the $S105_{\Delta TMD1}$ allele was expressed *in trans* to an induced S105 prophage, lysis of the host was blocked (Figure 3.4). Thus, the $S105_{\Delta TMD1}$ protein is an effective antiholin. Strikingly, unlike the block imposed by S107, the inhibition of the holin by expression of $S105_{\Delta TMD1}$ could not be subverted by addition of either KCN or DNP (Figure 3.4). When λ*S105* was plated on MC4100 carrying $pS105_{\Delta TMD1}$, the efficiency of plating (e.o.p.) was 0.01, compared to an e.o.p. of 0.6 for plating on pS107*. Plating λ*S105* on $pS105_{\Delta TMD1}$ also severely affected plaque morphology, giving rise to fuzzy, pinpoint plaques (Figure 3.5). The

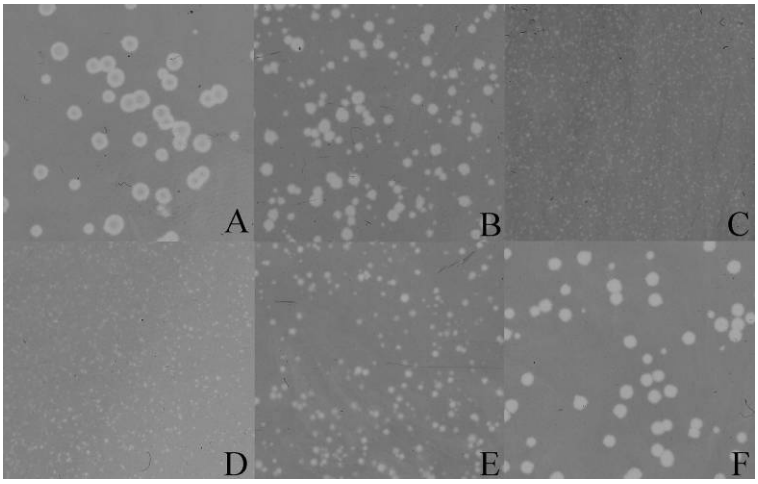

Figure 3.5. Effects of $pS105_{\Delta TMD1}$ on plaque morphology of λ*S105*. A, pKB1, B, pS107*, C, $pS105_{\Delta TMD1}$, D, $pS105_{\Delta TMD1\ A52V}$, E, $pS105_{\Delta TMD1\ A52G}$, F, $pS105_{\Delta TMD1\ C51S}$. Alleles that cause greater inhibition ($S105_{\Delta TMD1}$, and $S105_{\Delta TMD1\ A52V}$) have a greater effect on plaque morphology.

significance of these findings is two-fold. First, the inability to trigger hole formation in cells producing both S105 and $S105_{\Delta TMD1}$ suggests that the two proteins interact in a way that prevents the conformation or organizational changes in S105 that constitute the triggering event. Second, it is consistent with the notion that the antiholin activity of nascent S107 is abolished when its N-terminus penetrates the bilayer, a process we believe is promoted by membrane depolarization. Indeed, penetration of the N-terminus of S107 into the bilayer converts it from an antiholin to a holin. Thus, the continued antiholin activity of $S105_{\Delta TMD1}$ after membrane depolarization is due to its inability to be converted into a holin.

Antiholin activity of $S105_{\Delta TMD1}$ derivatives is correlated with their ability to heterodimerize with the holin

We previously studied the interaction between the mutant and wild type holin/antiholin proteins by co-expressing the desired *S105* and *S107* alleles (35). While this approach is clearly useful for demonstrating heterodimer formation by chemical crosslinking, assessing the antiholin activity of S107 variants by this method is complicated by the fact that the nascent S107 antiholin can be converted into a topological isomer that acts as a holin. Consequently, we decided to use the non-triggerable $S105_{\Delta TMD1}$ allele to test the effect of missense mutations on antiholin function. Quantitative Western blotting showed that S105 accumulates to approximately 1000-1500 molecules per cell when expressed from a prophage, and about 1.5-2 times that amount when expressed from pS105 (Figure 3.6). $S105_{\Delta TMD1}$ is expressed at much

higher levels in both contexts: approximately 3.5-fold more from the prophage and approximately 10.5-fold more from pS105$_{\Delta TMD1}$. The higher expression of *S105$_{\Delta TMD1}$* is presumable due to the loss of the regulatory stemloop structure spanning codons 11 through 16 (Figure 3.1A) in the *S* mRNA. Thus, when *S105* is expressed from the prophage with *S105$_{\Delta TMD1}$* expressed from a plasmid *in trans*, there is a ~1:10 ratio of S105 to S105$_{\Delta TMD1}$; the ratio of S105 to S107* in the same context is only ~1:2 (data not shown). Since this severe excess of S105$_{\Delta TMD1}$ may have masked the true extent of the interaction between S105$_{\Delta TMD1}$ and S105, *S105* was expressed from a plasmid *in trans* to *S105$_{\Delta TMD1}$* expressed from a prophage; transactivated pS105 derivatives produce

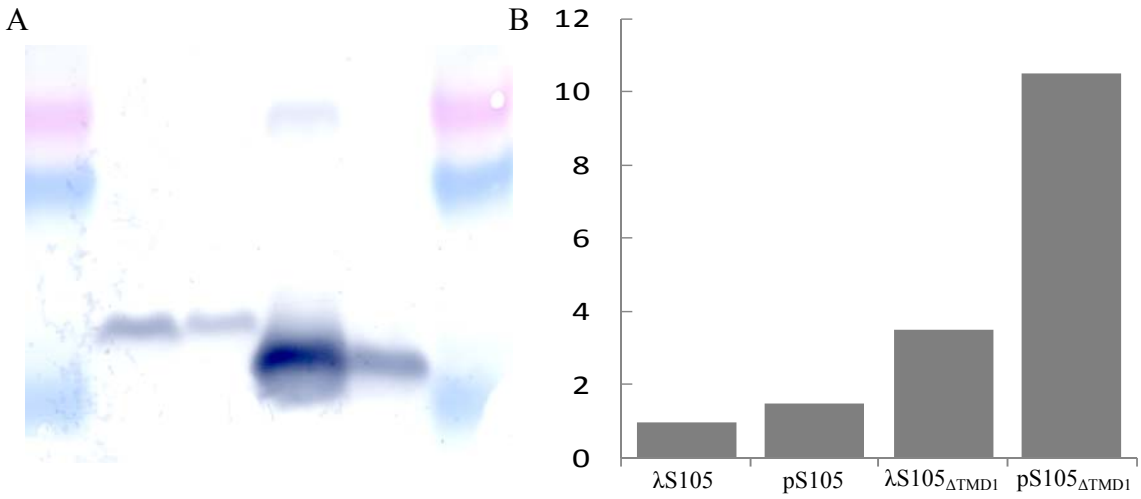

Figure 3.6. Comparison of expression levels of S105 and S105$_{\Delta TMD1}$ from plasmid and prophage. A, Western blot of cells expressing S105 or S105$_{\Delta TMD1}$ from either the plasmid or prophage; lanes 1 and 6, molecular weight marker, lane 2, pS105 sample, lane 3, λS105 sample, lane 4, pS105$_{\Delta TMD1}$ sample, lane 5, λS105$_{\Delta TMD1}$ sample. B, Comparison of band intensities; the intensity of the λS105 sample was used as the basis for comparison. Expression from pS105$_{\Delta TMD1}$ is clearly much higher than λS105, or even pS105.

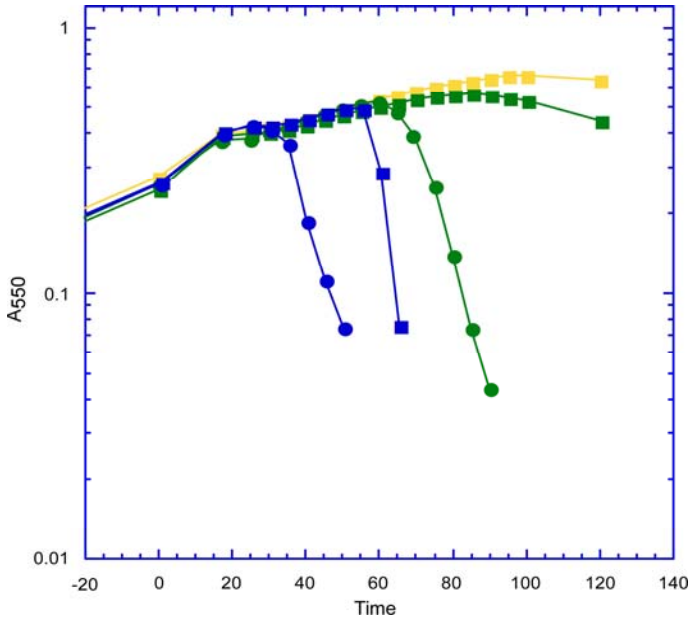

Figure 3.7. Inhibition of S105 by $S105_{\Delta TMD1}$. Lysis profiles of (●) λ*Sam7* + pS105, (■) λ*S105* + pKB1, (■) λ*S105* + $pS105_{\Delta TMD1}$, (●) λ$S105_{\Delta TMD1}$ + pS105, (■) λ*Sam7* + $pS105_{\Delta TMD1}$. The green curves show that by increasing the S105:$S105_{\Delta TMD1}$ ratio, inhibition is decreased.

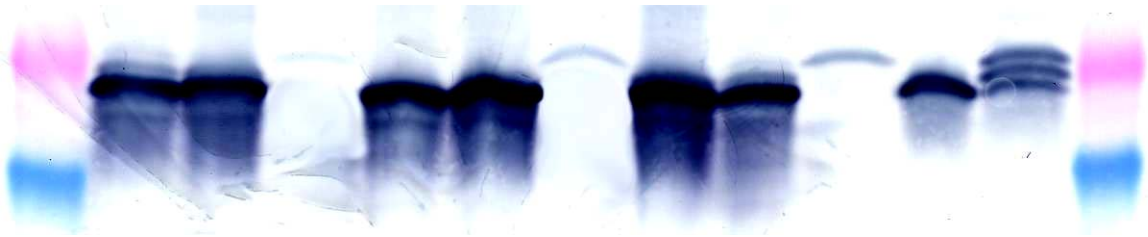

Figure 3.8. $Cu(Ph_3)$ crosslinking of S105 and $S105_{\Delta TMD1}$. Lanes 1, and 13, molecular weight marker Lane 2, λ$S105_{A52G}$ + $pS105_{\Delta TMD1}$, Lane 3, λS105 + $pS105_{\Delta TMD1\ A52G}$, Lane 4, λ$S105_{A52G}$, Lane 5, $pS105_{\Delta TMD1\ A52G}$, Lane 6, $pS105_{\Delta TMD1}$, Lane 7, λS105, Lane 8, λS105 + $pS105_{\Delta TMD1}$, Lane 9, λS105 + $pS105_{\Delta TMD1\ A52G}$, Lane 10, pS105, Lane 11, λ$S105_{\Delta TMD1}$, Lane 12, λ$S105_{\Delta TMD1}$ + pS105. For lanes 2-12, the top band is the S105 homodimer, the middle band is the S105/$S105_{\Delta TMD1}$, and the lower band is the $S105_{\Delta TMD1}$. Note the strong appearance of an S105 homodimer in the λ$S105_{\Delta TMD1}$ + pS105, but not in the λS105 + $pS105_{\Delta TMD1}$, and the appearance of a S105 homodimer band in the λ$S105_{A52G}$ + $pS105_{\Delta TMD1}$, and λS105 + $pS105_{\Delta TMD1\ A52G}$, but not in λ$S105_{A52G}$ + $pS105_{\Delta TMD1\ A52G}$, and λS105 + $pS105_{\Delta TMD1}$.

approximately 2-fold more S protein than a prophage (data not shown), so expressing *S105$_{\Delta TMD1}$* and *S105* this way increased the S105 to S105$_{\Delta TMD1}$ ratio to approximately 1:1.5. Interestingly, altering the ratio lead to a decrease in the amount of inhibition (Figure 3.7). Cu(Ph$_3$) crosslinking of S105 and S105$_{\Delta TMD1}$ in these different expression systems reveals that in addition to a decrease in inhibition, there is a decrease in crosslinking (Figure. 3.8), indicating that it is the amount of "free" S105 that determines lysis timing, since expressing less S105$_{\Delta TMD1}$ leads to more free S105 and earlier lysis.

Several mutants of S107 have been shown to interact less with S105 than S107$_{wt}$, and the weaker interaction also causes weaker inhibition (35). These mutations, and several others that were shown to be either recessive or dominant in mutational analysis studies, were put into S105$_{\Delta TMD1}$ and tested for inhibition (Table 3.3). Only the mutants A52G, C51S, G83D, and the double mutant C51S/S76C demonstrated decreased inhibition as compared to wild-type (Figure 3.9A). Since the test for interaction between S molecules is cysteine-specific crosslinking, and S has only a single cysteine at position 51, mutant C51S could not be used. Additionally, the interactions between TMD2 and TMD3 have not yet been demonstrated using Cu(Ph$_3$) crosslinking, so the mutantC51S/S76C was also not used. Western blot analysis of the G83D mutant showed that it does not accumulate to normal levels, indicating that the lack of inhibition exhibited by this allele is due to a lack of protein accumulation, and not a weaker interaction (data not shown). Cu(Ph$_3$) crosslinking of prophage expressed S105 and either plasmid expressed S105$_{\Delta TMD1}$, S105$_{\Delta TMD1\ A52V}$, or S105$_{\Delta TMD1\ A52G}$ showed that

decreased inhibition corresponds to a decreased interaction between S105 and $S105_{\Delta TMD1\ A52G}$ (Figure 3.10).

Table 3.3. $S105_{\Delta TMD1}$ alleles and inhibition of λ*S105.*

Allele	Inhibition of λS105	Phenotype in S105 in trans to λS105 (Table 2.2)
Wild-type	+++	NA
R59H	+++	R
M50I	+++	R
C51S	(+)	D(l)
A52G	+	D(l)
A52V	+++	D(n)
L71F	+++	R
C51S/S76C	(+)	D(l)
G83D	(+)	R

This decrease in inhibition is also correlated to the effect of the inhibitor on plaque morphology, since plating λS105 on either $S105_{\Delta TMD1\ C51S}$ and $S105_{\Delta TMD1\ A52G}$ gives larger plaques (Figure 3.5) at higher e.o.p.s (data not shown) than either $S105_{\Delta TMD1}$ or $S105_{\Delta TMD1\ A52V}$. Additionally, when $\lambda S105_{A52G}$ is expressed with $pS105_{\Delta TMD1\ A52G}$, strong inhibition is observed, similar to that of λS105 is expressed with $pS105_{\Delta TMD1}$, and when $\lambda S105_{A52G}$ is expressed with $pS105_{\Delta TMD1}$, less inhibition is observed, similar to that of λS105 is expressed with $pS105_{\Delta TMD1\ A52G}$ (Figure 3.9B). $Cu(Ph_3)$ crosslinking shows that the decreased inhibition is correlated with a decrease in crosslinking (Figure 3.8).

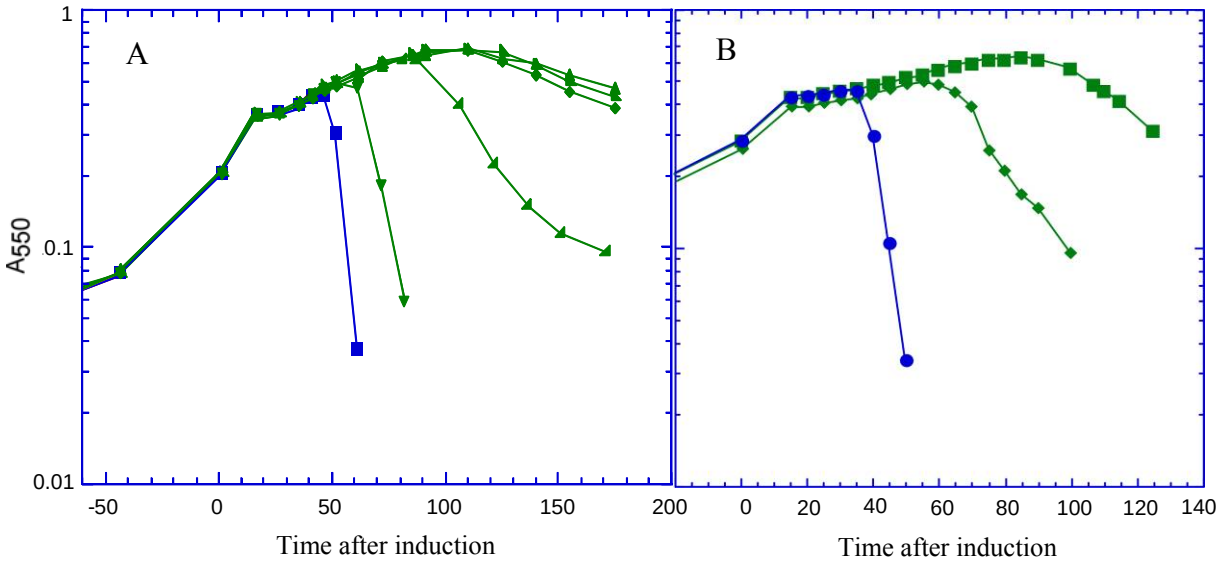

Figure 3.9. Inhibition of S105 by $S105_{\Delta TMD1}$ mutants. A, Lysis profiles of (■) λ*S105* + pKB1, (▼) λ*S105* + $pS105_{\Delta TMD1\ C51S}$, (◢) λ*S105* + $pS105_{\Delta TMD1\ A52G}$, (◣) λ*S105* + $pS105_{\Delta TMD1\ A52V}$, (▲) λ*S105* + $pS105_{\Delta TMD1\ A48V}$, (♦) λ*S105* + $pS105_{\Delta TMD1}$. B, Lysis profiles of (●) λ$S105_{A52G}$ + pKB1, (♦) λ$S105_{A52G}$ + $pS105_{\Delta TMD1}$, (♦) λ$S105_{A52G}$ + $pS105_{\Delta TMD1\ A52G}$. Only $S105_{\Delta TMD1\ C51S}$ and $S105_{\Delta TMD1\ A52G}$ show decreased inhibition of S105, while $S105_{\Delta TMD1}$ shows decreased inhibition of $S105_{A52G}$.

Figure 3.10. $Cu(Ph_3)$ crosslinking of S105 and $S105_{\Delta TMD1}$ or $S105_{\Delta TMD1mut}$. Lanes 1 and 9, molecular weight marker, Lane 2, $S105_{\tau 94}$ alone, Lane 3, $S105_{\tau 94}$ + S105, Lane 4, $S105_{\tau 94}$ + S107, Lane 5, S105 alone, Lane 6, S105 + $S105_{\Delta TMD1}$, Lane 7, S105 + $S105_{\Delta TMD1\ A52V}$, Lane 8, S105 + $S105_{\Delta TMD1\ A52G}$. For lanes 2-4, the top band is the S105τ94 homodimer, the middle band is the S105τ94/S105 or S107* heterodimer, and the lower band is either an S105 or S107* homodimer. For lanes 5-8, the top band is the S105 homodimer, the middle band is the S105/$S105_{\Delta TMD1(mut)}$ heterodimer, and the bottom band is the $S105_{\Delta TMD1}$ homodimer. Note the appearance of an S105 homodimer in the S105 + $S105_{\Delta TMD1\ A52G}$, but not in the S105 + $S105_{\Delta TMD1}$ or S105 + $S105_{\Delta TMD1\ A52V}$ samples, indicating a weaker interaction between S105 and $S105_{\Delta TMD1\ A52G}$.

Characterization and overexpression of SS-S107 and SS-S107$_{A52V}$

Previous studies on the ratio of S105:S107 (16-17) showed that the ratio remained constant under standard laboratory conditions; however, given the difficulties in identifying the two proteins on a normal SDS-PAGE gel, and the inviting prospect of real-time modulation of the ratio under different growth conditions, we wanted to revisit this question. Since S105 and S107 only differ by the two residue extension at the N-terminus of S107, the ability to identify the individual proteins from a single sample in which both are present proved problematic. To resolve this issue, we obtained S105-specific and S107-specific antibodies from Bethyl Laboratories (Conroe, TX) that were raised against the N-terminal 9 residues of S105 and S107, respectively, and then cross-adsorbed against the other peptide (S107 and S105, respectively). By using only the N-terminal 9 residues of each protein, the difference between the two epitopes is 33%. With these antibodies it is theoretically possible to quantify the amount of S105 and S107 from the native *S* gene (*Swt*) using either ELISA assays or quantitative Western blotting. Dot blots using purified S105 and purified S107* (which has a M3L mutation) showed that the α-S105 N-terminus antibodies recognized S105 and not S107*, and that the α-S107 N-terminus antibodies recognized neither S105 nor S107*.

Western blot analysis of cells expressing either *S105*, *S107** or *Swt*, showed that the α-S105 N-terminus antibody does recognize S107 and S107*, although to a lesser extent than the recognition of S105 and that blocking with the S107 N-terminal peptide did not significantly improve the specificity of the antibody (data not shown). This problem can be overcome by determining the background level of recognition that the α-

S105 N-terminus antibody exhibits using purified S107. Since both ELISA assays and quantitative Western blotting require standards of purified protein, and a standard for the background recognition of S107 by α-S105 N-terminus is also required, it was necessary to construct a mutant of S that only produces S107, and no S105, and preserves the sequence of the S107 N-terminus (since the α-S107 N-terminus antibodies do not recognize S107*). Early attempts to mutate and move the ribosome binding sites of the *S* gene showed that the ratio could be altered, but both proteins were still produced (data not shown). Further attempts to mutate the ribosome binding site using both site-directed mutagenesis and SOE PCR failed, presumably because the constructs were lethal.

Since mutating and moving the ribosome binding failed to produce a construct that produced only S107 and not S105, an alternative strategy was employed. A synthethic signal sequence was placed in front of the *S* gene, and the *sdi* stem loop was removed and replaced with a different ribosome binding site. The plasmid containing this construct, called pSS-S107, was detrimental to the growth of both the cloning strain XL1 Blue and the expression strain MC4100 *ΔtonA* (λΔSR), indicating that the plasmid expressed some level of the S protein, although this was not confirmed by Western blot. Interestingly, when the ribosome binding site in the construct was replaced with the native *sdi* stemloop, no effect on growth rate was observed, indicating that the structure is important for controlling basal level expression of the *S* gene. Induction of MC4100 *ΔtonA* (λΔSR) pSS-S107 showed that the lysis time of this construct is 11 minutes (Figure 3.11A). Given that the goal of using this construct is to purify the processed

protein, a construct that causes slow growth and fast lysis was not ideal. The non-lytic mutation, A52V, was introduced into pSS-S107. Surprisingly, although this construct did not alter the growth rate of the cells, it was extremely toxic to the cells beginning at 15 minutes after induction, causing the cells to passively rot (Figure 3.11A). A test of pS107*$_{A52V}$ with and without DNP revealed that S107*$_{A52V}$ could not be induced to cause lysis (Figure 3.11B), nor did it cause the "rotting" phenotype observed with SS-S107$_{A52V}$. A Western blot of cells expressing *SS-S107$_{A52V}$* revealed that two products were produced; the larger one corresponded to the molecular weight of the unprocessed form of SS-S107$_{A52V}$ and the smaller one corresponded to the processed form of SS-S107$_{A52V}$ (Figure 3.12). A His-tag ($G_2H_6G_2$) was introduced at codon 94 (73) in the *S*

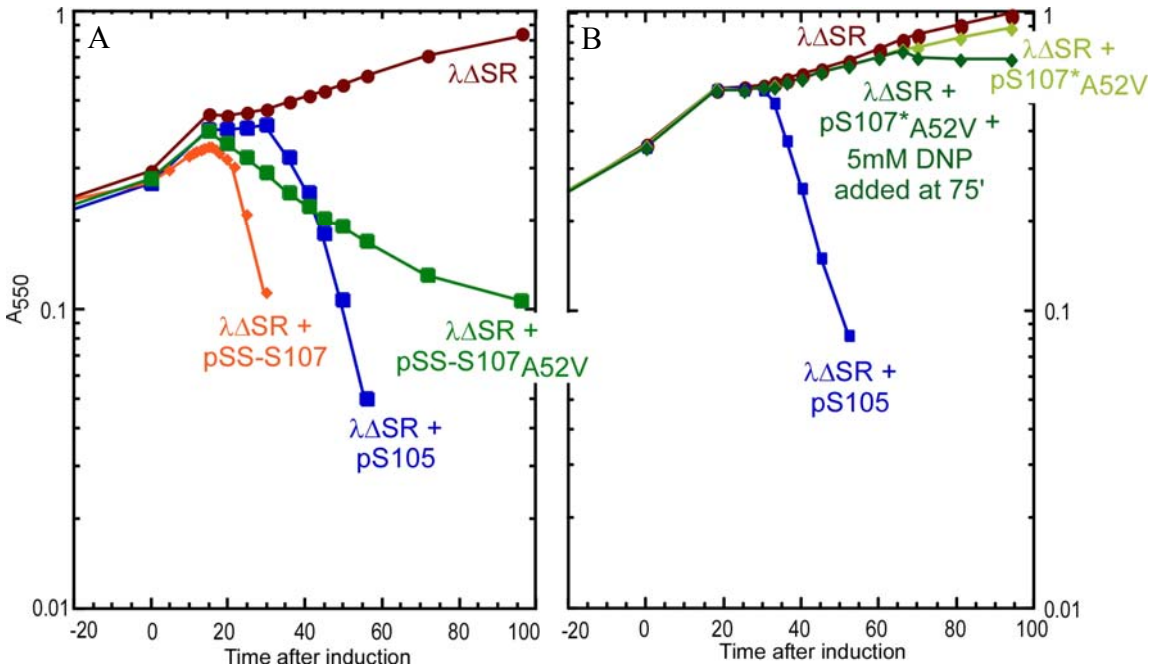

Figure 3.11. Lysis curves of SS-S107, SS-S107$_{A52V,}$ and S107*$_{A52V}$. A) SS-S107 causes lysis at 11' after induction; SS-S107$_{A52V}$ causes cell death and rotting starting at 15' after induction. B) S107*$_{A52V}$ is not harmful to cells, and does not cause lysis or rotting even after the addition of 5 mM DNP.

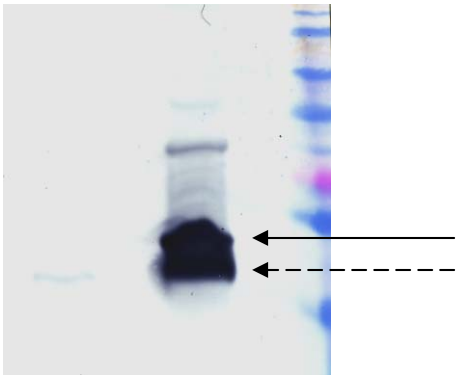

Figure 3.12. Western blot of cells expressing pS105 or pSS-S107$_{A52V}$. Sample was taken 15' after induction. Lane 1, S105 sample, lane 2, empty, lane 3, SS-S107$_{A52V}$, lane 4, empty, lane 5, molecular weight marker. Solid arrow indicates unprocessed form of SS-S107$_{A52V}$, dashed arrow indicates processed form.

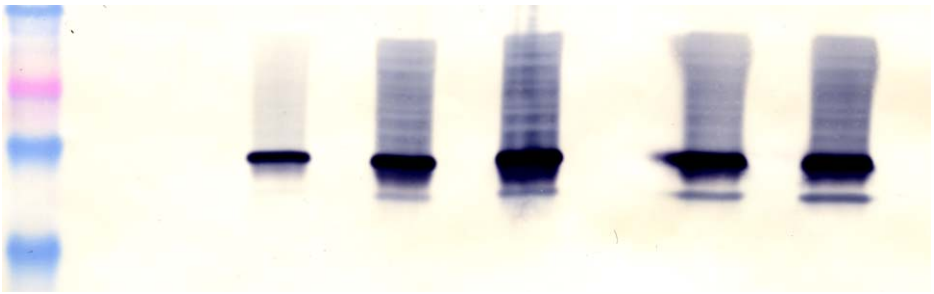

Figure 3.13. Overexpression of SS-S107$_{A52V\tau 94}$. Lane 1, molecular weight marker, lanes 2, 4, 6, 8, 10, and 12 are empty, lanes 3, 5, 7, 9, 11, 13, samples from cells overexpressing SS-S107A52Vτ94 at 0' 30' 60' 90' 120' and 150', respectively.

gene in this construct, and the *SS-S107$_{A52V\tau 94}$* gene was cloned into a pET vector (Novagen) for overexpression. Initial over-expression trials also showed that two products were produced, with the unprocessed form as the major (Figure 3.13). Western blots with the C-terminal S antibody, the His-tag antibody (Amersham), and the

N-terminal S107 antibody showed that the His-tag antibody had much lower sensitivity than the α-S C-terminus antibody, although this has previously been shown (C. Langlais and R. White, unpublished data), and that the α-S107 N-terminus antibody either had even lower sensitivity, or did not recognize the processed product (Figure 3.14). However, since the α-S C-terminus antibody recognizes a significant amount of S protein produced from the over-expression of *SS-S107*$_{A52V\ 94H}$, purification was performed as previously described. The processed and unprocessed forms of purified SS-S107$_{A52V\ 94H}$ were sequenced by Edman degredation and the sequence of the N-termini of both proteins were as predicted (data not shown), indicating that signal sequence of SS-S107$_{A52V\ 94H}$ is cleaved correctly.

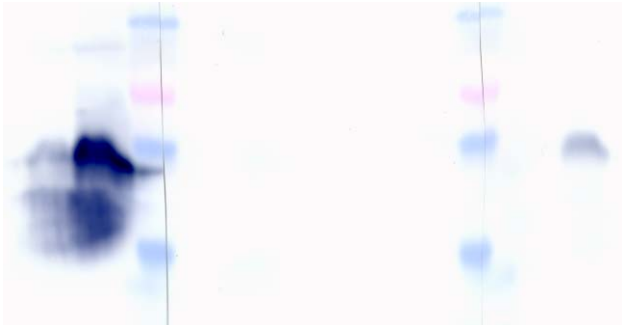

Figure 3.14. Western blot of overexpressed SS-S107$_{A52V\tau 94}$ with different antibodies. Lanes 1, 5, 10, 30' sample, lanes 2, 7, 11, 60' sample, lanes 3, 9, molecular weight marker, lanes 4, 6, 8 are empty; lanes 1, 2, α-S C-terminus antibody, lanes 4-8, α-S107 N-terminus antibody, lanes 10, 11, α-His-tag antibody.

Discussion

Although the holin and endolysin are the only two proteins required for lysis under standard laboratory conditions, many phage also encode an antiholin (11). For many phages, the holin and antiholin are encoded by the same gene, and are expressed via a dual-start motif, with the longer of the two products functioning as the antiholin and differing from the holin by only a few residues (one or more of which is positively charged) at the N-terminus (11). The most-well characterized dual-start holin/antiholin pair is S105 and S107 of bacteriophage λ. It has been proposed that S107 has different topology than S105, and that this altered topology gives S107 its antiholin character (76). The results presented here confirm that hypothesis, indicating that N-terminus (and therefore TMD1) of S105 exists the cytoplasm very rapidly, while the N-terminus of S107 does not, since S107's N-terminus (and TMD1) are prevented from transversing the membrane by the pmf.

Characterization of the deletion allele, $S105_{\Delta TMD1}$, revealed that in addition to being completely defective for lysis, it was also an effective antiholin. Thus, the absence of TMD1 from the membrane confers antiholin character to $S105_{\Delta TMD1}$, indicating that it is the absence of TMD1 from the membrane and not the presence of the N-terminus in the cytoplasm that makes S107 an antiholin, via its alternative topology. In addition to being completely lysis defective, $S105_{\Delta TMD1}$ cannot be artificially triggered to cause lysis with energy poisons, indicating that TMD1 is essential for hole formation. Unlike the block imposed by S107, the lysis block caused by co-expressing S105 and $S105_{\Delta TMD1}$ cannot be subverted by energy poisons, which means that the sentinel function of the

holin-antiholin complex has been abolished. The ability of the holin, and in the case of S107, the antiholin, to be triggered by depolarization of the membrane is critical, since it serves as a sensor of the outside environment. Without the sentinel function, other phages would be allowed to co-infect hosts that already have productive infections in progress, thus decreasing the ability of phage to compete with other phages.

In initial tests, the block imposed on S105 by $S105_{\Delta TMD1}$ was very strong, and could not be subverted even with the addition of energy poisons. Western blot analysis revealed that the expression systems used in those experiments gave a 1:7 ratio of S105 to $S105_{\Delta TMD1}$. Altering the expression system such that the ratio of expression was closer to 1:1-2 showed that in the absence of a severe excess of $S105_{\Delta TMD1}$, the block was temporary. This suggested that in the first experiments, the block was permanent because all of the S105 molecules were interacting with the $S105_{\Delta TMD1}$, and therefore a large enough population of S105 homodimers could not accumulate and effect hole formation. $Cu(Ph_3)$ crosslinking confirmed this hypothesis, since no S105 homodimer band was observed in the $S105_{\Delta TMD1}$ sample, and the amount of $S105_{\Delta TMD1}$ far exceeded the amount of S105 present in the sample. In the second set of experiments, since the ratio was only approximately 1:1.5, a significant portion of the S105 molecules were free to interact with each other, and eventually accumulated to a level that supported hole formation, resulting in lysis. This indicated that the ratio of holin:antiholin is important for the scheduling of lysis, although it is the amount of "free" S105 that determines lysis timing. Based on the dominance/recessiveness tests of many *S105* alleles, mutations were selected to create mutants to test whether the strength of the S105-$S105_{\Delta TMD1}$

interaction is also important. Only a few of those mutants, however, exhibited decreased inhibition of wild-type, despite the fact that all of the mutants, in the S105 context, presumably do not interact with S105 since they are either lytic dominant or recessive alleles. This indicates that TMD1, in addition to be essential for lysis, influences the intermolecular interactions of S. Several mutants of $S105_{\Delta TMD1}$ did not inhibit S105 as well as the wild-type $S105_{\Delta TMD1}$, and $Cu(Ph_3)$ crosslinking revealed that this is because they do not interact as well with S105. While no S105 homodimer band was observed for either the $S105_{\Delta TMD1}$ or $S105_{\Delta TMD1\ A52V}$, both of which cause a permanent lysis block when expressed in severe excess of the wild-type, an S105 homodimer band approximately equivalent to the one seen in the S105 only sample was observed in the $S105_{\Delta TMD1\ A52G}$ sample. This indicates that if a population of S105 is able to accumulate to the appropriate level in the absence of interaction with $S105_{\Delta TMD1}$, lysis will occur regardless of the amount of $S105_{\Delta TMD1}$ present. Similarly, when $S105_{A52G}$ is expressed with $S105_{\Delta TMD1\ A52G}$, strong inhibition of lysis is observed, and this inhibition is correlated with crosslinking, while expressing $S105_{A52G}$ is expressed with $S105_{\Delta TMD1}$ leads to decreased inhibition and crosslinking. The effects of the various $S105_{\Delta TMD1}$ alleles on plaque formation by λ*S105* confirmed this result. $S105_{\Delta TMD1}$ and $S105_{\Delta TMD1\ A52V}$ both cause a significant decrease in plaque size and in efficiency of plating, where $S105_{\Delta TMD1\ A52G}$, which shows decreased inhibition of S105, has a smaller and less dramatic effect. Thus, in addition to the ratio of holin to antiholin molecules, the strength of the interaction between the holin and antiholin molecules is also important for inhibition.

Given the apparent importance of the ratio of holin to antiholin ratio in the scheduling of lysis, further studies of the control of this ratio are required. Since S105 and S107 differ so little, and many conditions will need to be tested, a simple and sensitive assay, such as an ELISA or quantitative Western blotting, would ideally be employed. Antibodies specific to either protein with little cross recognition were obtained, but both ELISA assays and quantitative Western blotting require purified S105 and S107. S105 has been purified successfully in several studies (21, 67, 70, 72), but S107 with the native N-terminal sequence (MKMPEK…) has not been purified. Several attempts to create a construct that expressed only S107, and not S105, failed. Western blot analysis of the successful construct, pSS-S107$_{A52V\ 94H}$, revealed that a significant amount of protein was produced, although the expression of the SS-S107$_{A52V\ 94H}$ results in cell death observed due to membrane toxicity effects only 15 minutes after induction. Analysis of the processed, purified form of SS-S107$_{A52V\ 94H}$, revealed that the signal sequence is cleaved correctly, despite the fact that the N-terminal S107 antibody does not recognize the protein. It is not clear why the N-terminal S107 antibody does not recognize the processed, purified form of SS-S107$_{A52V\ 94H}$, and the issue is currently under investigation.

CHAPTER IV

LOCALIZATION STUDIES

Introduction

The timing of host lysis is the only decision made in the bacteriophage lytic cycle. To optimize timing, double-stranded DNA phages use a 2-component lysis system consisting of a soluble muralytic enzyme, the endolysin, and a small membrane protein, the holin. The holin is the key to timing; it accumulates harmlessly in the membrane until, at an allele-specific time, it triggers to form a lesion in the membrane, allowing the endolysin to escape across the bilayer and degrade the cell wall, causing lysis within seconds. The lysis genes of bacteriophage λ have been well characterized (86). The λ holin, S105, has been shown to oligomerize in the inner membrane (36, 87), and this oligomerization is required for hole formation (36). The hole formed by S105, with a diameter of at least 15 nm, is larger than any other known transmembrane channel formed by alpha-helical proteins, and is non-specific (81).

The current model for hole formation proposes that S105 forms "rafts" in the cytoplasmic membrane, and that these rafts grow until a defect occurs, causing local pmf depletion and holin triggering (81). Although oligomerization is required for hole formation (36), and the hole formed by S105 is very large, the exact steps of lesion formation, the number of holes per cell, and the exact size of the hole-forming complex are unknown.

Here, we report localization studies using GFP-fusion technology to investigate the process of hole formation at the single-cell level, in an attempt to determine the steps of hole formation and the number of holes per cell, and to characterize the "hole" or lesion complex .

Materials and methods

Materials, strains, bacteriophage, plasmids, and growth media

FM-464 was purchased from Invitrogen Molecular Probes (Eugene, OR). All other reagents were of the highest purity commercially available. The strains XL1Blue and BL21(DE3), the lysis-defective thermoinducible prophages *λΔSR,* $\lambda S105_{\Delta TMD1}$, and *λSam7*, and the lysis-proficient thermoinducible prophages λS105 (expressing *S105*) have been described previously (35, 57, 70, 73). The plasmids used in this work are described in Table 4.1.

Table 4.1. Strains, phage and plasmids.

Strain, phage or plasmid	Genotype/features	Source or reference
Strains		
MC4100 *ΔtonA*	E. coli K-12 F^- *araD139 Δ(argF-lac)U169 rpsL15 relA1flbB3501 deo pstF25 rbsR ΔtonA*	Lab stock
MDS12 *ΔtonA*	MG1655 with 12 deletions, totaling 376,180 nt including cryptic prophages; *ΔtonA*	(45)

Table 4.1 Continued

Strain, phage or plasmid	Genotype/features	Source or reference
XL1Blue	E. coli K-12 *recA endA1 gyrA96 thi1 hsdR17 supE44 relA1 lac* [F' *proAB lacZΔM15::tn10*]	Stratagene
Phage	Description	Source
λΔSR	*Δ(stf-tfa)::cat* cI_{857} Δ(*SR*)	(72)
λSam7	*Δ(stf-tfa)::cat* cI_{857} *Sam7*	(73)
λS105	*Δ(stf-tfa)::cat* cI_{857} S_{M1L}	(73)
Plasmid	Description	Source
pS105	λ lysis gene region with S_{M1L} cloned into pBR322, amp^R	(36)
pS105*R_{E19Q}	Same as pS105, but with R_{E19Q}	Lab stock
pS105*2	Same as pS105, but with Rz_{Q100am} and Rz_{W38am}	Lab stock
pλ81-2	Same as pλ81, but with Rz_{Q100am} and Rz_{W38am}	(82)
pS105(xR)GFP_{2aa}	Same as pS105, but with $GFP_{mut2\ A206K}$ fused to the C-terminus of S105 with a 2aa (PG) linker	This study
pS105(xR)GFP_{9aa}	Same as pS105, but with $GFP_{mut2\ A206K}$ fused to the C-terminus of S105 with a 9aa (PGASSGAGG) linker	This study
pS105(xR)GFP_{13aa}	Same as pS105, but with $GFP_{mut2\ A206K}$ fused to the C-terminus of S105 with a 13aa (PGSAGAASGSAGG) linker	This study
pS105(xR)GFP_{20aa}	Same as pS105, but with $GFP_{mut2\ A206K}$ fused to the C-terminus of S105 with a 20aa (PGASSGAGGSAGAASGSAGG) linker	This study
pS105(xR)GFP_{30aa} = pS105ΦGFP	Same as pS105, but with $GFP_{mut2\ A206K}$ fused to the C-terminus of S105 with a 30aa (PGSASGAAGAGSASSGAGGSAGAASGSAGG) linker	This study

Table 4.1 Continued

Strain, phage or plasmid	Genotype/features	Source or reference
pSwtΦGFP	Same as pS105 ΦGFP, but without the *Met1Leu* mutation (82)	This study
$pS105_{A52G}$ΦGFP	Same as pS105 ΦGFP, but with the *Ala52Gly* mutation (82)	This study
$pS105_{A52V}$ΦGFP	Same as pS105 ΦGFP, but with the *Ala52Val* mutation (82)	This study
$pS105_{\Delta TMD1}$ΦGFP	Same as pS105 ΦGFP, but with the *ΔTMD1* mutation (82)	This study
$pS105_{\Delta TMD1}$ΦCherry FP	Same as pS105 ΦGFP, but with the *ΔTMD1* mutation (82) and CherryFP (88) instead of GFP	This study

Media, growth conditions, and thermal induction of the λ lysis genes from a prophage and/or plasmid have been described previously (17, 37, 72). Bacterial cultures were grown in standard LB medium supplemented with ampicillin (100 μg/ml) and chloramphenicol (10 μg/ml) for the maintenance of plasmids and prophage, respectively.

Standard DNA manipulations, PCR, site-directed mutagenesis, and DNA sequencing

Isolation of plasmid DNA, DNA amplification by PCR, DNA transformation, and DNA sequencing were performed as previously described. Primers were obtained from Integrated DNA Technologies, Coralville, IA, and were used without further purification. Restriction and DNA-modifying enzymes were purchased from New England Biolabs; all reactions using these enzymes were performed according to the manufacturer's instructions. Site-directed mutagenesis was performed using the

QuikChange kit from Stratagene as described previously (37). The DNA sequence of all constructs was verified by automated fluorescence sequencing performed at the Laboratory for Plant Genome Technology at the Texas Agricultural Experiment Station.

Plasmid construction and generation of recombinant bacteriophage

The primers used in this study are listed in Appendix A. All enzymatic reactions were performed according to the manufacturer's instructions. The plasmid pR'GFP_{A206K} was created by subcloning the BamHI/HindIII GFP_{mut2} fragment from pDS439 (69) into pRE (52), creating the plasmid pR'GFP. The monomerization mutation *A206K* (88) was introduced into pR'GFP via site-directed mutagenesis. The plasmid pS105(xR)GFP_{2aa} was constructed via splicing by overlapping extension (SOE) PCR (42) from pS105 and pR'GFP_{A206K} using primers SEcoRI For, SxRGFP For-RC, SxRGFP For, and GFP ClaI/XhoI Rev. Briefly, these primers were used to amplify S105 from pS105 and GFP_{A206K} from pR'GFP_{A206K} (referred to as GFP in this work), respectively, with 26 nucleotides of S105 on the 5' end of the two amino acid linker and 26 nucleotides of GFP on the 3' end of the linker. The primers used for the initial amplification mutated the ATG of the *R* gene (via silent mutation of the *S* gene) to inactivate any translation from the *R* translational start site. The two products were PCR purified using the PCR Purification Kit (Qiagen), and then used as template in the second PCR reaction with SEcoRI For and GFP ClaI/XhoI Rev. The resulting PCR product was PCR purified, digested with EcoRI and AatII, ligated with T4 DNA ligase into EcoRI-AatII cut, gel-purified pS105, and transformed into XL1 Blue. Transformants were screened via

colony PCR, and plasmids from candidates that tested positive were sequenced. The linker was successively elongated to 9, 13, 20, and 30 amino acids using QuikChange Mutagenesis. Following DpnI digestion, the products were PCR purified, treated with T4 Polynucleotide kinase and ligated with T4 DNA ligase (according the manufacturer's instructions). The ligation was transformed into XL1 Blue; transformants were screened by colony PCR and plasmids from candidates that tested positive were sequenced. The resulting plasmids were called pS105(xR)GFP$_{9aa}$, pS105(xR)GFP$_{13aa}$, pS105(xR)GFP$_{20aa}$, and pS105(xR)GFP$_{30aa}$, respectively; the plasmid pS105(xR)GFP$_{30aa}$ was chosen for further study and will be called pS105ΦGFP for the remainder of this work. S105 mutants of pS105ΦGFP were created via site-directed mutagenesis as previously described (82).

To create pS105ΦGFP R^{+}Rz^{+}Rz1^{+}, the R, Rz and Rz1 genes from pS105 were amplified with R XhoI For and pS105 ClaI Rev. Following PCR purification and digestion with XhoI and ClaI, the PCR product was ligated into XhoI-ClaI cut, gel-purified pS105ΦGFP, and transformed into XL1 Blue. Transformants were screened by colony PCR and plasmids from candidates that tested positive were sequenced.

The plasmid pS105$_{\Delta TMD1}$ΦCherryFP was constructed via SOE PCR (42) from pS105$_{\Delta TMD1}$ΦGFP and pmCherry (88) using primers SEcoRI For, 30aa CherryFP For, 30aa CherryFP For-RC, and CherryFP Rev.

Recombinant phage were constructed as follows: Plasmids were transformed into MDS12 *ΔtonA* (λΔSR) and individual transformants were grown up and induced as previously described. Chloroform (final concentration, 1%) was added to the cultures 2

hours after induction, or when lysis was complete; in the case of R^- constructs, 10 mls of cells were harvested by centrifugation (3,000 rpm in clinical centrifuge), resuspended in 2 ml of λ dilution buffer, and disrupted by passage through a French pressure cell (Spectronic Instruments, Rochester, NY) at 16,000 lb/in^2 (1 lb/in^2 = 6.89 kPa) to release the progeny (chloroform was added to a final concentration of 1% after lysis). Lysates were cleared by centrifugation (3,000 rpm in a clinical centrifuge). Serial dilutions of the lysates were plated on either MDS12 or LE392. The resulting plaques were plaque purified by streaking on a fresh lawns of either MDS12 or LE392. Pickates of purified plaques were used to lysogenize MC4100 *ΔtonA*; lysogens were selected for by plating on LB plates containing chloramphenicol and were screened for single prophages using Single Prophage PCR (55). Positive candidates were used for lysis curves and to create phage stocks.

Protein sample preparation, SDS-PAGE and Western blotting

Detergent extracts enriched in inner membrane proteins were obtained as previously described (17). Briefly, cultures were induced at an A_{550} of 0.3-0.4. After lysis was complete or 100 minutes after induction in cases where lysis does not occur, 10 ml aliquots of the induced cultures were disrupted by passage through a French pressure cell (Spectronic Instruments, Rochester, NY) at 16,000 lb/in^2 (1 lb/in^2 = 6.89 kPa). Following a brief clearing spin, the membrane fraction was collected by centrifugation at 100,000 x *g* for 60 min at 18°C. The membrane pellet was resuspended in 50 µl of membrane extraction buffer (1% Empigen BB, 10% glycerol, 0.5 M NaCl, 20 mM Tris-

HCl, pH 8.0) containing 35 mM $MgCl_2$ to stabilize the outer membranes. This mixture was incubated for 12 to 14 h at 37°C and detergent-insoluble material was removed by centrifugation at 100,000 x *g* for 45 min at 18°C. The detergent-soluble fraction was diluted 1:1 with 2X protein sample loading buffer prior to sodium dodecyl sulfate-polyacrylamide gel electrophoresis (SDS-PAGE) analysis. Proteins were separated on 16.5% SDS-PAGE with a 4% stacking gel. Western blotting and immunodetection with anti-S antibodies were performed as described previously, with the exception that the GFP fusion proteins were detected with either the α-S105 N-terminus (Bethyl Laboratories, Conroe, TX) or α-GFP antibodies (Stressgen, Ann Arbor, MI) (37).

TCA precipitation

1 ml or 5 ml culture aliquots were added to 111 µl or 555 µl, respectively, of cold, 6.1 N trichloroacetic acid, then placed on ice for 30 minutes. The precipitate was collected by centrifugation (15,000 rpm in a tabletop microcentrifuge or 3,000 rpm in a clinical centrifuge, respectively) and washed once with acetone, resuspending the pellet completely. Pellets were air-dried and resuspended in SDS-PAGE loading buffer and run on gels as stated above.

Fluorescence microscopy

Fluorescence microscopy was performed as previously described (47, 54), with the exception that the cells were thermally induced. Briefly, 100 µl of an overnight culture was harvested and resuspended in 1 ml phosphate buffered saline (PBS); 10 µl of

the cell suspension was then placed on an agarose pad (1.2% agarose, 0.25X LB, 0.5 μg/ml FM 4–64; for cells expressing CherryFP fusions, the FM 4-64 was omitted). The agarose pad was heated to 30°C on the stage of the microscope via the WeatherStation™ environmental chamber; the pads were incubated for 2-2.5 hours, and then placed between two modular heating blocks in a 42°C incubator (the blocks were equilibrated to 42°C in the incubator overnight prior to the experiment) for 15 minutes to thermally induce the λ prophage. Following thermal induction, the pads were placed back on the stage (the temperature of the stage and WeatherStation™ was increased to 37°C during the thermal induction period) and images of cells were captured at the times indicated. For time lapse experiments, cells were grown on agarose pads as described and mid-plane images were captured at 1 minute intervals from 75' to 105' after induction. Images were captured with an Applied Precision Spectris optical sectioning microscope system equipped with an Olympus IX70 microscope, an Olympus Plan Apo 100X oil immersion objective (NA 1.4), a Photometrics Cool SNAP HQ digital camera and Delta Vision standard fluorescence filters: FITC for GFP visualization (excitation: blue 490/20 nm; emission: green 528/38 nm) and RD-TR-PE for FM-464 visualization (excitation: green 550/28 nm; emission: orange 617/73 nm). Using SoftWoRx software, 12 optical sections, 0.2 μm apart, were collected for each sample and deconvolved using the constrained iterative deconvolution algorithm. Following deconvolution, the brightness and contrast of each fluorochrome were adjusted with softWoRx software, setting the area outside of cells to be background; images were saved as TIFF files.

Fluorescence Recovery After Photobleaching (FRAP)

FRAP experiments were conducted as previously described (13, 18). Briefly, photobleaching experiments to assess the mobility of S105ΦGFP (or derivatives) used cells grown in liquid culture (0.25X LB, 0.5 μg/ml FM 4–64); 10 μl of cells were removed at the indicated times and applied to coverslips. After collecting a pre-bleach image, photobleaching was achieved using a 0.05 s pulse of a 488 nm argon laser at 50% power, and subsequent GFP images were collected at 3.5 second intervals for up to 10 minutes. Exposure times were limited to 1.5-2.5 seconds. Images were quantified as previously described (13). Briefly, the ‘‘edit polygon’’ function of the Delta Vision version 2.10 software was used to defined individual polygons to represent the background fluorescence, the entire membrane region, and completely unbleached or bleached regions of the cell. Average mean fluorescence from the background region was subtracted from all time points prior to data processing. Since there is an overall loss of fluorescence caused by photobleaching during image acquisition, mean fluorescence for each data region was adjusted for the losses by correcting the values with the application of a ratio created by dividing the first whole-cell fluorescence postbleach value by the last whole-cell fluorescence postbleach value. Data were plotted as time versus mean fluorescence for the unbleached region, the bleached region, and the whole cell fluorescence. To calculate the pixel intensity expected for the theoretical equilibration point, each whole-cell fluorescence ratio was applied to its corresponding mean whole-cell fluorescence value, and it is represented on the graphs as a dotted line.

Raft isolation experiments

Cells were induced as described. After holin triggering, cells from 30 ml samples were collected by centrifugation and the pellets were resuspended in 250 µl of 25% sucrose, 30 mM Tris-HCl, pH 8.0. Then, 10 µl of 0.25 M EDTA, 10 µl of lysozyme (20 mg/ml in water), and 250 µl of distilled water were added, sequentially, and the mixtures were incubated for 10 minutes at room temperature. Next, 100 µl of 1M $MgCl_2$, 10 µl of 10 mg/ml DNase I, and 10 µl of 10 mg/ml pancreatic RNase were added and the samples incubated at room temperature for 30 minutes with occasional mixing. When microscopic examination showed that ~95% of the cells had formed spheroplasts, an equal volume of 1% detergent was added to rupture the spheroplasts. Detergents were screened to determine which would solubilize the membrane but not disrupt the rafts. Digintonin was chosen for use in the gradients, since it yielded maximum preservation of the rafts. The cell extracts were then layered on were layered on the top of 12 ml gradients of 5–30% sucrose in the solubilization buffer with a 55% cushion (6 mM Tris, pH8.0, 2 mM EDTA, 0.1% digitonin), and centrifuged at 25°C in a SW41 rotor (Beckman) at 35,000 rpm for 4 hrs. Thirty-three, 400 µl fractions were collected from the top of the gradient. Protein distribution along the gradient was examined by SDS–PAGE, Coomassie brilliant blue staining, and S105 or S105ΦGFP were detected by immunoblotting as previously described.

Results

Effects of linker length on holin function

Mutants of S105 must be tested for both lysis timing and lysis efficiency to ensure that the hole is formed normally. Given S105's sensitivity to single amino acids changes, fusing it to green fluorescent protein (GFP), a protein approximately 2.5 times larger, would more than likely have a detrimental effect on lysis timing. Initial fusions of S105 and GFP, where GFP was inserted after codon 94 – the position of the His-tag insertion with the least affect on lysis timing or efficiency – were non-functional (data not shown). Fusing GFP to the extreme C-terminus with an intervening linker of only 2 amino acids resulted in a partially functional holin (Figure 4.1). Successively

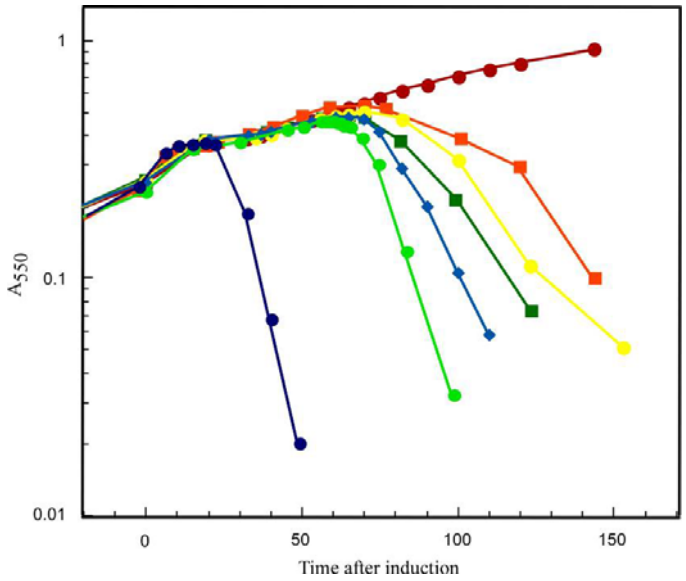

Figure 4.1. Lysis curves of S105ΦGFP fusions. (●) λ*Sam7* + pS105(xR)GFP$_{2aa,}$ (■) λ*Sam7* + pS105(xR)GFP$_{2aa,}$ (●) λ*Sam7* + pS105(xR)GFP$_{9aa,}$ (■) λ*Sam7* + pS105(xR)GFP$_{13aa,}$ (♦) λ*Sam7* + pS105(xR)GFP$_{20aa,}$ (●) λ*Sam7* + pS105(xR)GFP$_{30aa,}$ and (●) λ*Sam7* + pS105.

lengthening the linker resulted in increased holin function (Figure 4.1). All of the fusions were localized to the membrane (Figure 4.2), although there were slight differences in the amount of fusion protein produced. The fusion construct with the 30 amino acid linker was chosen for further study since it exhibited the best lysis phenotype, and will be called S105ΦGFP for the remainder of this work.

Figure 4.2. Western blot analysis of S105ΦGFP fusions. Samples were taken 75 minutes after induction and membrane samples were prepared as described in Materials and Methods. Lane 1, S105(xR)ΦGFP$_{2aa}$ soluble fraction, lane 2, S105(xR)ΦGFP$_{2aa}$ membrane fraction, lane 3, S105(xR)ΦGFP$_{9aa}$ soluble fraction, lane 4, S105(xR)ΦGFP$_{9aa}$ membrane fraction, lane 5, S105(xR)ΦGFP$_{13aa}$ soluble fraction, lane 6, S105(xR)ΦGFP$_{13aa}$ membrane fraction, lane 7, S105(xR)ΦGFP$_{20aa}$ soluble fraction, lane 8, S105(xR)ΦGFP$_{20aa}$ membrane fraction, lane 9, S105(xR)ΦGFP$_{30aa}$ soluble fraction, lane 10, S105(xR)ΦGFP$_{30aa}$ membrane fraction, lane 11, molecular weight marker. Note that S105(xR)ΦGFP$_{2aa}$ shows significantly less protein than the other samples.

S105ΦGFP forms multiple rafts per cell

To visualize S105ΦGFP, deconvolution fluorescence microscopy was employed. Cells were grown and induced on agar pads, and images were captured every 15 minutes beginning at 30 minutes after induction (Figure 4.3; medial focal planes are shown).

These images showed that raft formation occurs very late after induction; only small rafts were seen as late as 90 minutes after induction (Figure 4.3). Analysis of the optical sections from the 60 minute time point reveal that S105ΦGFP is very evenly distributed throughout the membrane (Figure 4.4); analysis of the optical sections from the 105 minute time point (Figure 4.5) reveal that there are multiple rafts per cell, multiple sizes of rafts per cell, and that these rafts do not seem to localize to any particular section of the cell. Although a direct analysis of the size of the rafts is not possible, based on the approximate number of S105ΦGFP molecules per cell (from quantitative Western blotting, data not shown), the largest of the rafts may consist of as many as 1,000 molecules, and the smallest of the rafts may consist of as few as 50 molecules. The number of large rafts per cell ranges from 0 to 9, with the average being 3.3 (for 229 cells counted, Figure 4.6). Analysis of S105 oligomerization mutants fused to GFP showed that the non-lytic mutants do not localize (Figure 4.7, only $S105_{A52V}$ΦGFP is shown), indicating that oligomerization is required for raft formation. When the fast-lysing mutant, the $S105_{A52G}$ is fused to GFP, it triggered with fewer molecules (as is the case without the fusion), and forms fewer smaller rafts than S105 (Figure 4.7), although the average number rafts is similar (3.7, 57 cells counted, Figure 4.6). The SwtΦGFP fusion, which expresses both S105 and S107, forms more rafts than S105ΦGFP, and forms more larger rafts than S105ΦGFP (Figure 4.7).

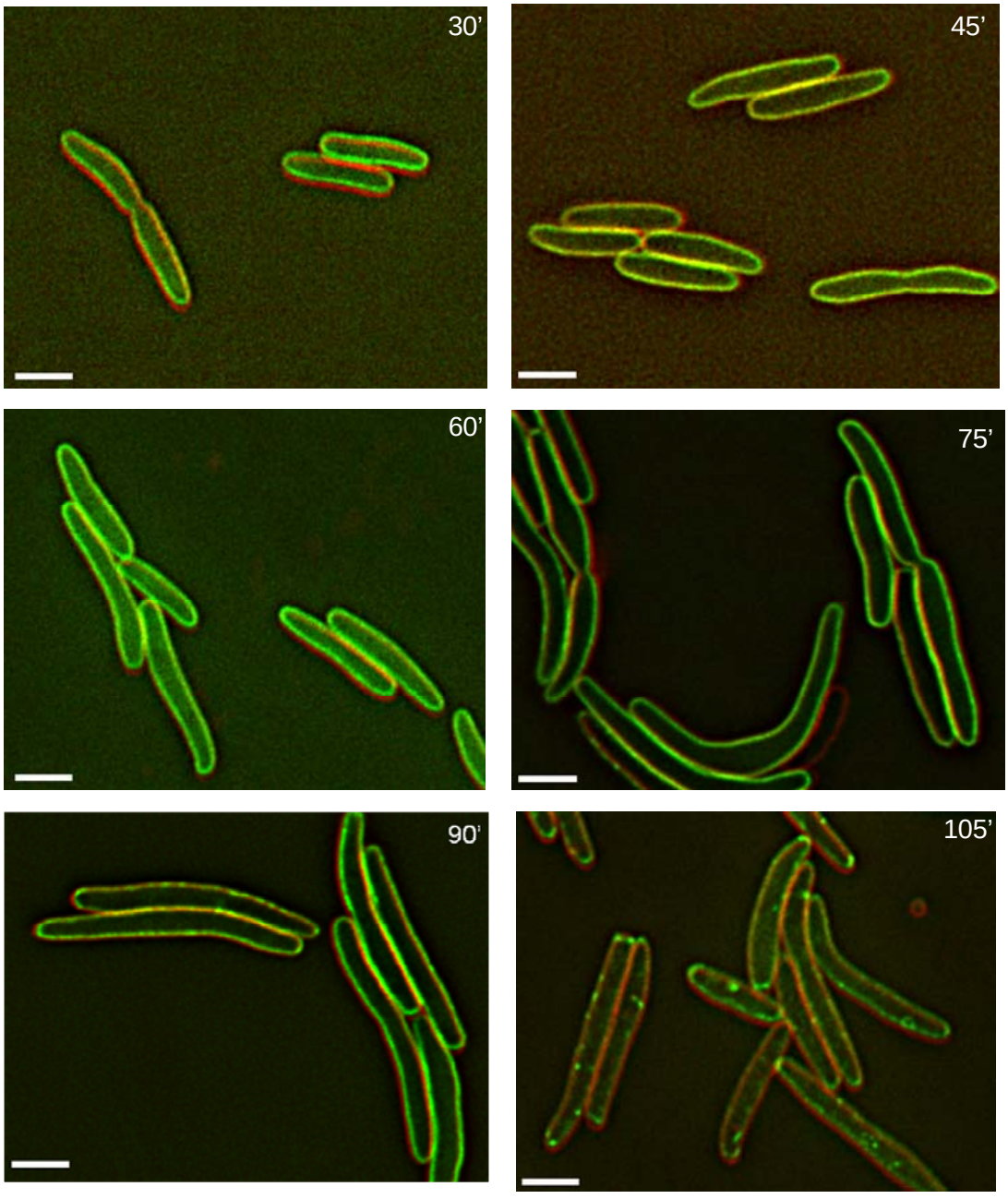

Figure 4.3. Fluorescence images of cells expressing *S105ΦGFP*. The times at which each image was captured are indicated in each panel. Membranes are stained with FM-464 (0.5 μg/ml). Bar = 3 μm. Some raft formation is observed in a few cells at 90' after induction. By 105' after induction, all cells show rafts.

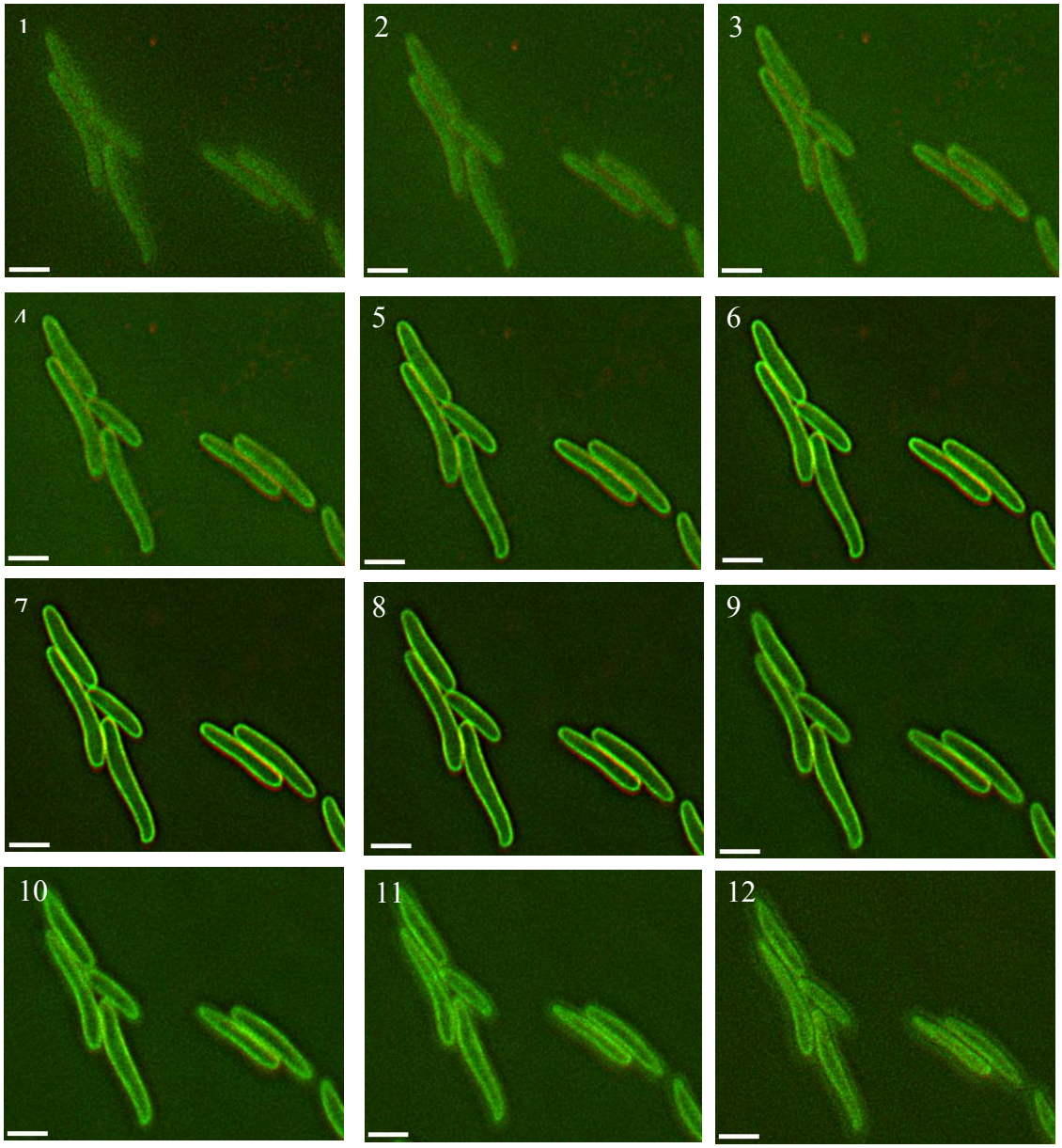

Figure 4.4. Optical sections of cells expressing *S105ΦGFP* before hole formation. Starting from the top left and moving left to right, top to bottom, the 12 optical sections show S105ΦGFP 60 minutes after induction, from the bottom of the cells through the top of the cells. Membranes are stained with FM-464 (0.5 μg/ml). Bar = 3 μm.

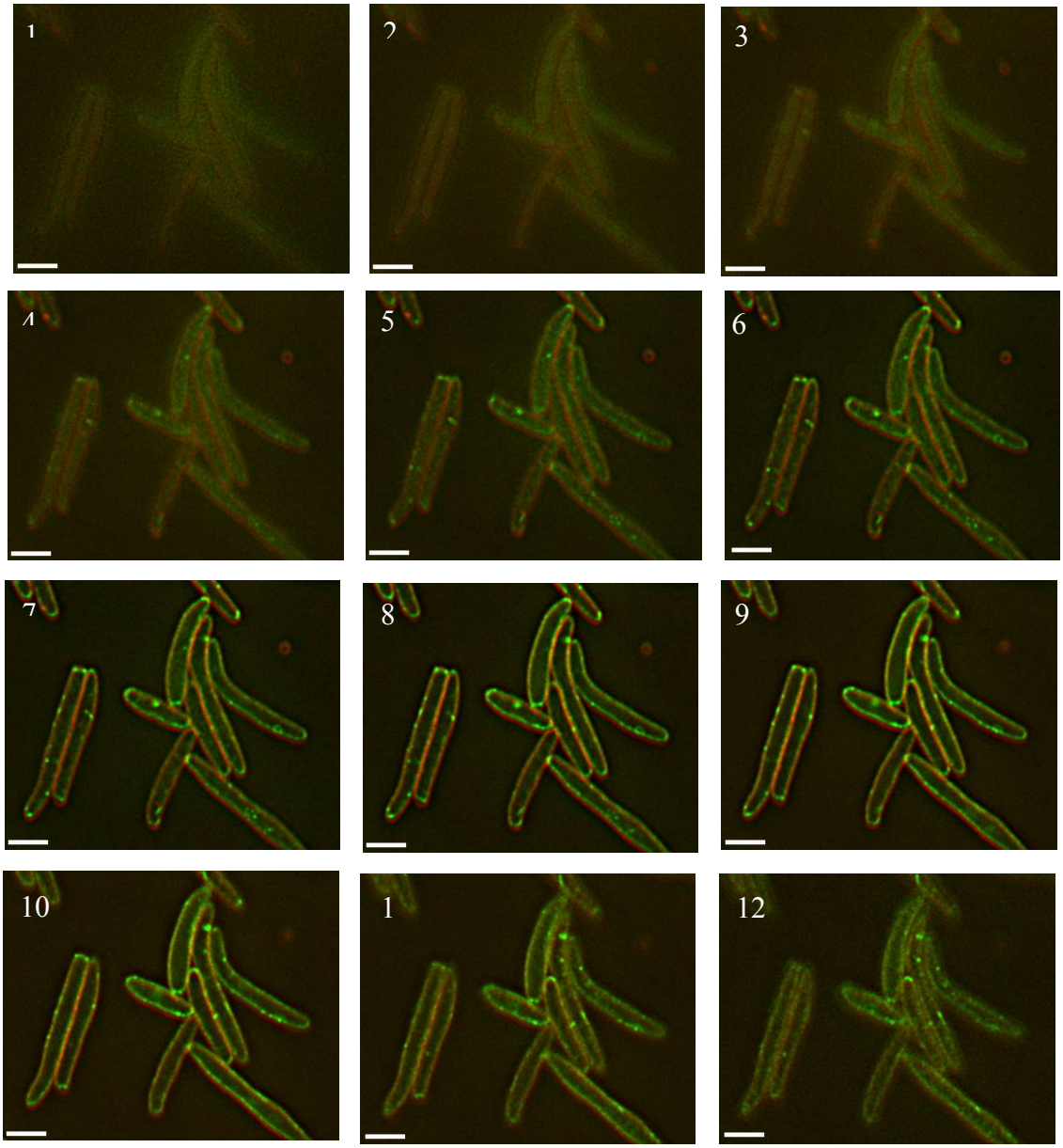

Figure 4.5. Optical sections of cells expressing *S105ΦGFP* after hole formation. Starting from the top left and moving left to right, top to bottom, the 12 optical sections show S105ΦGFP 105 minutes after induction, from the bottom of the cells through the top of the cells. Membranes are stained with FM-464 (0.5 μg/ml). Bar = 3 μm.

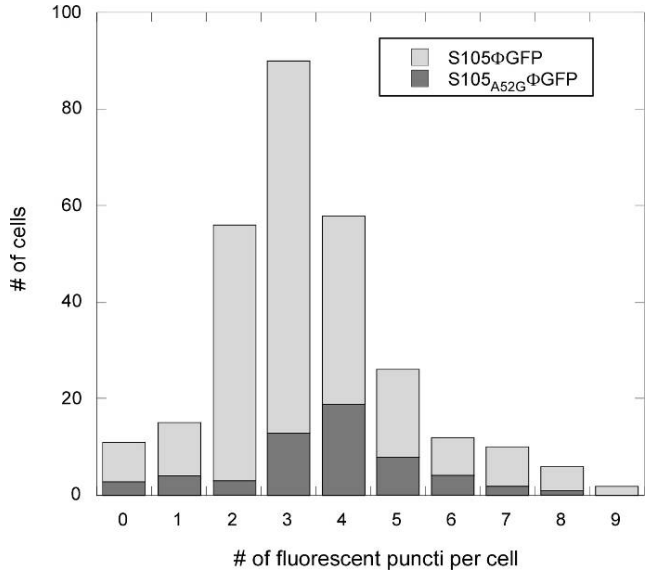

Figure 4.6. Histogram of the number of puncti per cell for S105ΦGFP and $S105_{A52G}$ΦGFP. Only fluorescent puncti, or rafts larger than 3 pixels in diameter were counted as "large" rafts.

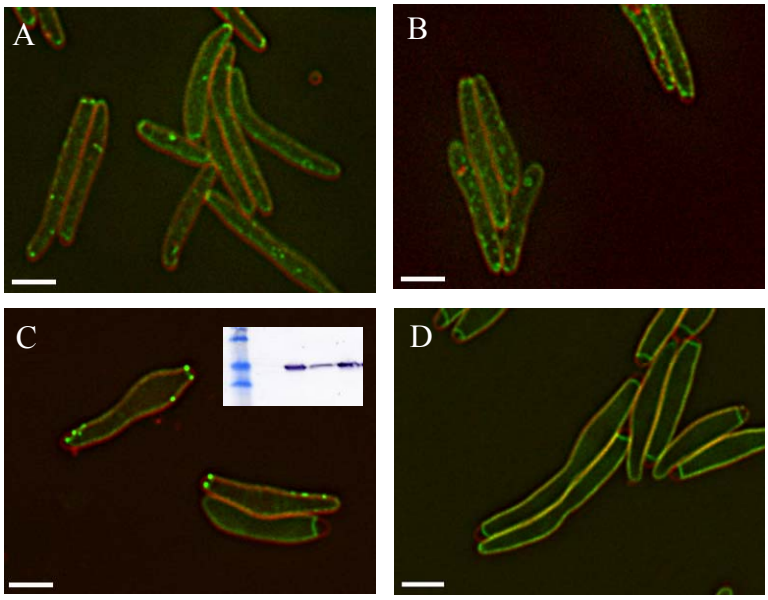

Figure 4.7. Fluorescence images of S105ΦGFP, SwtΦGFP, $S105_{A52G}$ΦGFP, and $S105_{A52V}$ΦGFP. A, S105ΦGFP, 105 minutes after induction, B, SwtΦGFP, C, $S105_{A52G}$ΦGFP, D, $S105_{A52V}$ΦGFP, 120 minutes after induction. Bar = 3 µm. C inset, Western blot of S105ΦGFP fusions. S105ΦGFP and $S105_{A52G}$ΦGFP samples were taken at the time of triggering, and $S105_{A52V}$ΦGFP sample was taken 120' after induction. Bar = 3 µm. Lane 1, molecular weight marker, lane 2, empty, lane 3, S105ΦGFP, lane 4, $S105_{A52G}$ΦGFP, lane 5, $S105_{A52V}$ΦGFP. Note the appearance of more rafts in SwtΦGFP and fewer in $S105_{A52G}$ΦGFP, and the lower amount of protein in the $S105_{A52G}$ΦGFP sample in the Western blot. Interestingly, it appears from these images that FM 4-64 binds only the outer membrane, and does not bind the inner membrane.

Large raft formation by S105ΦGFP is rapid

Since the time course experiments showed that raft formation occurs late after induction, between 90 and 105 minutes, a time-course experiment was conducted to determine when the rafts appeared, and if they grew in size prior to triggering. Images were captured every minute from 75 minutes after induction to 105 minutes after induction. These images show that although some small, transient rafts are present prior the appearance of large rafts, formation of the large, stable rafts occurs in less than a minute (Figure 4.8). The timing of the appearance of the large rafts coincides with the triggering time of S105ΦGFP under similar growth conditions (data not shown). This indicates that the rafts do not form and grow at a constant rate prior to triggering, but instead that appearance of the large rafts occurs suddenly, at or very near the time of triggering.

Formation of rafts by S105ΦGFP is inhibited by S105$_{\Delta TMD1}$ΦCherryFP

It has been recently shown that the allele S105$_{\Delta TMD1}$ is a non-triggerable inhibitor of S105 (82). To investigate the effects of S105$_{\Delta TMD1}$ on raft formation, *S105ΦGFP* and *S105$_{\Delta TMD1}$ΦCherryFP* were co-expressed and visualized. S105ΦGFP and S105$_{\Delta TMD1}$ΦCherryFP co-localize (Figure 4.9), and in the presence of S105$_{\Delta TMD1}$ΦCherryFP, S105ΦGFP does not forms rafts for at least 1 hour after the normal time of raft formation (Figure 4.9). Thus, S105$_{\Delta TMD1}$ inhibits the ability of S105 to form holes by preventing raft formation.

S105ΦGFP rafts are non-mobile

In contrast to the smaller rafts formed prior to triggering, the large rafts formed by S105ΦGFP appeared to be non-mobile. To test the mobility of S105ΦGFP, fluorescence recovery after photobleaching (FRAP) experiments were conducted. The results indicated that prior to triggering, S105ΦGFP is mobile in the membrane (Figure 4.10B) recovering fluorescence in 20 seconds. The control, the non-lytic mutant $S105_{A52V}$ΦGFP, which does not form rafts, showed similar mobility (Figure 4.10A). After triggering, however, the large rafts formed by triggered S105ΦGFP are non-mobile and stable complexes, showing very little recovery over a 2 minute period (Figure 4.10C).

S105ΦGFP and S105 rafts can be isolated

Since the rafts formed by S105ΦGFP are stable complexes, we attempted to isolate the rafts using sucrose velocity gradients. In order to do so, a detergent that solublized the membrane but did not disrupt the rafts was needed. Initial trials using 22 different detergents revealed that only digitonin preserved the rafts completely, although DDM also preserved the rafts to a much lesser extent (Figure 4.11). Velocity gradient analysis of the detergent extracts revealed that S105ΦGFP rafts were stable through the gradient preparation and fractionation, and were very large, with an S value greater than 19S (Figure 4.12). Isolation of S105 rafts showed that they were also stable through the gradient preparation and fractionation, and the approximate S value of the peak fraction was 19S (Figure 4.13). Initial attempts to visualize the rafts by transmission electron

microscopy failed because the samples were too dilute; however, several strategies to improve the method are currently being investigated.

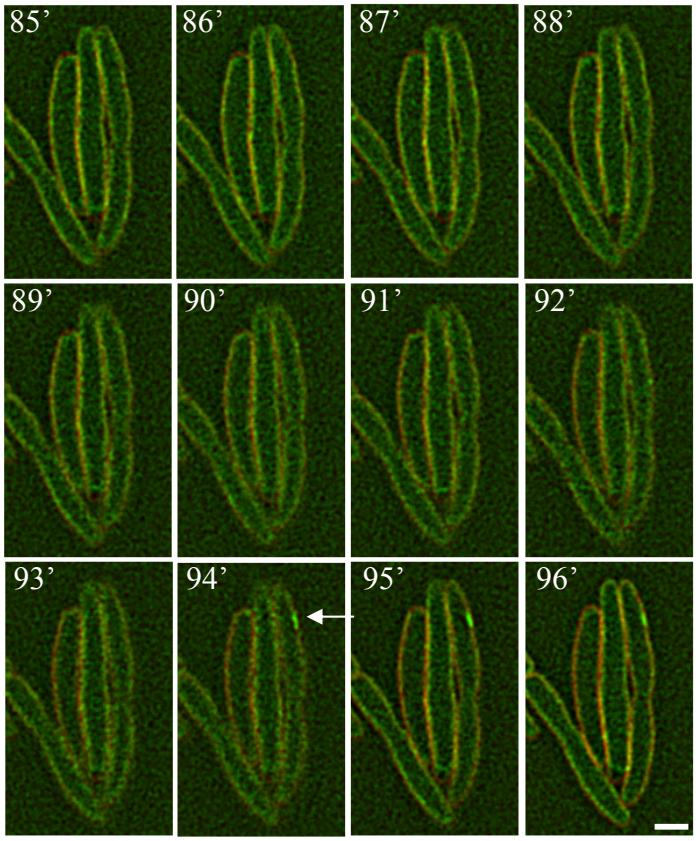

Figure 4.8. Time-lapse images of cells expressing *S105ΦGFP*. Starting at top left and moving left to right and top to bottom, the images were taken at 85’ to 96’. Note that the large raft (indicated by white arrow) appears first at 94’, and does not migrate.

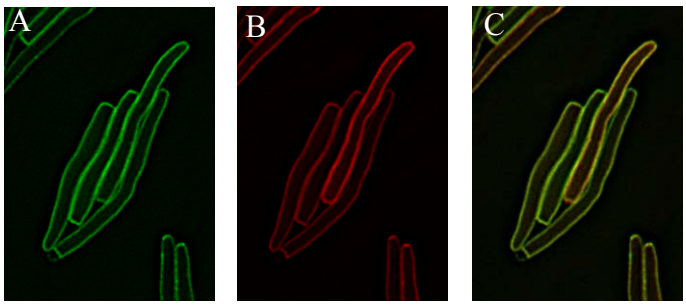

Figure 4.9. Cells co-expressing *S105ΦGFP* and *S105$_{\Delta TMD1}$ΦCherryFP* at 150’. A, S105ΦGFP, B, S105$_{\Delta TMD1}$ΦCherry, C, overlay. The presence of S105$_{\Delta TMD1}$ΦCherryFP prevents S105ΦGFP from forming rafts.

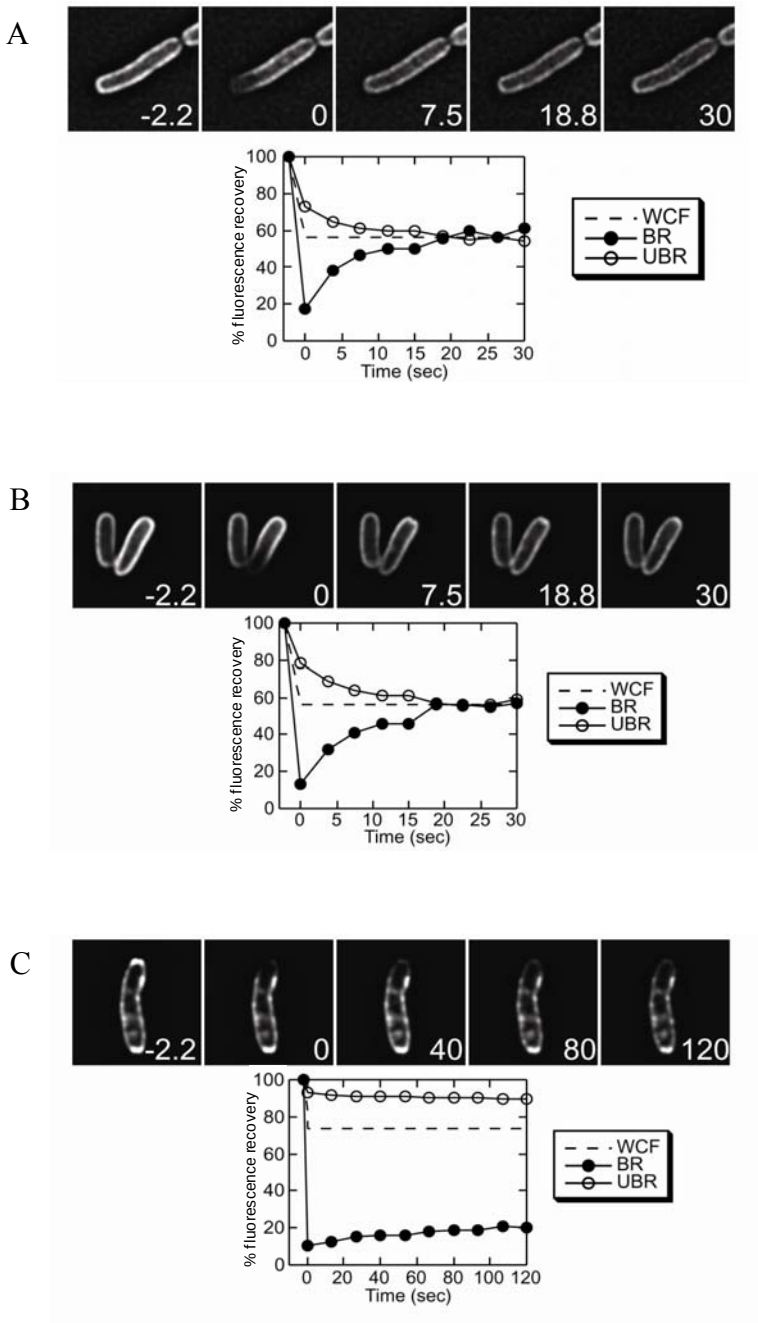

Figure 4.10. FRAP of S105ΦGFP and $S105_{A52V}$ΦGFP. A, $S105_{A52V}$ΦGFP samples were taken 140 minutes after induction. B and C, S105ΦGFP samples were taken at 45 and 140 minutes after induction. Relative fluorescence intensity of the bleached region (black circles) or an unbleached region (open circles) of the cell versus time. The dashed line indicates full recovery. The observed decrease in fluorescence for the unbleached region is due to photobleaching and to incorporation of bleached molecules into the unbleached region of the cell. The observed increase in fluorescence in the bleached region of the cell is due to unbleached molecules moving into the bleached region. Little recovery is observed for S105ΦGFP after triggering, as evidenced by the fact neither the line for the bleached and unbleached region reaches the dashed line, and the increase of fluorescence in the unbleached region is minor.

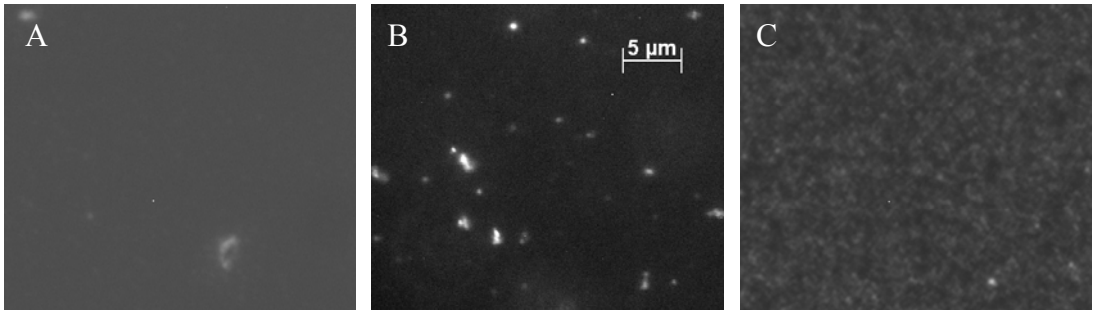

Figure 4.11. Fluorescence images of ruptured spheroplasts made from cells expressing *S105ΦGFP*. A, SDS-ruptured spheroplasts, B, digitonin ruptured spheroplasts, C, DDM ruptured spheroplasts. Note that there is only some large debris present in the SDS sample, while the digitonin sample shows punctuate fluorescence; the DDM sample also shows punctuate fluorescence, but the foci are much smaller than the foci present in the digitonin sample.

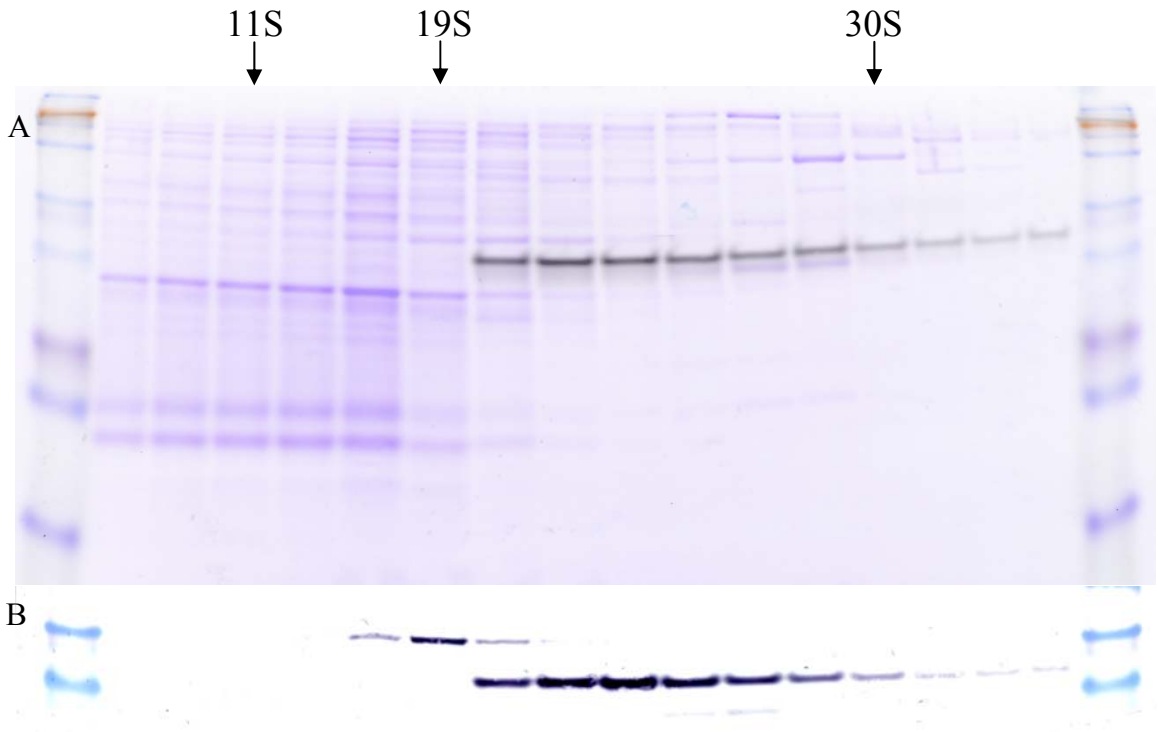

Figure 4.12. Fractionation of digitonin-solubilized S105ΦGFP cell extracts by velocity gradient centrifugation. The gels were loaded with the fractions from the top of the gradient on the left to the bottom of the gradient on the right. A, Coomassie stained gel and fluorescence scan overlay, B, Western blot using α-S105 N-terminus antibodies. The higher bands in the Western blot are due to the unfolding of GFP.

Figure 4.13. Fractionation of digitonin-solubilized S105 cells extracts by velocity gradient centrifugation. The gel was loaded with the fractions from the top of the gradient on the left to the bottom of the gradient on the right, and the Western blot was probed with α-S C-terminus antibodies. The S value peaks are indicated above the gel. The peak fraction of S105 corresponds to the 19S peak fraction.

Discussion

Although much is known about the regulation of S, little is known about the actual lesion formed by S. The λ holin, S105, accumulates harmlessly in the inner membrane until, at a genetically programmed time, it triggers to form the hole, releasing the endolysin and causing lysis (38). Since S105 is very small, and the hole it forms is very large (81), it must oligomerize to accomplish hole formation; S105 has indeed been shown to oligomerize, and this oligomerization is necessary, although not sufficient, for hole formation (36). Based on these and other data, it was proposed that S105 forms "rafts" in the inner membrane in order to form a hole (81). In order to test this hypothesis, a fusion of S105 and GFP was created. Initial fusions, where GFP was fused to S105 at position 94, were non-functional, in that they did not trigger and kill the cells, nor did they release the endolysin. When GFP was fused to the extreme C-terminus of S105 via a 2 amino acid linker, the construct exhibited a slow, inefficient lysis profile

indicating that the hole could form, but that it did not release endolysin efficiently. Subsequent fusions with longer linkers were created, and the lysis profile improved as the linker length increased. Interestingly, the construct with the 30 amino acid linker shows the most similar lysis profile to S105, except that the timing of lysis is significantly delayed. This indicates that the presence of GFP does not affect the size of the hole, since the slope of the lysis curves for S105ΦGFP and S105 are very similar, but that it affects timing. GFP is approximately 2.5 times larger than S105, and this may cause some steric hindrance, even with the 30 amino acid linker, which would explain why shorter linker length constructs were less effective holins. Western blot analysis of cells expressing the S105-GFP fusion constructs showed that the construct with the 2 amino acid linker accumulated less protein than the others, although it is not known whether this is due to a difference in translation rate or degradation. The mutant $S105_{A48V}$ does not form dimers or higher oligomers, and is proteolytically unstable (36). Accordingly, if the steric hindrance caused by fusing S105 to GFP with such a short linker prevents the protein from oligomerizing effectively, it may be degraded.

Visualization of S105ΦGFP at various times after induction reveals that for at least the first 60 minutes after induction, S105ΦGFP is evenly distributed throughout the membrane, and shows no subcellular localization. At the 75 minute and 90 minute time point however, small, transient rafts are observed, although there is no difference in the apparent size of the rafts for the two time points. This indicates that these small rafts do not grow in size prior to triggering. After triggering, multiple rafts of multiple sizes are visible in each cell; the average number of large rafts per cell is approximately 3.

Assuming that the rafts are actually the holes, the fact that there are smaller rafts in addition to the large ones is interesting. This could mean that once a large raft is formed, and presumably triggered to form a hole, the resulting pmf depletion would trigger all the other S105ΦGFP molecules to form holes, although those holes would be smaller. It is known that artificially triggering S105 with energy poisons results in smaller holes than when S105 triggers normally (81); the same process may occur during normal triggering, with the exception that there are also multiple large holes. It should be noted that the experiments which indicated a difference in hole size with or without artificial triggering showed that the smaller holes caused by prematurely triggering S105 with energy poisons were large enough to release the endolysin, implying that these smaller holes are fully functional, despite their size. Optical sections of the 105 minute time point reveal that some rafts are not visible at all planes of focus, indicating that there is no subcellular localization within the depth of the cell. This, taken together with a lack of specific subcellular localization along the length and width of the cell, indicates that S105ΦGFP does not localize to any particular part of the host cell. Time-lapse images of S105ΦGFP show that the large rafts appear suddenly at around 94 minutes after induction, which corresponds well with the lysis time for S105ΦGFP under the conditions used for microscopy (data not shown).

Mutants of S105 were also fused to GFP to test their localization pattern to determine the effects of the mutations on the ability of S105 to form rafts. All of the non-lytic alleles tested were blocked at the dimer stage of oligomerization, with the exception of $S105_{R59C}$, which forms higher oligomers (up to a heptamer), but is still non-

lytic. All of these mutants showed no raft formation, even well after the wild-type S105ΦGFP had triggered. This agrees with previous findings (36) that oligomerization is necessary but not sufficient for hole formation or raft formation. The early lysing mutant, $S105_{A52G}$, showed similar raft formation to S105ΦGFP when fused to GFP, with the exception that there were fewer smaller rafts. Like $S105_{A52G}$, $S105_{A52G}$ΦGFP triggers with much less protein than the wild-type. This, taken together with the fact that $S105_{A52G}$ΦGFP forms fewer smaller rafts, implies that $S105_{A52G}$ΦGFP has a higher self-affinity that the wild-type.

FRAP analysis of $S105_{A52V}$ΦGFP and S105ΦGFP prior to triggering reveals that the two proteins behave similarly, recovering from photobleaching within 20 seconds. After triggering, however, FRAP of S105ΦGFP showed that the large rafts are immobile, and little recovery was observed. These results indicate that S105ΦGFP prior to triggering is freely diffusible in the membrane, as is $S105_{A52V}$ΦGFP; since $S105_{A52V}$ΦGFP is blocked at the dimer stage of oligomerization, it is conceivable that S105ΦGFP exists as dimers prior to raft formation. Little to no recovery after photobleaching is observed for the large rafts for more than 2 minutes after bleaching. A $t_{1/2}$ of 2 minutes corresponds to a diffusion coefficient of 0.002 μm^2 sec^{-1}; this approximately 50 lower than the diffusion coefficient for either $S105_{A52V}$ΦGFP or S105ΦGFP prior to triggering. The small amount of recovery observed in the FRAP analysis of S105ΦGFP after triggering is most likely due to the smaller rafts present in the cell, since they would be mobile, and could thus diffuse into the bleached area.

Since the rafts are stable and seem to be very large, we attempted to isolate the rafts using a velocity gradient. Using S105ΦGFP as a screening tool, we determined that only the detergent digitonin preserved the rafts while solubilizing the membrane. Velocity gradient analysis of the digitonin extracts of cells expressing S105ΦGFP showed that the rafts were stable enough to withstand the gradient procedure, and that they are indeed very large, with an S value greater than 19S. Similarly, the extracts from cells expressing S105 showed that rafts formed by S105 are also stable and very large; the S105 peak fraction coincided with the 19S peak fraction. Unfortunately, attempts to visualize the rafts by transmission electron microscopy failed because the samples were too dilute.

A recent study modeling the process of hole formation by S105 predicted several of these results (65). The authors of that study show mathematically that lysis timing is dominated by raft formation, and that raft formation occurs very close to the lysis time, and that late raft formation is necessary for precise lysis timing. Additionally, they show that the delay between large raft formation and hole formation should be very small (65). Our time-lapse data show the rapid formation of large rafts very late after induction, and we assume that these large rafts correspond to holes. Interestingly, the authors also point out that in their model, holin molecules can form small, transient rafts prior to the nucleation of the large rafts and hole formation; this fits our observations of small rafts appearing as early as 75 minutes after induction. The modeling study also shows that stronger interactions between holin molecules (i.e., self-affinity) will lead to earlier raft nucleation and thus an earlier lysis time. Additionally, their model indicates that there

will be on average 2 rafts per cell, and that the average number of S105 molecules per raft will be 505 (65), which correspond with the numbers from our localization studies.

This study has answered several questions about the lesion formed by S105; the model for hole formation based on this data is presented in Figure 4.14. Since S105 accumulates in the inner membrane without localizing or forming rafts until just before lysis; the large rafts, which we believe are holes, form suddenly just before or at the time of hole formation. Lysis timing, then, is controlled by the formation of these large rafts. Future studies will focus on visualizing the hole using cryo-electron tomography and improving the sucrose gradient isolation protocol so that the rafts can be further characterized and visualized by transmission electron microscopy.

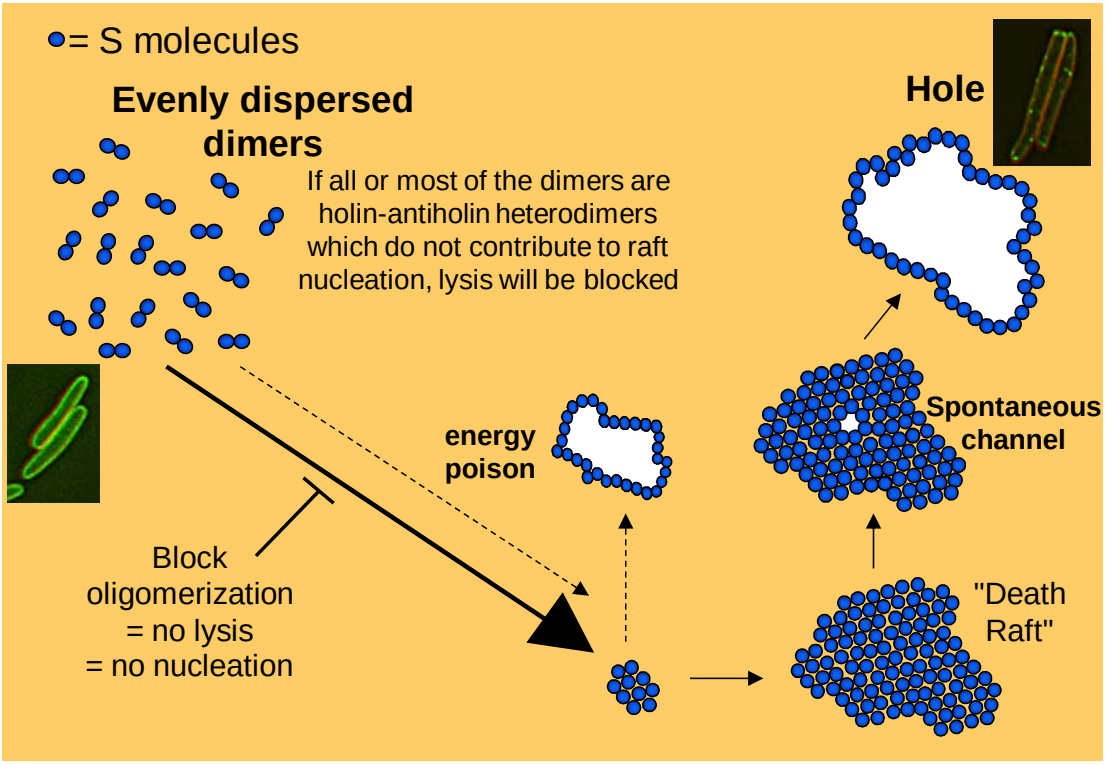

Figure 4.14. Model for hole formation by S105. S105 accumulates in the membrane as dimers and is evenly distributed throughout the membrane until just before triggering. Given that the antiholin inhibits hole formation by directly interacting with the holin, inhibition probably occurs through the formation of holin/antiholin heterodimers; the higher the number of heterodimers formed, the greater the inhibition of lysis. If oligomerization is blocked, as in the case of $S105_{A52V}$, no nucleation occurs and lysis is blocked. Adding an energy poison prematurely triggers the formation of holes, and presumably precipitates raft formation, although the holes formed are smaller than holes that trigger normally (10). The rate limiting step of hole formation is the formation of large rafts, which appear suddenly just before or at the time of hole formation.

CHAPTER V

CONCLUSIONS AND FUTURE DIRECTIONS

It is not often appreciated that the timing of host lysis is the only decision made in the bacteriophage lytic cycle. Double-stranded DNA phages use a 2-component lysis system, the holin-endolysin system, to optimize lysis timing. The holin, a small membrane protein, accumulates harmlessly in the membrane until, at a genetically programmed timed, it suddenly triggers to form "holes" in the membrane. This allows the endolysin, a muralytic enzyme and the second component of the system, to escape into the periplasm, where subsequent cell wall degradation leads to lysis. The best characterized holin gene to date is the *S* gene of bacteriophage λ, which has been studied as the effector of lysis since its discovery in 1967. The work in this dissertation has built on the previously accumulated knowledge and has made a number of advances. First, the work in this dissertation has shown that: 1) all three transmembrane domains must interact to accomplish the hole, and the effects of single amino acid substitutions in the TMDs are unpredictable; 2) TMD1 is essential for hole formation and influences the strength of interactions between different holin molecules; 3) the N-terminus of S105 exists the cytoplasm rapidly, and the N-terminus of S107 does not; 4) the alternative topology of S107 makes it a triggerable antiholin, and deleting TMD1 from S105 creates an untriggerable antiholin; 5) both the strength of the interaction between holin and antiholin and the ratio of holin to antiholin are important for the scheduling of lysis; 6) prior to triggering, S105ΦGFP is evenly distributed in the membrane and after triggering

forms multiple rafts of multiple sizes in the inner membrane; 7) the large rafts form rapidly and appear at or just before the time of lysis; 8) the rafts formed by S105ΦGFP are stable and immobile; and 9) the rafts formed by S105ΦGFP and S105 are very large and can be isolated.

Defining the surface of the S hole

Although the mutational analysis presented in this dissertation revealed that all three TMDs must interact to form the hole, there is still little known about the arrangement of the TMDs in the hole forming complex. Recently, Pang et al. (51) showed, using a collection of single cysteine mutants, that the hole facing residues of the S68 holin from phage 21 could be identified using the membrane-impermeable cysteine-modifying reagent, (2-sulfonatoethyl)-methanethiosulfaonate (MTSES) followed by PEGylation with maleimide-PEG_{5000}. In this assay, cysteines that are available for modification by MTSES must be exposed to the aqueous environment; thus, residues in the TMDs are only exposed if they face the hole. Residues that are modified by MTSES are unavailable for modification by maleimide-PEG_{5000}. Therefore, residues that get PEGylated face the lipid and those that do not face the hole. A similar study with S105 should be conducted in order to determine the regions of each TMD that face the hole. This assay requires that the single cysteine mutants forms holes, and a number of the previously characterized single-cysteine mutants are non-lytic and therefore do not form holes (36-37). Because of this, more single-cysteine mutants still need to be created so that there are lytic alleles representing all faces of all three TMDs. Once this collection

is created, it can also be used for cysteine-specific crosslinking to probe the TMD interactions in the hole forming complex as well.

Visualizing the S hole

Although the studies presented in this dissertation show that S105 forms rafts rapidly just prior to or at the time of triggering, a more detailed structure of the rafts needs to be obtained. Recently, Savva et al. (67) showed that S105 forms rings in detergent *in vitro*, and that the ability to form rings in detergent correlates with the ability to form holes *in vivo*, although it is not known if the rings themselves form *in vivo*. Attempts to isolate the rafts were successful, although attempts to visualize the rafts via transmission electron microscopy were not. Attempts to improve the raft isolation method are currently underway. Cryo-electron tomography will be employed in an attempt to visualize the lesions in whole cells. Combined with the single-cysteine mutant experiments listed above, these experiments should give a clear picture of the structure of the S hole complex.

Determining the triggering event

Despite these advances in the study of S, questions about the triggering event remain. We have previously equated "triggering" with hole formation, but these may be separate events. The fluorescence microscopy data indicate that S105 is distributed throughout the membrane until just before or at the time of lysis, when large rafts rapidly form. These results indicate that the triggering event may be the formation of these large

rafts, and that hole formation follows almost instantaneously. This notion is supported by the mathematical model, which says that the rate limiting step in creating a hole is the formation of large rafts and that hole formation proceeds very rapidly afterwards (65). Additionally, mathematical modeling of hole formation indicates that artificially depleting the pmf strengthens holin-holin interactions, leading to the nucleation of rafts (65). Preliminary results in localization studies of S107*ΦGFP show that it is evenly distributed throughout the membrane for more than 2 hours after induction; treating the cells with energy poisons results in rapid conversion of the distributed fluorescence to large rafts (data not shown). This also indicates that triggering may be the formation of the large rafts. Further investigations of the triggering event are required, and future experiments could utilize S107*ΦGFP since it is not lytic until triggered artificially by energy poisons. Experiments similar to the ones performed by Gründling et al. (38) using S105ΦGFP fusions may also help to elucidate the nature of the triggering event.

What does the S hole look like in the membrane of *E. coli*? What is the structure of the hole? How are the TMDs arranged in the hole forming complex? What is triggering? These questions and others will arise as we continue to study the S protein and hole formation.

REFERENCES

1. **Abergel, C., E. Bouveret, J.-M. Claverie, K. Brown, A. Rigal, C. Lazdunski, and H. Bénédetti.** 1999. Structure of the *Escherica coli* TolB protein determined by MAD methods at 1.95Å resolution. Structure. **7**:1291-1300.

2. **Adhya, S., A. Sen, and S. Mitra.** 1970. Role of gene S, p.743-746. *In* A.D. Hershey (ed.), The Bacteriophage Lambda. Cold Spring Harbor Laboratory Press, Cold Spring Harbor, NY.

3. **Agu, C.A., R. Klein, J. Lengler, F. Schilcher, W. Gregor, T. Peterbauer, U. Bläsi, B. Salmons, W.H. Günzburg, and C. Hohenadl.** 2007. Bacteriophage-encoded toxins: the lambda-holin protein causes caspase-independent non-apoptotic cell death of eukaryotic cells. Cell Microbiol. **9**:1753-1765

4. **Altman, E., K. Young, J. Garrett, R. Altman, and R. Young.** 1985. Subcellular localization of lethal lysis proteins of bacteriophages λ and ϕX174. J. Virology. **53**:1008-1011.

5. **Altman, E.A., R.K. Altman, J.M. Garrett, R.J. Grimaila, and R. Young.** 1983. *S* gene product: identification and membrane localization of a lysis control protein. J. Bacteriol. **155**:1130-1137.

6. **Barik, S. and N.C. Mandal.** 1982. Role of *S* gene product of bacteriophage lambda in host cell lysis. J. Biosci. **4**:361-368.

7. **Bernadac, A., M. Gavioli, J.C. Laxxaroni, S. Raina, and R. Lloubès.** 1998. *Escherichia coli tol-pal* mutants form outer membrane vesicles. J. Bacteriol. **180**:4872-2878.

8. **Berstein, A., B. Rolfe, and K. Onodera.** 1972. Pleiotropic properties and genetic organization of the *tolA, B* Locus of *Escherichia coli* K-12. J. Bacteriol. **112**:74-83.

9. **Bläsi, U., K. Nam, D. Hartz, L. Gold, and R. Young.** 1989. Dual translational initiation sites control function of the λ *S* gene. EMBO J. **8**:3501-3510.

10. **Bläsi, U., C.-Y. Chang, M. T. Zagotta, K. Nam, and R. Young**. 1990. The lethal λS gene encodes its own inhibitor. EMBO J. **9**:981-989.

11. **Bläsi, U., and R. Young.** 1996. Two beginnings for a single purpose: the dual-start holins in the regulation of phage lysis. Mol. Microbiol. **21:**675-682.

12. **Bläsi, U., P. Fraisl, C.-Y. Chang, N. Zhang, and R. Young.** 1999. The C-terminal sequence of the λ holin constitutes a cytoplasmic regulatory domain. J. Bacteriol. **181**:2922-2929.

13. **Broder, D.H. and K. Pogliano.** 2006. Forespore engulfment mediated by a ratchet-like mechanism. Cell. **126**:917-928.

14. **Campbell, J.H., and B.G. Rolfe.** 1975. Evidence for a dual control of the initiation of host-cell lysis caused by bacteriophage lambda. Mol. Gen. Genet. **139**:1-8.

15. **Catterall, W.A.** 2000. From ionic currents to molecular mechanisms: the structure and function of voltage-gated sodium channels. Neuron **26**:13-25.

16. **Chang, C.-Y., K. Nam, and R. Young.** 1993. Synthesis of two bacteriophage λ S proteins in an in vivo system. Gene. **133**:9-16.

17. **Chang, C.-Y., Nam, K., and R. Young.** 1995. S gene expression and the timing of lysis by bacteriophage λ. J. Bacteriol. **177**:3283-3294.

18. **Chiba, S., K. Coleman, and K. Pogliano.** 2007. Impact of membrane fusion and proteolysis on SpoIIQ dynamics and interaction with SpoIIIAH. J. Biol. Chem. **282**:2576-2586.

19. **Cormack, B.P., R.H. Valdivia, and S. Falkow.** 1996. FACS-optimized mutants of green fluorescent protein (GF). Gene **173**:33-38.

20. **Dankenbring, C.A., R.L. White, and R. Young.** 2008. Intragenic suppressors of the lambda holin. Manuscript in preparation.

21. **Deaton, J., C.G. Savva, J. Sun, A. Holzenburg, J. Berry, and R. Young.** 2004. Solubilization and delivery by GroEL of megadalton complexes of the λ holin. Prot. Sci. **13**:1778-1786.

22. **Doermann, A. H.** 1948. Lysis and lysis inhibition of *Escherichia coli* bacteriophage. J. Bacteriol. **55**:257-276.

23. **Engelberg-Kulka, H., M. Reches, S. Narasimhan, R. Schoulaker-Schwarz, Y. Klemes, E. Aizenman, and G. Glaser.** 1998. *rexB* of Bacteriophage λ is an anti-cell death gene. Proc. Natl. Acad. Sci. USA. **95**:15481-15486.

24. **Evrard, C., J. Fastrez, and J.P. Declercq.** 1998. Crystal structure of the lysozyme from bacteriophage lamba and its relationahip with V and C-type lysozymes. J. Mol. Biol. **276**:151-164.

25. **Fields, R.** 1972. The rapid determination of amino froup with TNBS. Methods in Enzymology. **25**: 464-46.

26. **Fung., D.C., and H.C. Berg.** 1995. Powering the flagellar motor of *Escherichia coli* with an external voltage source. Nature. **375**:809-812

27. **Gabel, C.V., and H.C. Berg.** 2003. The speed of the flagellar rotary motor of Escherichia coli varies linearly with protonmotive force. Proc. Natl. Acad. Sci. USA **100**:8748-8751.

28. **Garrett, J., R. Fusselman, J. Hise, L. Chiou, D. Smith-Grillo., J. Schulz, and R. Young.** 1981. Cell lysis by induction of cloned lambda lysis genes. Mol. Gen. Genet. **182**:326-331.

29. **Garrett, J., C. Bruno, and R. Young.** 1990. Lysis protein S of phage lambda functions in *Saccharomyces cerevisiae*. J. Bacteriol. **172**:7275-7277.

30. **Garret, J.M., and R. Young.** 1982. Lethal action of bacteriophage λ *S* gene. J. Bacteriol. **44**:886-892.

31. **Goldberg, A.R., and M. Howe.** 1969. New mutations in the S cistron of bacteriophage lambda affecting host cell lysis. Virology. **38**:200-202.

32. **Goldberg, E., L. Grinius, and L. Letellier.** 1994. Recognition, attachment and injection, p. 347-356. *In* J. D. Karam (ed.), Molecular Biology of Bacteriophage T4. ASM Press, Washington, DC.

33. **Graschopf, A., and U. Bläsi.** 1999. Functional assembly of the λ S holin requires periplasmic localization of its N-terminus. Arch. Microbiol. **172**:31-39.

34. **Graschopf, A., and U. Bläsi**. 1999. Molecular function of the dual-start motif in the lambda S holin. Mol. Microbiol. **33**:569-582.

35. **Gründling, A., D. Smith, U. Bläsi, and R. Young.** 2000. Dimerization between the holin and holin inhibitor of phage λ. J. Bacteriol. **182**:6075-6081.

36. **Gründling, A., U. Bläsi, and R. Young**. 2000. Genetic and biochemical analysis of dimer and oligomer interactions of the lambda S holin. J. Bacteriol. **182**:6082-6090.

37. **Gründling, A., U. Bläsi, and R. Young**. 2000. Biochemical and genetic evidence for three transmembrane domains in the class I holin, lambda S. J. Biol. Chem. **275**:769-776.

38. **Gründling, A., M. D. Manson, and R. Young**. 2001. Holins kill without warning. Proc. Natl. Acad. Sci. USA **98**:9348-9352.

39. **Harris, A.W., D.W. Mount, C.R. Fuerst, and L. Siminovitch.** 1967. Mutations in bacteriophage lambda affecting host cell lysis. Virology. **32**:553-569.

40. **Hartz., D., D.S. McPheeters, and L. Gold.** 1988. Extension inhibition analysis of translation initiation complexes. Methods Enzymol. **164**:419-425.

41. **Hartz., D., D.S. McPheeters, L. Green, and L. Gold.** 1991. Detection of *Escherica coli* ribosome binding at translation initiation sites in the absence of tRNA. J. Mol. Biol. **218**:99-105

42. **Ho, S.N., H.D. Hunt, R.M. Horton, J.K. Pullen, and L.R. Pease.** 1989. Site-directed mutagenesis by overlap extension using the polymerase chain reaction. Gene. **77**:51-59.

43. **Johnson-Boaz, R., C.-Y. Chang, and R. Young** 1994. A dominant mutation in the bacteriophage lambda *S* gene causes premature lysis and an absolute defective plating phenotype. Mol. Microbiol. **13**:495-504.

44. **Kaiser, K.** 1980. The origin of Q-independent derivatives of phage λ. Mol. Gen. Genet. **179**:547-554.

45. **Kolisnychenko, V., G. Plunkett III, C. D. Herring, T. Fehér, J. Pósfai, F. R. Blattner, and G. Pósfai.** 2002. Engineering a reduced *Escherichia coli* genome. Genome Research **12**:640-647.

46. **Labedan, B., and L. Letellier.** 1981. Membrane potential changes during the first steps of coliphage infection. Proc. Natl. Acad. Sci. USA. **78**:215-219

47. **Liu, N.-J.L., R.J. Dutton, and K. Pogliano.** 2006. Evidence that the SpoIIIE DNA translocase participates in membrane fusion during cytokinesis and engulfment. Mol. Microbiol. **59**:1087-1113.

48. **Matz, K., M. Schmandt, and G.N. Gussin.** 1982. The *rex* gene of bacteriophage lambda is really two genes. Genetics. **102**:319-327.

49. **Mount, D.W.A., A.W. Harris, C.R. Fuerst, and L. Siminovitch.** 1968. Mutations in bacteriophage lambda affecting particle morphogenesis. Virology. **35**:134-149.

50. **Mullineaux, C.W., A. Nenninger, N. Ray, and C. Robinson.** 2006. Diffusion of green fluorescent protein in the three cell environments in *Escherichia coli*. J. Bacteriol. **188**:3442-3448.

51. **Pang, T., C. Savva, D.K. Struck, and R. Young.** 2008. Structure of the S^{21} hole. Manuscript in preparation.

52. **Park, T., D.K. Struck, J.F. Deaton, and R. Young.** 2006. Topological dynamics of holins in programmed bacterial lysis. Proc. Natl. Acad. Sci. USA. **103**:19713-19718.

53. **Parma, D.H., M. Snyder, S. Sobolevski, M. Nawroz, E. Brody, and L. Gold.** 1992. The rex system of bacteriophage lambda: tolerance and altruistic cell death. Genes and Dev. **6**:497-510.

54. **Pogliano, J., T.Q. Ho, Z. Zhong, and D.R. Helinski.** 2001. Multicopy plasmids are clustered and localized in Escherichia coli. Proc. Natl. Acad. Sci. USA. **98**:4486-4491.

55. **Powell, B.S., M.P. Rivas, D.L. Court, Y. Nakamura, and C.L. Turnbough, Jr.** 1994. Rapid confirmation of single copy lambda prophage integration by PCR. Nucleic Acids Res. **22**:5765-5766.

56. **Raab, R., G. Neal, J. Garrett, R. Grimaila, R. Fusselman, and R. Young.** 1986. Mutational analysis of bacteriophage lambda lysis gene *S*. J. Bacteriol. **167**:1035-1042.

57. **Raab, R., G. Neal, C. Sohaskey, J. Smith, and R. Young.** 1988. Dominance in lambda S mutations and evidence for translational control. J. Mol. Biol. **199**:95-105.

58. **Rajagopalan, P. T. R., S. Grimme, and D. Pei.** 2000. Characterization of cobalt(II)-substituted peptide deformylase: function of the metal ion and the catalytic residue Glu-133. Biochemistry. **39**:779-790.

59. **Reader, R.W., and L. Siminovitch.** 1971. Lysis defective mutants of bacteriophage lambda: genetics and physiology of S cistron mutants. Virology. **43**:607-622.

60. **Reader, R.W., and L. Siminovitch.** 1971. Lysis defective mutants of bacteriophage lambda: on the role of the S function of lysis. Virology **43**:623-637.

61. **Rietsch, A., and U. Bläsi.** 1993. Non-specific hole formation in the *Escherichia coli* inner membrane by λ S proteins is independent of cellular *secY* and *secA*

functions and of the proportion of membrane acidic phospholipids. FEMS Microbiol. Lett. **107**:101-106.

62. **Rietsch, A., P. Fraisl, A. Graschopf, and U. Bläsi.** 1997. The hydrophilic C-terminal part of the lambda S holin is non-essential for intermolecular interactions. FEMS Microbiol. Lett. **153**:393-398.

63. **Rolfe, B.G., and J.H. Campbell.** 1974. A relationship between tolerance to colicin K and the mechanism of phage-induced host cell lysis. Mol. Gen. Genet. **133**:293-297.

64. **Rolfe, B.G., and J.H. Campbell.** 1977. Genetic and physiological control of host cell lysis by bacteriophage lambda. J. Virology. **23**:626-636.

65. **Ryan, G.L. and A.D. Rutenberg.** 2007. Clocking out: modeling phage-induced lysis of *Escherichia coli*. J. Bacteriol. **189**:4749-4755.

66. **Saikawa, N., Y. Akiyama, and K. Ito.** 2004. FtsH, exists as an exceptionally large complex containing HflKC in the plasma membrane of *Escherichia coli*. J. Struct. Biol. **270**:23485-23490.

67. **Savva, C., J.S. Dewey, J. Deaton, R.L. White, D.K. Struck, A. Holzenburg, and R. Young.** 2008. The holin of bacteriophage lambda forms rings with large diameter. Mol. Microbiol. Submitted.

68. **Schoulaker-Schwarz, R., L. Dekel-Gorodetsky, and H. Engelberg-Kulka.** 1991. An additional function for the bacteriophage λ *rex*: the rexB product prevents degradation of the λ O protein. Proc. Natl. Acad. Sci. USA. **88**:4996-5000.

69. **Siegele, D.A. and J.C. Hu.** 1997. Gene expression from plasmids containing the araBAD promoter at subsaturating inducer concentrations represents mixed populations. Proc. Natl. Acad. Sci. USA. **94**:8168-8172.

70. **Smith, D. L.** 1998. Purification and biochemical characterization of the bacteriophage lambda holin. Ph.D. dissertation. Texas A&M University, College Station.

71. **Smith, D.L., C.-Y. Chang, and R. Young.** 1998. The λ holin accumulates beyond the lethal triggering concentration under hyperexpression conditions. Gene Expr. **7**:39-52.

72. **Smith, D. L., D. K. Struck, J. M. Scholtz, and R. Young.** 1998. Purification and biochemical characterization of the lambda holin. J. Bacteriol. **180**:2531–2540.

73. **Smith, D. L., and R. Young.** 1998. Oligohistidine mutagenesis of the λ holin gene. J. Bacteriol. **180**:4199–4211.

74. **Sohaskey, C.D.** 1992. Analysis of the λ*S* gene function by mutational suppressors. M.S. thesis. Texas A&M University, College Station.

75. **Solbiati, J., A. Chapman-Smith, J.L. Miller, C.G. Miller, and J.E. Cronan, Jr.** 1999. Processing of the N termini of nascent polypeptide chains requires deformylation prior to methionine removal. J. Mol. Biol. **290**:607-614.

76. **Steiner, M., and U. Bläsi.** 1993. Charged amino-terminal amino acids affect the lethal capacity of Lambda lysis proteins S107 and S105. Mol. Microbiol. **8**:525-533.

77. **Studier, F.W., and B.A. Moffatt.** 1986. Use of bacteriophage T7 RNA polymerase to direct selective high-level expression of cloned genes. J. Mol. Biol. **189**:112-130.

78. **Summer, E.J., J. Berry, T.A.T. Tran, L. Nu, D.K. Struck, and R. Young.** 2007. Rz/Rz1 lysis gene equivalents in phages of Gram-negative hosts. J. Mol. Biol. **373**:1098-1112.

79. **Wang, I. N., A. E. Dykhuizen, and L. B. Slobodkin**. 1996. The evolution of phage lysis timing. Evolution Ecology **10**:545-558.

80. **Wang, I. N., D. L. Smith, and R. Young**. 2000. Holins: the protein clocks of bacteriophage infections. Annu. Rev. Microbiol. **54**:799-825.

81. **Wang, I. N., J. Deaton, and R. Young**. 2003. Sizing the holin lesion with an endolysin-β-galactosidase fusion. J. Bacteriol. **185**:779-787.

82. **White, R.L., C.A. Dankenbring, T.A.T. Tran, J. Deaton, D.K. Struck, and R. Young.** 2008. The N-terminal transmembrane domain of lambda S is required for holin but not antiholin function. Manuscript in preparation.

83. **White, R.L., S. Chiba, K. Pogliano, D.K. Struck, and R. Young.** 2008. Subcellular localization of the lambda holin. Manuscript in preparation.

84. **Wilson, D.B.** 1982. Effect of the lambda *S* gene product on properties of the *Escherichia coli* inner membrane. J. Bacteriol. **151**:1403-1410.

85. **Xu, M., D. K. Struck, J. Deaton, I. N. Wang, and R. Young**. 2004. A signal-arrest-release sequence mediates export and control of the phage P1 endolysin. Proc. Natl. Acad. Sci. USA **101**:6415-6420.

86. **Young, R. and R. White.** 2008. Lysis of the host by bacteriophage. *In*: B.J.W.Mahy and M.H.V. Van Regenmortel (Ed.), Encyclopedia of Virology, Third Ed. Elsevier Ltd., Oxford, U.K. In press.

87. **Zagotta, M.T., and D.B. Wilson.** 1990. Oligomerization of the bacteriophage lambda S protein in the inner membrane of *Escherichia coli*. J. Bacteriol. **172**:912-921.

88. **Zhang, J., R.E. Campbell, A.Y. Ting, and R.Y. Tsien.** 2002. Creating new fluorescent probes for cell biology. Nat. Rev. Mol. Cell. Biol. **3**:906-918.

89. **Zheng, Y., D.K. Struck, C.A. Dankenbring, and R. Young.** 2008. Evolutionary dominance of holin lysis systems derives from superior genetic malleability. Micriobology. Accepted.

APPENDIX A

PRIMERS

Primer	Sequence (mutations underlined and in bold)
A12T For	AAACATGACCTGTTGGCC**ACG**ATTCTCGCGGCAAAGGAA
A12T Rev	TTCCTTTGCCGCGAGAAT**CGT**GGCCAACAGGTCATGTT
A16N For	GGCCGCCATTCTCGCG**AAT**AAGGAACAAGGCATCGGGGC
A16N Rev	GGCCCGATGCCTTGTTCC**TTA**TTCGCGAGAATGGCGGCC
E18K For	CCGCCATTCTCGCGGCAAAG**AAA**CAAGGCATCGGGC
E18K Rev	GCCCCGATGCCTTC**TTT**CTTTGCCGCGAGAATGGCGG
I21T For	CGCGGCAAAGGAACAAGGC**ACC**GGGGCAATCCTTGCGTTTGCAA TGGC
I21T Rev	GCCATTGCAAACGCAAGGATTGCCCC**GGT**GCCTTGTTCCTTTGC CGCG
G22E For	GGCAAAGGAACAAGGCATC**GAG**GCAATCCTTGCGTTTGCAATGG CG
G22E Rev	CGCCATTGCAAACGCAAGGATTGC**CTC**GATGCCTTGTTCCTTTG CC
G22R For	GGCAAAGGAACAAGGCATC**AGG**GCAATCCTTGCGTTTGCAATGG CG
G22R Rev	CGCCATTGCAAACGCAAGGATTGC**CCT**GATGCCTTGTTCCTTTG CC
G22W For	GGCAAAGGAACAAGGCATC**TGG**GCAATCCTTGCGTTTGCAATGG CG
G22W Rev	CGCCATTGCAAACGCAAGGATTGC**CCA**GATGCCTTGTTCCTTTG CC
A23T For	GGAACAAGGCATCGGG**ACA**ATCCTTGCGTTTGCAATGG
A23T Rev	CCATTGCAAACGCAAGGAT**TGT**CCCGATGCCTTGTTCC
A23V For	GGCAAAGGAACAAGGCATCGGG**GTA**ATCCTTGCGTTTGCAATGG CG
A23V Rev	CGCCATTGCAAACGCAAGGAT**TAC**CCCGATGCCTTGTTCCTTTG CC
L25G For	CAAGGCATCGGGGCAATC**GGC**GCGTTTGCAATGGCGTAC
L25G Rev	GTACGCCATTGCAAACGC**GCC**GATTGCCCCGATGCCTTG
L25V For	GGAACAAGGCATCGGGGCAATC**GTT**GCGTTTGCAATGGCGTACC
L25V Rev	GGTACGCCATTGCAAACGC**AAC**GATTGCCCCGATGCCTTGTTCC

A28T For	CGGGGCAATCCTTGCGTTT**ACA**ATGGCGTACCTTCGCGGC
A28T Rev	GCCGCGAAGGTACGCCAT**TGT**AAACGCAAGGATTGCCCCG
M29I For	GGCAATCCTTGCGTTTGCA**ATA**GCGTACCTTCGCGGC
M29I Rev	GCCGCGAAGGTACGC**TAT**TGCAAACGCAAGGATTGCC
A30S For	GGCAATCCTTGCGTTTGCAATG**TCG**TACCTTCGCGGC
A30S Rev	GCCGCGAAGGTA**CGA**CATTGCAAACGCAAGGATTGCC
A30V For	GCAATCCTTGCGTTTGCAATG**GTG**TACCTTCGCGGCAGATATAA TGGC
A30V Rev	GCCATTATATCTGCCGCGAAGGTA**CAC**CATTGCAAACGCAAGGA TTGC
Y31I For	CTTGCGTTTGCAATGGCG**ATA**CTTCGCGGCAGATATAAT
Y31I Rev	ATTATATCTGCCGCGAAG**TAT**CGCCATTGCAAACGCAAG
R33C For	GCGTTTGCAATGGCGTACCTT**TGC**GGCAGATATAATGGCGGTGC G
R33C Rev	CGCACCGCCATTATATCTGCC**GCA**AAGGTACGCCATTGCAAACG C
R33H For	GCGTTTGCAATGGCGTACCTT**CAC**GGCAGATATAATGGCGGTGC G
R33H Rev	CGCACCGCCATTATATCTGCC**GTG**AAGGTACGCCATTGCAAACG C
R33L For	GCGTTTGCAATGGCGTACCTT**CTC**GGCAGATATAATGGCGGTGC G
R33L Rev	CGCACCGCCATTATATCTGCC**GAG**AAGGTACGCCATTGCAAACG C
G34S For	GCAATGGCGTACCTTCGC**AGC**AGATATAATGGCGGTGCG
G34S Rev	CGCACCGCCATTATATCT**GCT**GCGAAGGTACGCCATTGC
G38S For	CGCGGCAGATATAAT**AGC**GGTGCGTTTACAAAAACAG
G38S Rev	CTGTTTTTGTAAACGCACC**GCT**ATTATATCTGCCGCG
D47Y For	GCGTTTACAAAAACAGTAATC**TAC**GCAACGATGTGCGCCATTAT CG
D47Y Rev	CGATAATGGCGCACATCGTTGC**GTA**GATTACTGTTTTTGTAAAC GC
A48T For	CAAAAACAGTAATCGAC**ACA**ACGATGTGCGCA
A48T Rev	TGGCGCACATCGT**TGT**GTCGATTACTGTTTTTG
A48V For	CAAAAACAGTAATCGAC**GTA**ACGATGTGCGCA

A48V Rev	TGGCGCACATCGT**TCC**GTCGATTACTGTTTTTG
M50A For	CAGTAATCGACGCAACG**GCG**TGCGCCATTATCGCCTGG
M50A Rev	CCAGGCGATAATGGCGCA**CGC**CGTTGCGTCGATTACTG
M50G For	ACAGTAATCGACGCAACG**GGA**TGCGCCATTATCGCCTGG
M50G Rev	CCAGGCGATAATGGCGCA**TCC**CGTTGCGTCGATTACTGT
M50I For	GTAATCGACGCAACG**ATA**TGCGCCATTATCGCC
M50I Rev	GGCGATAATGGCGCA**TAT**CGTTGCGTCGATTAC
C51A For	CAGTAATCGACGCAACGATG**GCC**GCCATTATCGCCTGG
C51A Rev	CCAGGCGATAATGGC**GGC**CATCGTTGCGTCGATTACTG
C51D For	CAGTAATCGACGCAACGATG**GAT**GCCATTATCGCCTGG
C51D Rev	CCAGGCGATAATGGC**ATC**CATCGTTGCGTCGATTACTG
C51E For	CAGTAATCGACGCAACGATG**GAA**GCCATTATCGCCTGG
C51E Rev	CCAGGCGATAATGGC**TTC**CATCGTTGCGTCGATTACTG
C51F For	CAGTAATCGACGCAACGATG**TTT**GCCATTATCGCCTGG
C51F Rev	CCAGGCGATAATGGC**AAA**CATCGTTGCGTCGATTACTG
C51G For	CAGTAATCGACGCAACGATG**GGT**GCCATTATCGCCTGG
C51G Rev	CCAGGCGATAATGGC**ACC**CATCGTTGCGTCGATTACTG
C51H For	CAGTAATCGACGCAACGATG**CAT**GCCATTATCGCCTGG
C51H Rev	CCAGGCGATAATGGC**ATG**CATCGTTGCGTCGATTACTG
C51I For	CAGTAATCGACGCAACGATG**ATC**GCCATTATCGCCTGG
C51I Rev	CCAGGCGATAATGGC**GAT**CATCGTTGCGTCGATTACTG
C51K For	CAGTAATCGACGCAACGATG**AAA**GCCATTATCGCCTGG
C51K Rev	CCAGGCGATAATGGC**TTT**CATCGTTGCGTCGATTACTG
C51L For	CAGTAATCGACGCAACGATG**CTC**GCCATTATCGCCTGG
C51L Rev	CCAGGCGATAATGGC**GAG**CATCGTTGCGTCGATTACTG
C51M For	CAGTAATCGACGCAACGATG**ATG**GCCATTATCGCCTGG
C51M Rev	CCAGGCGATAATGGC**CAT**CATCGTTGCGTCGATTACTG
C51N For	CAGTAATCGACGCAACGATG**AAT**GCCATTATCGCCTGG

C51N Rev	CCAGGCGATAATGGC**ATT**CATCGTTGCGTCGATTACTG
C51P For	CAGTAATCGACGCAACGATG**CCC**GCCATTATCGCCTGG
C51P Rev	CCAGGCGATAATGGC**GGG**CATCGTTGCGTCGATTACTG
C51Q For	CAGTAATCGACGCAACGATG**CAA**GCCATTATCGCCTGG
C51Q Rev	CCAGGCGATAATGGC**TTG**CATCGTTGCGTCGATTACTG
C51R For	CGACGCAACGATG**CGC**GCCATTATCGCC
C51R Rev	GGCGATAATGGC**GCG**CATCGTTGCGTCG
C51S For	CAGTAATCGACGCAACGATG**AGC**GCCATTATCGCCTGG
C51S Rev	CCAGGCGATAATGGC**GCT**CATCGTTGCGTCGATTACTG
C51T For	CAGTAATCGACGCAACGATG**ACA**GCCATTATCGCCTGG
C51T Rev	CCAGGCGATAATGGC**TGT**CATCGTTGCGTCGATTACTG
C51V For	CAGTAATCGACGCAACGATG**GTG**GCCATTATCGCCTGG
C51V Rev	CCAGGCGATAATGGC**CAC**CATCGTTGCGTCGATTACTG
C51W For	CAGTAATCGACGCAACGATG**TGG**GCCATTATCGCCTGG
C51W Rev	CCAGGCGATAATGGC**CCA**CATCGTTGCGTCGATTACTG
C51Y For	CAGTAATCGACGCAACGATG**TAC**GCCATTATCGCCTGGTTCATTCG
C51Y Rev	CGAATGAACCAGGCGATAATGGC**GTA**CATCGTTGCGTCGATTACTG
A52C For	CAGTAATCGACGCAACGATGTGC**TGT**ATTATCGCCTGGTTCATTCG
A52C Rev	CGAATGAACCAGGCGATAAT**ACA**GCACATCGTTGCGTCGATTACTG
A52D For	CAGTAATCGACGCAACGATGTGC**GAT**ATTATCGCCTGGTTCATTCG
A52D Rev	CGAATGAACCAGGCGATAAT**ATC**GCACATCGTTGCGTCGATTACTG
A52E For	CAGTAATCGACGCAACGATGTGC**GAA**ATTATCGCCTGGTTCATTCG
A52E Rev	CGAATGAACCAGGCGATAAT**TTC**GCACATCGTTGCGTCGATTACTG
A52F For	CAGTAATCGACGCAACGATGTGC**TTC**ATTATCGCCTGGTTCATTCG
A52F Rev	CGAATGAACCAGGCGATAAT**GAA**GCACATCGTTGCGTCGATTACTG

A52G For	CGACGCAACGATGTGC**GGC**ATTATCGCCTGGTTC
A52G Rev	GAACCAGGCGATAAT**GCC**GCACATCGTTGCGTCG
A52H For	CAGTAATCGACGCAACGATGTGC**CAT**ATTATCGCCTGGTTCATT CG
A52H Rev	CGAATGAACCAGGCGATAAT**ATG**GCACATCGTTGCGTCGATTAC TG
A52I For	CAGTAATCGACGCAACGATGTGC**ATC**ATTATCGCCTGGTTCATT CG
A52I Rev	CGAATGAACCAGGCGATAAT**GAT**GCACATCGTTGCGTCGATTAC TG
A52K For	CAGTAATCGACGCAACGATGTGC**AAA**ATTATCGCCTGGTTCATT CG
A52K Rev	CGAATGAACCAGGCGATAAT**TTT**GCACATCGTTGCGTCGATTAC TG
A52L For	CGCAACGATGTGC**CTC**ATTATCGCCTGG
A52L Rev	CCAGGCGATAAT**GAG**GCACATCGTTGCG
A52M For	CAGTAATCGACGCAACGATGTGC**ATG**ATTATCGCCTGGTTCATT CG
A52M Rev	CGAATGAACCAGGCGATAAT**CAT**GCACATCGTTGCGTCGATTAC TG
A52N For	CAGTAATCGACGCAACGATGTGC**AAC**ATTATCGCCTGGTTCATT CG
A52N Rev	CGAATGAACCAGGCGATAAT**GTT**GCACATCGTTGCGTCGATTAC TG
A52P For	CAGTAATCGACGCAACGATGTGC**CCA**ATTATCGCCTGGTTCATT CG
A52P Rev	CGAATGAACCAGGCGATAAT**TGG**GCACATCGTTGCGTCGATTAC TG
A52Q For	CAGTAATCGACGCAACGATGTGC**CAG**ATTATCGCCTGGTTCATT CG
A52Q Rev	CGAATGAACCAGGCGATAAT**CTG**GCACATCGTTGCGTCGATTAC TG
A52R For	CAGTAATCGACGCAACGATGTGC**AGA**ATTATCGCCTGGTTCATT CG
A52R Rev	CGAATGAACCAGGCGATAAT**TCT**GCACATCGTTGCGTCGATTAC TG
A52S For	CAGTAATCGACGCAACGATGTGC**AGC**ATTATCGCCTGGTTCATT CG
A52S Rev	CGAATGAACCAGGCGATAAT**GCT**GCACATCGTTGCGTCGATTAC TG
A52T For	CAGTAATCGACGCAACGATGTGC**ACA**ATTATCGCCTGGTTCATT CG

A52T Rev	CGAATGAACCAGGCGATAAT**TGT**GCACATCGTTGCGTCGATTAC TG
A52V For	CGACGCAACGATGTGC**GTC**ATTATCGCCTGGTTCATTCG
A52V Rev	CGAATGAACCAGGCGATAAT**GAC**GCACATCGTTGCGTCG
A52W For	CAGTAATCGACGCAACGATGTGC**TGG**ATTATCGCCTGGTTCATT CG
A52W Rev	CGAATGAACCAGGCGATAAT**CCA**GCACATCGTTGCGTCGATTAC TG
A52Y For	CAGTAATCGACGCAACGATGTGC**TAC**ATTATCGCCTGGTTCATT CG
A52Y Rev	CGAATGAACCAGGCGATAAT**GTA**GCACATCGTTGCGTCGATTAC TG
I53Y For	GACGCAACGATGTGCGCC**TAT**ATCGCCTGGTTCATTCGT
I53Y Rev	ACGAATGAACCAGGCGAT**ATA**GGCGCACATCGTTGCGTC
A55T For	CGATGTGCGCCATTATC**ACC**TGGTTCATTCGTGACC
A55T Rev	GGTCACGAATGAACCA**GGT**GATAATGGCGCACATCG
W56S For	CGATGTGCGCCATTATCGCC**AGT**TTCATTCGTGACCTTCTCG
W56S Rev	CGAGAAGGTCACGAATGAA**ACT**GGCGATAATGGCGCACATCG
W56Y For	CGATGTGCGCCATTATCGCC**TAT**TTCATTCGTGACCTTCTCG
W56Y Rev	CGAGAAGGTCACGAATGAA**ATA**GGCGATAATGGCGCACATCG
Sam7 For	CGATGTGCGCCATTATCGCC**TAG**TTCATTCGTGACCTTCTCG
Sam7 Rev	CGAGAAGGTCACGAATGAA**CTA**GGCGATAATGGCGCACATCG
R59C For	GCCATTATCGCCTGGTTCATT**TGT**GACCTTCTCGACTTCGCCGG
R59C Rev	CCGGCGAAGTCGAGAAGGTC**ACA**AATGAACCAGGCGATAATGGC
R59H For	GCCATTATCGCCTGGTTCATT**CAT**GACCTTCTCGACTTCGCCGG
R59H Rev	CCGGCGAAGTCGAGAAGGTC**ATG**AATGAACCAGGCGATAATGGC
R59L For	GCGCCATTATCGCCTGGTTCATT**CTT**GACCTTCTCGACTTCGCC GG
R59L Rev	CCGGCGAAGTCGAGAAGGTC**AAG**AATGAACCAGGCGATAATGGC GC
D60N For	GCCATTATCGCCTGGTTCATTCGT**AAC**CTTCTCGACTTCGCCGG
D60N Rev	CCGGCGAAGTCGAGAAG**GTT**ACGAATGAACCAGGCGATAATGGC
L62F For	GCCTGGTTCATTCGTGACCTT**TTC**GACTTCGCCGGACTAAGTAG C

L62F Rev	GCTACTTAGTCCGGCGAAGTC**GAA**AAGGTCACGAATGAACCAGGC
G66E For	GACCTTCTCGACTTCGCC**GAG**CTAAGTAGCAATCTCGCT
G66E Rev	AGCGAGATTGCTACTTAG**CTC**GGCGAAGTCGAGAAGGTC
L71F For	GCCGGACTAAGTAGCAAT**TTC**GCTTATATAACGAGCGTGTTTATCGGC
L71F Rev	GCCGATAAACACGCTCGTTATATAAGC**GAA**ATTGCTACTTAGTCCGGC
A72C For	/Phos/AATCTC**TGC**TATATAACGAGCGTG
A72C Y73C Rev	GCTACTTAGTCCGGCGAAG
Y73C For	/Phos/AATCTCGCT**TGC**ATAACGAGCGTGTTTATCGGC
Y73F For	CGGACTAAGTAGCAATCTCGCT**TTC**ATAACGAGCGTGTTTATCGGC
Y73F Rev	GCCGATAAACACGCTCGTTAT**GAA**AGCGAGATTGCTACTTAGTCCG
Y73T For	CGGACTAAGTAGCAATCTCGCT**ACC**ATAACGAGCGTGTTTATCGGC
Y73T Rev	GCCGATAAACACGCTCGTTAT**GGT**AGCGAGATTGCTACTTAGTCCG
T75C For	GCAATCTCGCTTATATA**TGC**AGCGTGTTTATCGGC
T75C Rev	GCCGATAAACACGCT**GCA**TATATAAGCGAGATTGC
S76C For	GCAATCTCGCTTATATAACG**TGC**GTGTTTATCGGCTACATCGG
S76C Rev	CCGATGTAGCCGATAAACAC**GCA**CGTTATATAAGCGAGATTGC
V77T For	CTCGCTTATATAACGAGC**ACC**TTTATCGGCTACATCGGT
V77T Rev	ACCGATGTAGCCGATAAA**GGT**GCTCGTTATATAAGCGAG
F78G For	GCAATCTCGCTTATATAACGAGCGTG**GGG**ATCGGCTACATCGGTACTGACTCG
F78G Rev	CGAGTCAGTACCGATGTAGCCGAT**CCC**CACGCTCGTTATATAAGCGAGATTGC
I79C For	/Phos/AGCGTGTTT**TGC**GGCTACATCGGTACTGACTCG
I79C G80C Rev	CGTTATATAAGCGAGATTGC
G80C For	/Phos/AGCGTGTTTATC**TGC**TACATCGGTACTGACTCG
G80S For	CGCTTATATAACGAGCGTGTTTATC**AGC**TACATCGGTACTGACTCG
G80S Rev	CGAGTCAGTACCGATGTA**GCT**GATAAACACCGTCGTTATATAAG

	CG
G83D For	CGTGTTTATCGGCTACATC**GAT**ACTGACTCGATTGGTTCG
G83D Rev	CGAACCAATCGAGTCAGT**ATC**GATGTAGCCGATAAACACG
G83I For	GTGTTTATCGGCTACATC**ATC**ACTGACTCGATTGGTTCG
G83I Rev	CGAACCAATCGAGTCAGT**GAT**GATGTAGCCGATAAACAC
I87Y For	TACATCGGTACTGACTCG**TAT**GGTTCGCTTATCAAACGC
I87Y Rev	GCGTTTGATAAGCGAACC**ATA**CGAGTCAGTACCGATGTA
G88K For	CATCGGTACTGACTCGATT**AAA**TCGCTTATCAAACGCTCGC
G88K Rev	GCGAGCGTTTGATAAGCGA**TTT**AATCGAGTCAGTACCGATG
A99C For	CGCTTCGCTGCTAAAAAA**TGC**GGAGTAGAAGATGG
A99C Rev	CCATCTTCTACTCC**GCA**TTTTTTAGCAGCGAAGCG
V101T For	GCTGCTAAAAAAGCCGGA**ACC**GAAGATGGTAGAAATCAA
V101T Rev	TTGATTTCTACCATCTTC**GGT**TCCGGCTTTTTTAGCAGC
Y31 For	TACCTTCGCGGCAGATATAATGGCGG
D8 Rev	GTCATGTTTTTCTGGCATCTTCAGG
SS-S107 For	/Phos/TCTCTTTTATTTCTATTCTCGAGTGCGTATGCGATGAA GATGCCAGAAAAACATGACCTGTTGGCC
SS-S107 Rev	AATGAAAGTTACCCACTTCATATGTATATGTCCTTCTTGCTCTA TTTAATTAGGAATAAG
sdi SS-S107 For	CCTAATTAAATAGAGCAAATCCCCTTATTGGGGGTAAGACATGA AGTGGGTAACTTTC
sdi SS-S107 Rev	GAAAGTTACCCACTTCATGTCTTACCCCCAATAAGGGGATTTGC TCTATTTAATTAGG
NdeI SS-S107 For	GGCGCGGCCATATGAAGTGGGTAACTTTCATTTC
BamHI SS-S107 Rev	GCGACAGGATCCTTATTGATTTCTACCATCTTC
SEcoRI For	TCCTGAATTCATTAGTAATAGTTAC
SxRGFP For	CCGGAGTAGAAGA**C**GGTAGAAATCAACCCGGGAGTAAAGGAGAA GAACTTTTCACTGG
SxRGFP For-RC	CCAGTGAAAAGTTCTTCTCCTTTACTCCCGGGTTGATTTCTACC **G**TCTTCTACTCCGG
GFP ClaI/XhoI Rev	CAGCTTATAATCGATATGGGCCTCGAGCCTGCAGTTATTTGTAT AGTTCATCCATGCC

9aa Linker For	GGGGCTAGCAGTGGAGCAGGTGGGAGTAAAGGAGAAGAACTTTTCACTGG
9aa Linker Rev	GGGTTGATTTCTACCGTCTTCTACTCCGGC
12aa Linker For	GGGAGTAAAGGAGAAGAACTTTTCACTGG
12aa Linker Rev	AACTGCACTTCCGCTAGCTGCTCCAGCACTCCCGGGTTGATTTCTACCGTCTTCTACTCC
20aa Linker For	GGGGCAAGCAGTGGGGCCGGCGGAAGTGCTGGAGCAGCTAGCGG
30aa Linker For	GGGAGCGCAAGTGGCGCCGCGGGAGCTGGTAGTGCAAGCAGTGGGGCCGGCGG
GFP A206K For	CCTGTCCACACAATCT**AAG**CTTTCCAAAGATCCC
GFP A206K Rev	GGGATCTTTGGAAAG**CTT**AGATTGTCTGGACAGG
R XhoI For	CCGCCGCTCGAGGCTAAAAAAGCCGGAGTA
30aa CherryFP For	GGAGCAGCTAGCGGAAGTGCAGGTGGGAGCAAGGGCGAGGAGGATAACATGG
30aa CherryFP ForRC	CCATGTTATCCTCCTCGCCCTTGCTCCCACCTGCACTTCCGCTAGCTGCTCC
CherryFP Rev	GCCACCTGACGTCTAAATCGATTCGGCAACTCGAGTTACTTGTACAGCTCG
BamHI pS105 Rev	CCCCGGGATCCAAAAGTGCCACCTGACGTCTAAGAAACC
pS105 ClaI Rev	TTGACAGCTTATCATCGATATG
mid-GFP Seq	CTCACACAATGTATACATCATGGC
2-AatII For	CCAGAAATCATGGTTATGA**T**GTCATTGTAGGCGGAGAGC
2-AatII Rev	GCTCTCCGCCTACAATGCC**A**TCATAACCATGATTTCTGG
Lys Cas Rev	TGCTCACAATAATTGCATGAGT
Ram54 KpnI For	GCTGGCGTGGTCGGAGGG**T**AC**C**GATAACGGACGT**T**AGAAAAC
Ram54 KpnI Rev	GGTTTTCT**A**ACGTCCGTTATC**G**GT**A**CCCTCCGACCACGCCAGC
RevBor	AAAGCATCGGGAATAACACCATGA
lbdRSeqFor	TTCTCGACTTCGCCGGACTAAG

gal attB For (SPP primer 1)	GAGGTACCAGCGCGGTTTGATC
lbd attP For (SPP primer 2)	TTTAATATATTGATATTTATATCATTTTACGTTTCTCGTTC
lb dint Rev (SPP primer 3)	ACTCGTCGCGAACCGCTTTC
lbd S Seq For	CCGTTTTGCCCGTGCATATCGG
S Seq 350	GCAGGACCGGATCACCAAATGCG
PstI PR’ For	GGCGCCCTGCAGGAAGGAAATACTAAGGCAAAGG
XhoI PR’ For	GGCGGCGGCTCGAGCCATGGTACAGGCCGTGCG
lbd PR’ seq For	ATGCCAGCAAGCGCAGCATATCGCG
-130bp S EcoRI For +150bp	GGTTAGCCAGTGCTCTTTCCG
pS105 ClaI Rev	TAGGGGTTCCGCGCACATTTCC

VITA

Rebecca Lynn White received her Bachelor of Science degree with honors in biology from the University of North Texas in 2001. She entered the doctoral program in microbiology at Texas A&M University as a fellow of the Program in Microbial Genetics and Genomics. She received a National Science Foundation Graduate Research Fellowship in 2003. Her research interests include the molecular biology and genetics of viruses and membrane protein biochemistry. Ms. White served as the Biology Department Representative to the Texas A&M University Graduate Student Council (GSC) for 4 years; during her tenure on the GSC, she served as the GSC Vice President of University Affairs, the Executive Vice President, and the Director of Student Research Week 2006. She also served on a number of University committees, including the Student Health Insurance Advisory Committee, and several Department of Biology committees, including the Faculty Search Committee. In addition to teaching microbiology laboratory sections and serving as a teaching assistant for cell and molecular biology lecture classes, Ms. White supervised a number of undergraduate students and mentored several graduate students. Upon completion of her doctoral studies, she will join the John Elder lab at The Scripps Research Institute in La Jolla, California to study pathogenicity determinants of feline immunodeficiency virus (FIV).

Ms. White may be reached at P.O. Box 818, Clarendon, Texas, 79226. Her email address is reba.white@yahoo.com.